

AD-A189 876

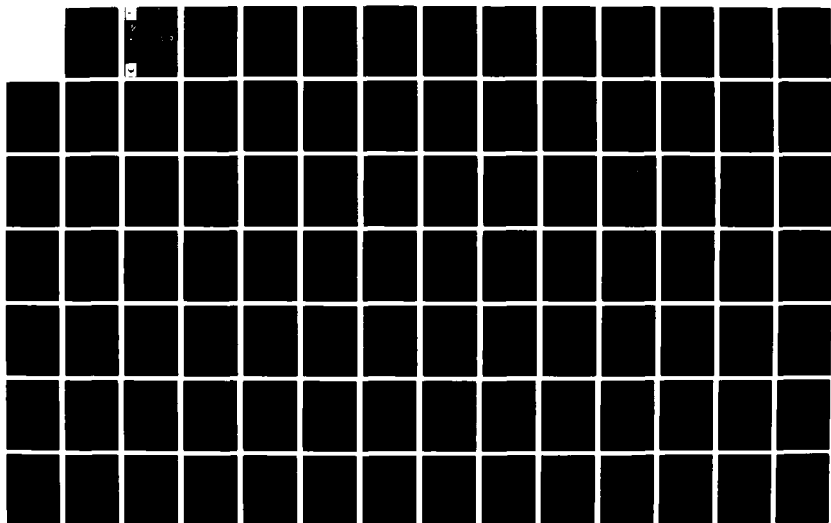
LOWER GREEN BAY HYDRODYNAMIC AND MASS TRANSPORT:
NUMERICAL MODEL STUDY(U) COASTAL ENGINEERING RESEARCH
CENTER VICKSBURG MS A SHAIN ET AL. DEC 87
CERC-MP-87-19

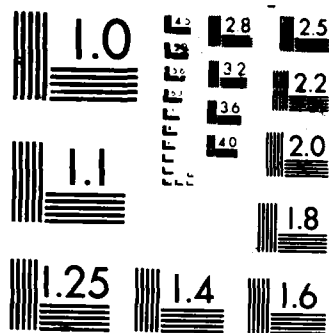
1/2

UNCLASSIFIED

F/G 8/8

NL





DTIC FILE COPY

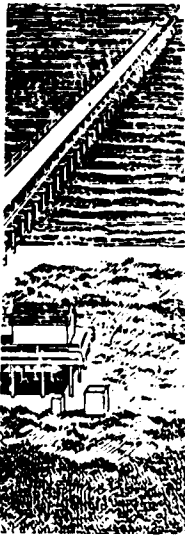
MISCELLANEOUS PAPER CERC-87-19

4



US Army Corps
of Engineers

AD-A189 076



LOWER GREEN BAY HYDRODYNAMIC AND MASS TRANSPORT

Numerical Model Study

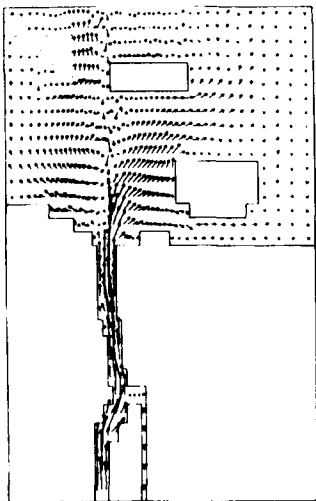
by

A. Swain, Sandra Bird

Coastal Engineering Research Center
Environmental Laboratory

DEPARTMENT OF THE ARMY
Waterways Experiment Station, Corps of Engineers
PO Box 631, Vicksburg, Mississippi 39180-0631

DTIC
ELECTE
JAN 27 1988
S H D



December 1987
Final Report

Approved For Public Release, Distribution Unlimited



88 1 19 104

Prepared for US Army Engineer District, Detroit
PO Box 1027, Detroit, Michigan 48231-1027

Destroy this report when no longer needed. Do not return
it to the originator.

The findings in this report are not to be construed as an official
Department of the Army position unless so designated
by other authorized documents.

The contents of this report are not to be used for
advertising, publication, or promotional purposes.
Citation of trade names does not constitute an
official endorsement or approval of the use of
such commercial products.

Unclassified
SECURITY CLASSIFICATION OF THIS PAGE

A189 576

REPORT DOCUMENTATION PAGE				Form Approved OMB No 0704-0188 Exp Date Jun 30 1986	
1a REPORT SECURITY CLASSIFICATION Unclassified			1b RESTRICTIVE MARKINGS		
2a SECURITY CLASSIFICATION AUTHORITY			3 DISTRIBUTION/AVAILABILITY OF REPORT		
2b DECLASSIFICATION/DOWNGRADING SCHEDULE			Approved for public release; distribution unlimited.		
4 PERFORMING ORGANIZATION REPORT NUMBER(S) Miscellaneous Paper CERC-87-19			5 MONITORING ORGANIZATION REPORT NUMBER(S)		
6a NAME OF PERFORMING ORGANIZATION See reverse		6b OFFICE SYMBOL (If applicable)	7a NAME OF MONITORING ORGANIZATION		
6c ADDRESS (City, State, and ZIP Code) PO Box 631 Vicksburg, MS 39180-0631			7b ADDRESS (City, State, and ZIP Code)		
8a NAME OF FUNDING/SPONSORING ORGANIZATION US Army Engineer District, Detroit		8b OFFICE SYMBOL (If applicable)	9 PROCUREMENT INSTRUMENT IDENTIFICATION NUMBER		
8c ADDRESS (City, State, and ZIP Code) PO Box 1027 Detroit, MI 48231-1027			10 SOURCE OF FUNDING NUMBERS		
			PROGRAM ELEMENT NO	PROJECT NO	TASK NO
					WORK UNIT ACCESSION NO
11 TITLE (Include Security Classification) Lower Green Bay Hydrodynamic and Mass Transport; Numerical Model Study					
12 PERSONAL AUTHOR(S) Swain, A.; Bird, Sandra					
13a TYPE OF REPORT Final report		13b TIME COVERED FROM Mar 86 TO Jun 86		14 DATE OF REPORT (Year, Month, Day) December 1987	
15 PAGE COUNT 110					
16 SUPPLEMENTARY NOTATION Available from National Technical Information Service, 5285 Port Royal Road, Springfield, VA 22161.					
17 COSATI CODES			18 SUBJECT TERMS (Continue on reverse if necessary and identify by block number)		
FIELD	GROUP	SUB-GROUP	Confined Disposal Facility evaluation Transport Green Bay, Wisconsin, Hydrodynamics		
19 ABSTRACT (Continue on reverse if necessary and identify by block number) The US Army Engineer-Waterways Experiment Station's Implicit Flooding Model (WIFM) and the transport model WIFM-SAL were applied to investigate the hydrodynamic and mass transport in Lower Green Bay and Fox River, before and after the proposed Confined Disposal Facility (CDF) expansion. WIFM was calibrated and verified using prototype data. Three hydrodynamic conditions (high, intermediate, and low flow) were simulated in WIFM with the existing CDF and the proposed expansion in place. The hydrodynamic results of these simulations were conducted in the Lower Green Bay area. The first group of simulations consisted of an instantaneous injection of tracer released at the mouth of the Fox River. The second group involved a continuous injection of tracer across the numerical grid boundaries. All simulations were conducted with and without the CDF expansion. (Continued)					
20 DISTRIBUTION STATEMENT (If applicable) <input type="checkbox"/> UNCLASSIFIED <input type="checkbox"/> CONFIDENTIAL <input type="checkbox"/> SECRET			21 ABSTRACT AVAILABILITY STATEMENT <input type="checkbox"/> UNCLASSIFIED <input type="checkbox"/> CONFIDENTIAL <input type="checkbox"/> SECRET		
22a NAME OF RESPONSIBLE PERSON			22b NAME OF RESPONSIBLE PERSON		

DD FORM 1473, 84 MAR

REPRODUCTION OF THIS FORM IS PROHIBITED
WITHOUT THE WRITTEN PERMISSION OF THE
GOVERNMENT OF THE UNITED STATES OF AMERICA

Unclassified

Dist

A-1

City Codes
Avail and/or
Special

Unclassified

SECURITY CLASSIFICATION OF THIS PAGE

6a&b. NAME AND OFFICE SYMBOL OF PERFORMING ORGANIZATION

USAEWES Coastal Engineering Research Center, CEWES-CR-P, and USAEWES Environmental Laboratory, CEWES-ES-Q.

19. ABSTRACT (Continued).

These results it was found that the flow exchange differences caused by the proposed CDF with Peats Lake Bay are insignificant, and the CDF expansion simply redistributes flow by increasing, by way of the main channel, to Middle Bay and by reducing discharge through the cross section between Grassy Island and the expanded CDF. The transport test for instantaneous dye injection, in the presence of the CDF expansion, showed an insignificant effect on the movement of material from the mouth of the Fox River through the Lower Green Bay area. For the continuous boundary injection patterns of concentration, contours were similar for both the existing and proposed conditions.

Unclassified

SECURITY CLASSIFICATION OF THIS PAGE

PREFACE

This report presents the results of a hydrodynamic and mass transport study conducted to quantify the distribution of Fox River discharge into Lower Green Bay under existing conditions and for a proposed expansion of the Confined Disposal Facility located northeast of the river mouth.

The project was requested and funded by the US Army Engineer District, Detroit, under specific direction of Messrs. T. C. Nuttle and John Niemiec, under the general direction of Mr. B. Malamud, Acting Chief, Engineering Division.

Field data required for numerical model calibration and verification were provided by Dr. Kwang Lee, University of Wisconsin, Madison, Wisconsin, and Messrs. D. J. Patterson and B. K. Holmstrom, Department of Natural Resources, Wisconsin, and US Department of Interior, Geological Survey, Madison, Wisconsin.

This study was conducted at the US Army Engineer Waterways Experiment Station (WES). The numerical investigation was completed and this report was prepared by Dr. A. Swain, Coastal Engineering Research Center (CERC), and Ms. Sandra Bird, Environmental Laboratory (EL). Dr. Richard Schmalz provided invaluable technical advice throughout this project.

Providing general supervision were Dr. J. R. Houston and Mr. C. C. Calhoun, Jr., Chief and Assistant Chief, respectively, CERC; Dr. John Harrison, Chief, EL; and Mr. D. L. Robey, Chief, Environmental Research and Simulation Division (ERSD), EL. Direct supervision of the project was provided by Mr. H. L. Butler, Chief, Research Division, CERC, and Mr. Mark Dortch, Chief, Water Quality Modeling Group, ERSD, EL.

Commander and Director of WES during the course of this study and preparation and publication of this report was COL Dwayne G. Lee, CE. Technical Director was Dr. Robert W. Whalin.

CONTENTS

	<u>Page</u>
PREFACE.....	1
CONVERSION FACTORS, NON-SI TO SI (METRIC) UNITS OF MEASUREMENT.....	3
PART I: INTRODUCTION.....	4
Description of Study Area and Objectives.....	4
Approach.....	5
PART II: COMPUTATIONAL METHODS.....	7
Governing Equations.....	7
Numerical Formulation.....	8
Grid Schematization.....	11
PART III: DATA REQUIREMENTS.....	12
Prototype Data.....	12
Model Data.....	12
Boundary Conditions.....	13
PART IV: NUMERICAL MODEL CALIBRATION AND VERIFICATION.....	15
WIFM Calibration.....	15
WIFM Verification.....	15
WIFM-SAL Dispersion Test.....	16
PART V: PRODUCTION RUNS.....	17
Flow Distribution Test.....	17
Hydrodynamic Test Cases.....	17
Transport Test Cases.....	19
Transport Test Results.....	20
PART VI: SUMMARY AND CONCLUSIONS.....	22
REFERENCES.....	24
TABLES 1-7	
FIGURES 1-7	
PLATES 1-68	
APPENDIX A: NOTATION.....	A1

CONVERSION FACTORS, NON-SI TO SI (METRIC)
UNITS OF MEASUREMENT

Non-SI units of measurement used in this report can be converted to SI (metric) units as follows:

<u>Multiply</u>	<u>By</u>	<u>To Obtain</u>
cubic feet per second	0.02831685	cubic metres per second
degree (angle)	0.01745329	radians
feet	0.3048	metres
knots (international)	0.5144444	metres per second
miles (US nautical)	1.852	kilometres
miles (US statute)	1.609344	kilometres
square miles (US statute)	2.589988	square kilometres

LOWER GREEN BAY HYDRODYNAMIC AND MASS TRANSPORT

Numerical Model Study

PART I: INTRODUCTION

Description of Study Area and Objectives

1. Green Bay is a relatively small bay separated from Lake Michigan by the Door Peninsula. The northern (upper) part of Green Bay north of Oconto, Wisconsin, is generally deeper than 60 ft* and the southern (lower) part of the bay south of Long Tail Point is shallower than 20 ft. The Fox River enters Green Bay at the southernmost end of the bay (Figure 1). The Corps of Engineers maintains a navigation channel in the lower Fox River and into Green Bay, dredging as necessary to maintain navigability. Kidney Island, a Confined Disposal Facility (CDF), is located in Lower Green Bay east of the navigation channel.

2. The Corps of Engineers has proposed an expansion of Kidney Island to accommodate continued disposal of dredged materials from the maintenance dredging (Figure 2). However, several point source discharges of oxygen demanding wastes located along a 7.3 mile stretch of the Fox River between De Pere Dam and Lower Green Bay directly impact dissolved oxygen primarily in the lower Fox River and one-fourth mile into the southern end of Green Bay (Patterson 1984). The Wisconsin Department of Natural Resources (WDNR) has developed wasteload allocations for dischargers into the Fox River for upgrading water quality in the lower Fox River and southern Green Bay. The WDNR is concerned that possible changes in the transport and mixing characteristics of Lower Green Bay induced by the proposed expansion of Kidney Island might require an alteration in wasteload allocation.

3. To aid the WDNR in the assessment of the impacts of the Kidney Island expansion, the US Army Engineer District, Detroit (NCE) sponsored a numerical model study by Kwang Lee (1984) to investigate the hydrodynamic impacts resulting from the proposed CDF enlargement. The NCE requested the US Army Engineer Waterways Experiment Station's (WES) Coastal Engineering

* A table of factors for converting non-SI units of measurement to SI (metric) units is presented on page 3.

Research Center review and comment on the model study conducted by Dr. Kwang Lee. The review revealed a number of problems concerning the validity of the results and conclusions. Data presented in the study report were not sufficient to support the conclusions drawn in the report. Consequently, WES was asked to conduct an additional numerical modeling effort to quantify the distribution of Fox River discharge into Lower Green Bay under existing and proposed CDF conditions. WES applied the WES Implicit Flooding Model (WIFM), a two-dimensional (2-D) vertically averaged hydrodynamic model, and the transport model WIFM-SAL to investigate the currents and mass transport in Lower Green Bay and Fox River before and after the proposed CDF expansion. This report summarizes the results of the WES study.

Approach

4. The study was conducted in two parts. The first part involved the application of the numerical hydrodynamic model WIFM (Butler in preparation). This model uses finite difference techniques to represent the vertically integrated Navier-Stokes equations of fluid flow. Description of several special features of WIFM can be found elsewhere (Leenknecht, Earickson, and Butler 1984).

5. WIFM was calibrated and verified using field data collected by Kwang Lee (1984) and data provided by the WDNR and the US Department of Interior Geological Survey, Madison, Wisconsin. After calibration and verification, flow distribution tests were conducted to examine how flow from the Fox River is distributed into various Lower Green Bay regions under the existing and proposed CDF conditions.

6. Three hydrodynamic conditions were simulated in WIFM with the existing CDF and with the proposed expansion in place. These used the fixed flow, seiche, and wind approach developed by Patterson (1984). The hydrodynamic results of these simulations were saved on a subgrid for use in the transport calculations.

7. The second part of the study involved the application of the numerical transport model WIFM-SAL (Schmalz 1985). The transport algorithm in WIFM-SAL was decoupled from the hydrodynamic computations producing a stand-alone transport model which is driven by the previously obtained hydrodynamic simulation data. This eliminates the need for repeating hydrodynamic

simulations. Constituent computations were performed on a subgrid of the hydrodynamic computational grid and used the same time-step as the hydrodynamic computations.

8. The transport model was tested to determine model sensitivity to variations in the input value for the dispersion coefficient. After these tests, the output from WIFM was used as the input to WIFM-SAL for the transport simulations. Two types of transport tests were conducted in the Lower Green Bay area. The first test consisted of an instantaneous injection of tracer released at the mouth of the Fox River. The second type of test was a continuous injection of tracer across the boundaries (the lower Fox River boundary and upper open water boundary of the subgrid). All tests were conducted with and without the proposed CDF expansion.

PART II: COMPUTATIONAL METHODS

Governing Equations

9. The governing equations WIFM uses for hydrodynamic calculations are as follows:

Continuity

$$\frac{\partial \eta}{\partial t} + \frac{\partial}{\partial x} (ud) + \frac{\partial}{\partial y} (vd) = R \quad (1)$$

Momentum (x-direction)

$$\begin{aligned} \frac{\partial u}{\partial t} + u \frac{\partial u}{\partial x} + v \frac{\partial u}{\partial y} - fv + g \frac{\partial}{\partial x} (\eta - \eta_a) + \frac{gu}{C_d^2} (u^2 + v^2)^{1/2} \\ - \epsilon \left(\frac{\partial^2 u}{\partial x^2} + \frac{\partial^2 u}{\partial y^2} \right) + F_x = 0 \end{aligned} \quad (2)$$

Momentum (y-direction)

$$\begin{aligned} \frac{\partial v}{\partial t} + u \frac{\partial v}{\partial x} + v \frac{\partial v}{\partial y} + fu + g \frac{\partial}{\partial y} (\eta - \eta_a) + \frac{gv}{C_d^2} (u^2 + v^2)^{1/2} \\ - \epsilon \left(\frac{\partial^2 v}{\partial x^2} + \frac{\partial^2 v}{\partial y^2} \right) + F_y = 0 \end{aligned} \quad (3)$$

These equations are solved for η , u , and v which are the dependent variables, and represent water surface elevation above datum and the vertically integrated velocities in the x- and y-direction, respectively. The independent variables in the above equations include:

∂ = partial differential operator

t = time

x, y = wind stress direction

$d = \eta - h$, total water depth

h = bed elevation above datum

R = source/sink terms (rate of water volume change through rainfall and evaporation)

f = Coriolis parameter

- g = acceleration due to gravity
 η_a = hydrostatic water elevation due to atmospheric pressure differences
 C = Chezy coefficient
 F_x, F_y = external forcing functions in the x- and y-direction, respectively (i.e., wind stress)
 ϵ = eddy viscosity coefficient

10. The governing equation WIFM-SAL used for transport simulation is the conservative form of the vertically integrated constituent transport equation

$$\frac{\partial}{\partial t} (hs) + \frac{\partial}{\partial x} (hus) + \frac{\partial}{\partial y} (hvs) = \frac{\partial}{\partial x} \left(hK_x^* \frac{\partial s}{\partial x} \right) + \frac{\partial}{\partial y} \left(hK_y^* \frac{\partial s}{\partial y} \right) \quad (4)$$

where s is the vertically integrated constituent concentration, K_x^* and K_y^* are the effective dispersion coefficients in the x- and y-direction, respectively. Details of the derivation of this equation may be found in Schmalz (1985).

Numerical Formulation

11. WIFM uses the alternating-direction-implicit (ADI) scheme to solve Equations 1-3. However, due to the inclusion of the advective terms in these equations, the ADI scheme encountered stability problems. To minimize this problem, WIFM uses a centered stabilizing-correction (SC) scheme that is accurate to second-order in space and time. Boundary conditions can be formulated to the same order of accuracy. A brief description of this technique is given here. More details of the SC scheme can be found in Butler (in preparation).

12. Equations 1, 2, and 3 can be written in matrix form as:

$$U_t + AU_x + BU_y = 0 \quad (5)$$

where

$$U = \begin{bmatrix} \eta \\ u \\ v \end{bmatrix}, \quad A = \begin{bmatrix} 0 & d & 0 \\ g & 0 & 0 \\ 0 & 0 & 0 \end{bmatrix}, \quad B = \begin{bmatrix} 0 & 0 & d \\ 0 & 0 & 0 \\ g & 0 & 0 \end{bmatrix}$$

The SC scheme for solving Equation 5 is

$$(1 + \lambda_x) U^* = (1 - \lambda_x - 2\lambda_y) U^{k-1} \quad (6)$$

$$(1 + \lambda_y) U^{k+1} = U^* + \lambda_y U^{k-1} \quad (7)$$

where

$$\lambda_x = \frac{1}{2} \frac{\Delta t}{\Delta x} A \delta_x \quad \text{and} \quad \lambda_y = \frac{1}{2} \frac{\Delta t}{\Delta y} B \delta_y \quad (8)$$

In the above equations (Equations 6 through 8) the variables are defined as follows:

- λ_x, λ_y = two-dimensional difference operators
- U^* = value of u at an intermediate time-step level ($k+1$ time level, where k counts time levels)
- U = matrix consisting of η, u, v as function of x, y , and t
- k = integer time-step counter
- Δt = time-step
- $\Delta x, \Delta y$ = length of computational cell in x - and y -direction
- A, B = matrixes coefficient
- δ_x, δ_y = centered difference operators

13. The SC scheme consists of two steps. The first step approximates the grid in the x -direction. The second step sweeps the grid in the y -direction. Completing both sweeps constitutes a full time-step and marches the solution from the k^{th} time-level to the $(k+1)$ time-level. The form of the continuity and momentum equations employed in the multioperational hydrodynamic scheme for the x -sweep are given by

$$\frac{1}{2\Delta t} (\eta^* - \eta^{k-1}) + \frac{1}{2\Delta x} \delta_x (u^*d + u^{k-1}d) + \frac{1}{\Delta y} \delta_y (v^{k-1}d) = 0 \quad (9)$$

$$\frac{1}{2\Delta t} (u^* - u^{k-1}) + \frac{g}{2\Delta x} \delta_x (\eta^* + \eta^{k-1}) = 0 \quad (10)$$

$$\frac{1}{2\Delta t} (v^* - v^{k-1}) + \frac{g}{\Delta y} \delta_y (\eta^{k-1}) = 0 \quad (11)$$

and the y-sweep by

$$(12) \quad \frac{1}{2\Delta t} (\eta^{k+1} - \eta^*) + \frac{1}{2\Delta y} \delta_y (v^{k+1}_d - v^{k-1}_d) = 0$$

$$u^{k+1} = u^* \quad (13)$$

$$\frac{1}{2\Delta t} (v^{k+1} - v^*) + \frac{g}{2\Delta y} \delta_y (\eta^{k+1} - \eta^{k-1}) = 0 \quad (14)$$

14. Note that v^* in Equation 11 represents a functional value computed at the $(k-1)$ time-level. If the value of v^* from Equation 11 and the value of u^* from Equation 13 are substituted into Equations 9 and 10, the following simplified equations are obtained:

x-sweep

$$\frac{1}{2\Delta t} (\eta^* - \eta^{k-1}) + \frac{1}{2\Delta x} \delta_x (u^{k+1}_d + u^{k-1}_d) + \frac{1}{\Delta y} \delta_y (v^{k-1}_d) = 0 \quad (15)$$

$$\frac{1}{2\Delta t} (u^{k+1} - u^{k-1}) + \frac{g}{2\Delta x} \delta_x (\eta^* + \eta^{k-1}) = 0 \quad (16)$$

y-sweep

$$\frac{1}{2\Delta t} (\eta^{k+1} - \eta^*) + \frac{1}{2\Delta y} \delta_y (v^{k+1}_d - v^{k-1}_d) = 0 \quad (17)$$

$$\frac{1}{2\Delta t} (v^{k+1} - v^{k-1}) + \frac{g}{2\Delta y} \delta_y (\eta^{k+1} + \eta^{k-1}) = 0 \quad (18)$$

Equations 15 and 16 and 17 and 18 are alternatively solved in WIFM by applying these difference equations to one column (x-sweep) or row (y-sweep), respectively, of the numerical grid. The method of solution can be found in Butler (in preparation).

15. WIFM-SAL contains a flux-corrected transport scheme (Zelasek 1979) capable of resolving sharp fronts without oscillation or numerical dispersion. Details of the solution technique can be found in Schmalz (1985).

Grid Schematization

16. Both WIFM and WIFM-SAL use a stretching transformation of the form

$$X = a + bz^c \quad (19)$$

where

X = physical distance

a, b, c = arbitrary constants

Z = computational distance

for mapping distances along each coordinate direction. A detailed description of the program MAPIT, which maps a variable grid in real space into a uniform grid in computational space is described by Butler (in preparation). MAPIT maps each coordinate direction independently and maximizes grid resolution (finer cells) in areas of hydrodynamic importance and minimizes the number of computational cells (coarser cells) in areas of less importance.

Hydrodynamic grid

17. Based on the previously mentioned technique, a numerical hydrodynamic grid was developed to cover the areas of interest. This grid overlaid on the National Oceanic and Atmospheric Administration (NOAA) Chart 1498 is shown in Figure 3. There are 86 grid indices ($N = 86$) in the longitudinal direction and 65 grid indices ($M = 65$) in the transverse direction. The entire grid consists of 5,590 (N, M) cells.

Transport grid

18. Any impacts of the CDF expansion on the transport of material are expected to occur primarily in Lower Green Bay, south of Grassy Island. A subset of the hydrodynamic grid, centered on this area, was selected for transport calculations. This grid consisted of 2,405 cells and covered 37 of the 86 cells in the direction ($N = 24$ to 60) and the entire 65 cells in the transverse direction ($M = 1$ to 65). This subgrid covered approximately 2 miles beyond Grassy Island inside Long Tail Point and about 2 miles upstream of the Fox River mouth. The transport subgrid overlaid on the hydrodynamic grid is also shown in Figure 3.

PART III: DATA REQUIREMENTS

Prototype Data

19. Prototype data required for numerical model calibration and verification were obtained from the following two sources:

- a. US Department of Interior, Geological Survey, Madison, Wisconsin, provided water surface elevation data for the Angle Light Station and east shore sites on Green Bay, East River, and Fox River for portions of the 1984 water level records.
- b. Velocity and weather data collected by Dr. Kwang Lee were obtained from the Department of Natural Resources (DNR), Madison, Wisconsin. Figure 4 shows locations of water level gages, current meter stations, and weather stations.

Model Data

20. The input data required to run WIFM comprises 26 different input groups. Key information required includes water depth of each cell, a friction characteristic (Manning's n) of each cell, water-surface elevation tabular data along the open water boundary as a function of time, discharge at De Pere Dam as a function of time, and appropriate wind over the entire grid. A 60-sec time-step was used for the numerical simulations.

21. Transport simulations require the hydrodynamic simulation results. Grid geometry information, flag arrays, depths, friction coefficient data, water-surface elevations, and velocities are output by the hydrodynamic code on the transport subgrid, written onto magnetic tape, and supplied as input to the transport code for transport simulation.

22. The dispersion coefficient was calculated in the transport model based on the following formulation (Taylor 1954, Elder 1959):

$$K^* = C_1 U_*^1 h \quad (20)$$

where

C_1 = constant of proportionality

U_*^1 = fluid shear velocity

h = water depth

Based on the work of Elder (1959) a value of 6.0 was used for C_1 to account

for effects of turbulent diffusion and spatial averaging over the depth. Sensitivity to this parameter was tested.

Boundary Conditions

23. A variety of boundary conditions are permissible in WIFM, which can be classified into three general groups: open boundaries, water-land boundaries, and subgrid barrier (thin-wall barriers) boundaries. A brief summary of these boundary conditions are described below. A complete description is given in Butler (in preparation).

Open boundaries

24. This category includes seaward boundaries of the computational grid or locations where channels exit the 2-D grid. Water elevations or flow velocities can be prescribed as functions of location and time. This information can be input to WIFM either as tabular input data or as constituent tidal components from which water elevations can be calculated within the code during the time-marching process.

Land-water boundaries

25. Included in this category are land-water boundaries which are either fixed or variable to allow flooding and drying of cells. The usual condition used at these boundaries is that of "no flow" normal to the boundary. This is accomplished by setting $u = 0$ or $v = 0$ at the appropriate cell face. Low-lying terrain may alternately dry and flood within a tidal cycle or surge history. Flooding in WIFM is simulated by making the location of the land-water boundary a function of local water depth. Once the water levels in adjacent cells rise above the level of adjacent land height (possibility of flooding), water is allowed into the "dry" cell using a broad crested weir formula (Reid and Bodine 1968). When the water level on the dry cell exceeds some small prescribed value, the boundary face is treated as open and computations for η , u , and v are made for that cell ("wet" cell). The drying of cells is the inverse of this process, and water mass balance is conserved in both procedures.

Subgrid barriers

26. These barriers are defined along cell faces and are of three types: exposed, submerged, and overtopping. Exposed barriers permit no flow across a cell face. Submerged barriers are simulated by controlling flow

across cell faces with the use of a time dependent frictional coefficient. An overtopping barrier is treated by using the broad crested weir formula which calculates the proper flow rate across the barrier. The barrier's characteristics are determined by its height and water elevations in the two adjoining cells.

PART IV: NUMERICAL MODEL CALIBRATION AND VERIFICATION

WIFM Calibration

27. The numerical model was calibrated by using field data recorded on 30 July 1982. The forcing conditions used in the calibration included water surface elevation at Angle Light Station as an open water boundary condition, variable discharge at De Pere Dam, and appropriate wind speed and direction.

28. Results of WIFM water surface elevation computations were compared with prototype water surface elevations and numerical model results obtained by Lee (1984) for a 16-hr period. Plates 1-4 show a comparison of calculated and measured water surface elevations above mean lake level at the open water boundary, Angle Light Station, the Fox River mouth, and at De Pere Dam. The calculated WIFM water elevations (shown by the solid line) compare favorably with the field measurements.

29. Plates 5 and 6 present computed current fields in the form of vector plots for a selected grid area in Lower Green Bay. These plots were generated for the numerical model calibration period (at hours 8 and 16) with existing CDF conditions. Plates 7 and 8 show similar plots obtained for the proposed CDF conditions. Simulation time and vector scale relationships to velocity magnitude are given at the bottom of each plate (Plates 5-8).

WIFM Verification

30. Verification of WIFM consists of its ability to reproduce accurately the hydrodynamics of the area of interest without adjusting model parameters. To test this, a period on 25 June 1984 was simulated by WIFM and the calculated results were compared to measured data. This verification period was selected because good field data were available at a number of locations. Boundary conditions used in the verification included measured water surface elevations at Angle Light Station (modified as necessary to represent an open water boundary condition (Plate 9)), variable measured discharge at De Pere Dam, and appropriate wind data.

31. Calculated water surface elevations above mean lake level and calculated current vectors were compared with prototype data. Plate 10 presents a comparison of calculated (solid line) and measured water surface elevations

above mean lake level at Angle Light Station. It should be noted that the comparisons of computed results with measured data for water surface elevations at the mouth of the Fox River and at De Pere Dam are not shown due to the lack of prototype data.

32. Plates 11-15 show a comparison of WIFM current computations with prototype data collected by Dr. Kwang Lee (26 June 1984). The calculated currents compare favorably to the measurements with respect to amplitude and phase.

33. Plates 16 and 17 present computed current fields in the form of vector plots obtained for existing CDF conditions during the numerical model verification period (at hours 8 and 16). Plates 18 and 19 present similar plots obtained for the proposed CDF conditions. Simulation time and vector scale are given at the bottom of each plate (Plates 16-19).

WIFM-SAL Dispersion Test

34. The value of the dispersion coefficient depends on the assigned value of C_1 in Equation 20. Numerical model results may be sensitive to dispersion coefficient changes. To investigate this, dispersion tests were conducted by varying the value of C_1 from 1.0 to 10.0 and using hydrodynamics from a low-discharge scenario (1,000 cfs). Test scenarios will be discussed in detail in the following section. An initial injection of 25.0 mg/l of an arbitrary conservative tracer was made at the mouth of the Fox River in the block of cells ($N = 22$, $M = 35-39$) shown in Plate 20. After 24 hr of simulation the maximum concentration in the dye patch was reduced by only 2 percent by the 10-fold increase in the value of the dispersion coefficient (see Table 1). The concentration contours are nearly identical after 24 hr (Plates 21 and 22). Based on these results and Elder's (1959) recommendation, a value of 6 was used for C_1 in this study.

PART V: PRODUCTION RUNS

Flow Distribution Test

35. Two flow distribution tests were conducted in WIFM to examine how flow from Fox River is distributed into three Lower Green Bay regions (Lower East, Middle, and Peats Lake region; see Figure 5) under the existing and proposed CDF conditions. Ranges were established in WIFM across the east, north, and west side of the Lower Green Bay to facilitate quantification of flow distribution into Lower Green Bay.

36. In the first test, a constant flow of 2,000 cfs was applied as the boundary condition at De Pere Dam. No other forcing conditions (no wind or seiche transmission type boundary condition was applied at the northern open water boundary) were used in the model.

37. In the second test, a constant flow of 4,000 cfs was applied at De Pere Dam, and no other forcing conditions were used in WIFM.

38. Figures 6 and 7 present results from these tests and quantify the distribution of flow from the Fox River into three Lower Green Bay regions under the existing and proposed CDF conditions. It is seen that insignificant exchange of water mass occurs between the Fox River mouth and Peats Lake Bay. The discharge into the Lower Bay is slightly reduced by the proposed CDF, while discharge into Middle Bay is increased by a corresponding amount.

Hydrodynamic Test Cases

39. On the basis of the results presented for the numerical model calibration, verification and flow distribution test, it can be concluded WIFM is correctly simulating the Lower Green Bay hydrodynamics and can therefore be used for hydrodynamic input to drive transport of a conservative substance.

40. Three synthetic hydrodynamic conditions were simulated. The first test was with a constant low flow of 1,000 cfs at De Pere Dam, the second test with an intermediate flow of 2,000 cfs at De Pere Dam, and the third test with a high flow of 4,000 cfs at De Pere Dam. These hydrodynamic scenarios used the fixed flow, mean seiche, and mean wind conditions developed by Patterson (1984). Table 2 lists the seiche magnitude, wind speed and direction, and appropriate fixed flow conditions used in WIFM. Additional information about

seiche data and wind data used in this study can be found in Patterson (1984).

41. The first test was conducted with the following forcing conditions: flow at De Pere Dam = 1,000 cfs; seiche = 0.64 ft with a period of 12 hr was applied at open water boundary; wind speed = 7.60 knots; and wind direction = 210 deg were applied to the entire study area. No other boundary conditions were used in the model.

42. Hydrodynamic results were simulated for a period of 36 hr using a 60-sec time-step. Test conditions are given in Table 3. Plate 23 shows calculated water surface elevations above the mean lake level for selected gage locations for existing and CDF conditions. An examination of Plate 23 reveals that hydrodynamic results repeat after 18 hr of simulation. Since the hydrodynamics reached a near steady-state condition only 36 hr were simulated.

43. A subset of the numerical grid was selected to save hydrodynamic data for use in the transport code. This included cells 24 through 60 ($N = 24$ to 60) in the longitudinal direction, and the entire 65 cells ($M = 1$ to 65) in the vertical direction. This region is shown in Figure 3. Results from the last 12 hr (from 24 to 36 hr) of simulation were saved for use in the transport tests.

44. Table 3 displays the data used to simulate the first tests and the resulting flow distribution across the established ranges for the existing and proposed CDF conditions. The directions of flow in and out of the region are shown by arrows. The convention used to define a positive flow or a negative flow into the region is the same as established in WIFM (u positive downward and v positive to the right).

45. Plates 24 and 25 and 26 and 27 present the computed current vector fields for the existing and proposed CDF, respectively. Plots are given for the selected grid area for both flood and ebb conditions in the river. The simulation time and the vector scale are given at the bottom of each plate.

46. The second test was conducted for a fixed flow of 2,000 cfs applied at De Pere Dam. The forcing conditions are given in Table 4 along with the calculated flow distribution across the established ranges for the existing and proposed CDF conditions. Plate 28 displays calculated water surface elevations above the mean lake level for selected gage locations for existing CDF conditions. Plates 29-32 present the computed vector current fields for the existing and proposed CDF. Plots are given for the same area and simulation times used in the first test.

47. The final hydrodynamic test was simulation for a fixed flow of 4,000 cfs applied at De Pere Dam along with the appropriate seiche and wind data (Table 2). Table 5 shows the data used in WIFM for this test along with the resulting flow distribution across the established ranges for the existing and proposed CDF conditions. Plate 33 displays calculated water surface elevations above mean lake level for selected gage locations for existing CDF conditions. Plates 34-37 present the computed current vector fields for the existing and proposed CDF. The plots are for the same area and simulation times used in the first test.

48. Table 6 shows percentage change in flow distribution between bay regions (Lower East, Middle, and Peats Lake) and the region near mouth of Fox River. These tabulated results were calculated from Tables 3-5.

49. These results indicate that flow exchange differences caused by the existing and proposed CDF with Peats Lake Bay are insignificant. Results indicate the CDF expansion simply redistributes flow by increasing discharge by way of the main channel to Middle Bay while reducing discharge through the cross section between Grassy Island and the expanded CDF.

Transport Test Cases

50. Two types of transport tests were made in the Lower Green Bay area. An instantaneous injection of tracer, as described in the dispersion sensitivity test, was made at the mouth of the Fox River for both a low and high flow condition with and without the proposed CDF expansion, respectively. Movement and dilution of the dye patch was followed for 24 hr.

51. The second type of test was a continuous injection of a conservative tracer across the boundary. A dye concentration of 6.0 mg/l was set at the lower Fox River boundary and a value of 0.15 mg/l was set at the upper open water boundary. These values are based on typical loading rates of biochemical oxygen demand (BOD) into the system (Patterson 1984). It should be emphasized that the resulting concentrations from the tests are not exactly equivalent to BOD since transport simulations are for a conservative substance. Additionally, material that moves across the open water boundary is lost from the system. However, this test will indicate the order of magnitude of the change in BOD which might be expected for the CDF expansion compared to the present conditions. This boundary condition injection was run for 96 hr and a cyclical pattern established.

Transport Test Results

52. For the low flow instantaneous injection, concentration contours for the existing and proposed CDF conditions are shown at 6 hr in Plates 38 and 39 and at 24 hr in Plates 40 and 41. At the gage locations shown in Plate 42, concentration versus time profiles are shown in Plates 43-48. With and without the CDF expansion in place, mass is initially advected up the Fox River as indicated in the 6-hr contour plots (Plates 38 and 39) and the gage located in the Fox River shown in Plate 49. By 6 hr the velocity vectors (Plates 25 and 27) have reversed. The mass moves out of the river back into the lower bay area. With and without the CDF the material moves primarily east of the main channel between the CDF and Grassy Island as shown in Plates 40 and 41, while relatively low concentrations are found west of the channel (Plate 45) toward the Peats Lake region. Only a small concentration of dye reaches Gage 2 (Plate 44) which is in the main channel about one-half mile north of the Fox River mouth.

53. This distribution of material is very similar for both the proposed and existing CDF conditions. Small differences exist in phase for the movement of the mass. Due to increased mixing induced by the slightly increased velocities, there is a very slight decrease in concentrations which have dropped from the initial value of 25.0 mg/l to less than 7.0 mg/l (see Table 1) for both the present CDF and the proposed facility.

54. Under the high flow condition, transport of mass is similar for the instantaneous release condition with and without the CDF expansion. Major differences exist, however, in the movement of mass given the high flow condition as opposed to the low flow condition. For the high flow condition, the dye is not initially moved as far back up the Fox River as would be expected. At 6 hr no significant concentrations of the mass remain in the Fox River (Plates 49 and 50) and virtually no mass reaches gage point 6 (Plate 58). A significant portion of the material moves west of the channel (Plates 51, 52, and 55) for this flow condition under both present and proposed CDF conditions. The 24-hr contours (Plates 51 and 52) indicate that for the high flow, as in the low flow case, the dye is diluted slightly faster with the CDF expansion in place than without it. Plates 53, 54, 56, 57, and 58 show dye movement at different gage locations.

55. The contours of the continuous boundary injections at 91 and 96 hr

are shown in Plates 59-62. Concentrations at the six gage locations are shown in Plates 63-68. For the gage points located in the Fox River and the main channel (Plates 67 and 68), there are no significant differences in concentrations with and without the expansion. The greatest differences occur at Gage 4 (Plate 66) which is located near the CDF and at Gage 1 (Plate 63) which is located between the CDF and Grassy Island. At Gage 1 peak concentrations are on the order of 5 percent higher with the expansion than without it. At Gage 4 the peak value is slightly higher for the existing condition but higher concentration material remains in that area for more of the cycle under expansion conditions.

56 Examination of the contour plots at 91 hr (Plates 59 and 60) illustrates the concentration gradient that forms across the channel particularly during the river outflow cycle. For both the proposed and existing condition an area of high concentration material moves out on the east side of the channel. This is consistent with the observation that the peak concentrations at Gage 5 located near the river mouth are lower than those at Gage 4 which is farther in the bay but on the east side of the channel. Patterns of the concentration contours are similar for both the existing and proposed conditions.

57. The WDNR requested information at a series of gage points forming a rectangle around the mouth of the Fox River and one-half mile into Green Bay. This rectangle is bounded by a row of cells across the mouth of the Fox River ($N = 49$, $M = 37$ to 40); a row of cells extending across the navigation channel ($N = 44$, $M = 30$ to 46); a column of cells east of the navigation channel but west of the CDF ($M = 30$, $N = 44$ to 47); and a column of cells west of the navigation channel ($M = 45$, $N = 44$ to 47). Time averaged concentrations in each of these cells for the last 12 hr cycle (84-96 hr) are given for both the existing and proposed CDF conditions in Table 7. A time-averaged, volume-weighted concentration for all cells in the area was calculated. For the existing conditions this average concentration was 2.75 mg/l and for the proposed condition this value was 2.76 mg/l or an average increase of 0.4 percent for the area.

PART VI: SUMMARY AND CONCLUSIONS

58. The hydrodynamic model WIFM was calibrated and verified by using field data provided by WDNR and the US Department of Interior, Geological Survey, Madison, Wisconsin.

59. A flow distribution test was conducted to investigate the impact of the proposed CDF on water mass circulation in Lower Green Bay and to calculate the distribution of flow across established ranges parallel to and across the Fox River channel. Test results indicated a reduction of flow into Lower East Bay with the proposed CDF in place, and an increase in flow by the corresponding amount into Middle Bay. An insignificant flow exchange with Peats Lake Bay was noted.

60. Three hydrodynamic tests were conducted to generate input data for a transport model. The forcing conditions for these tests included constant flow ($Q = 1,000, 2,000, \text{ and } 4,000 \text{ cfs}$) at De Pere Dam, mean seiche at the open boundary, and appropriate mean wind conditions. A subset of the numerical grid was selected to save the hydrodynamic data from these tests for use in the transport model. The hydrodynamic test results indicated flow exchange differences caused by proposed CDF with Peats Lake Bay are insignificant. Results show the CDF expansion simply redistributes flow by increasing discharge by way of the main channel to Middle Bay and by reducing discharge through the cross section between Grassy Island and the expanded CDF.

61. The 1,000 and 4,000 cfs hydrodynamic simulations were used in WIFM-SAL to drive transport. Two different types of transport tests were conducted in the Lower Green Bay area. These were an instantaneous injection of tracer and a continuous injection of tracer. Both tests were for the low flow ($Q = 1,000 \text{ cfs}$) and high flow ($Q = 4,000 \text{ cfs}$) conditions with and without the proposed CDF expansion in place.

62. For the instantaneous injection test cases, the presence of the CDF expansion does not significantly affect the movement of material from the mouth of the Fox River through the Lower Green Bay area. The material is diluted and moved in a similar fashion for both a high and low flow condition with and without the expansion in place. A slight increase in dilution rate of material is observed with the CDF expansion in place.

63. For the continuous boundary injection, there is very little difference in concentrations at the gage points located in the Fox River and in

the main channel (area considered critical in terms of dissolved oxygen. The gage point located adjacent to the CDF shows local changes in the concentrations but the peak and trough values are still nearly equal even at this location. At Gage 3, which is west of the main channel, with the CDF in place, there is an insignificant increase in the peak concentration of material that is moved into this area, but it moves back out and drops to a preexpansion level in each seiche cycle. Similar patterns are observed in the concentration contours under proposed and expansion conditions. For the rectangular area centered on the mouth of the Fox River, the time-averaged, volume-weighted concentration changes by less than 1 percent following the CDF expansion.

REFERENCES

- Butler, H. L. "WIFM-WES Implicit Flooding Model: Theory and Program Documentation" (in preparation), US Army Engineer Waterways Experiment Station, Coastal Engineering Research Center, Vicksburg, Miss.
- Elder, J. W. 1959. "The Dispersion of Marked Fluid in Turbulent Shear Flow," Journal of Fluid Mechanics, Vol 5, pp 544-560.
- Lee, Kwang K. 1984. "Lower Green Bay and Fox River Currents and Mass Transports Hydrodynamics Study for Two Proposed Confined Disposal Facilities," US Army Engineer District, Detroit, Detroit, Mich.
- Leenknecht, David A., Earickson, Jeff A., and Butler, H. Lee. 1984. "Numerical Simulation of Oregon Inlet Control Structures' Effects on Storm and Tide Elevations in Pamlico Sound," US Army Engineer Waterways Experiment Station, Coastal Engineering Research Center, Vicksburg, Miss.
- Patterson, Dale. 1984. "Water Quality Modeling of the Lower Fox River for Wasteload Allocation Development Cluster 111 - Water Quality Modeling," Wisconsin Department of Natural Resources, Madison, Wis.
- Reid, R. O., and Bodine, B. R. 1968. "Numerical Model for Storm Surges in Galveston Bay," Journal of Waterways and Harbor Division, American Society of Civil Engineers, Vol 94, No. WW1, pp 33-57.
- Schmalz, R. A., Jr. 1985 (May). "User Guide for WIFM-SAL: A Two-Dimensional Vertically Integrated, Time-Varying Estuarine Transport Model," Instruction Report EL-85-1, US Army Engineer Waterways Experiment Station, Vicksburg, Miss.
- Taylor, G. I. 1954. "Dispersion of Matter in Turbulent Flow through a Pipe," Proceedings of the Royal Society of London (A), Vol 223, pp 446-468.
- Zelasek, S. T. 1979. "Fully Multi-Dimensional Flux-Corrected Transport. Algorithms for Fluids," Journal of Computational Physics, Vol 31, pp 333-362.

Table 1
Maximum Plume Concentration at 24 hr

Flow Condition	Maximum		Grid Element Dispersion Constant
	mg/l	N, M	
Low flow, existing CDF	7.0	16, 20	1.0
Low flow, existing CDF	6.9	16, 20	10.0
Low flow, existing CDF	6.9	16, 20	6.0
Low flow, proposed CDF	6.8	19, 26	6.0
High flow, existing CDF			
West of channel	6.0	17, 56	6.0
East of channel	4.7	20, 19	6.0
High flow, proposed CDF			
West of channel	4.6	17, 56	6.0
East of channel	4.6	19, 24	6.0

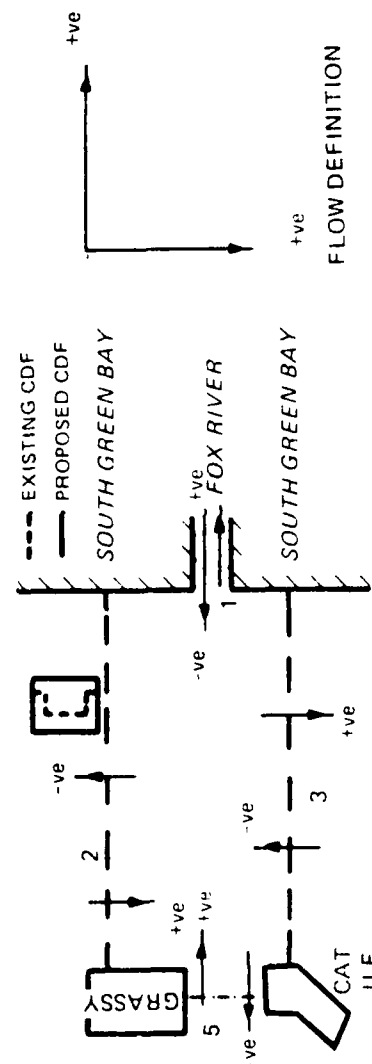
Table 2
Hydrodynamic Test Conditions to Drive Transport

Flow at De Pere Dam cfs	Mean Seiche Magnitude ft	Mean Wind Speed knots	Wind Direction deg
1,000	0.64	7.60	210
2,000	0.46	6.40	210
4,000	0.60	8.04	210

Table 3

Lower Green Bay Numerical Study, Range Computations, 1,000 cfs

Range No.	Results				Item
	Existing		Proposed		
	+ve Flow	-ve Flow	+ve Flow	-ve Flow	
	* 10 ⁶ ft ³	* 10 ⁶ ft ³	* 10 ⁶ ft ³	* 10 ⁶ ft ³	
1	197.81	334.06	197.71	333.93	Mouth of Fox River
2	166.81	351.44	166.78	328.80	Grassy Island and South Green Bay
3	258.70	145.60	258.53	145.52	Cat Island and South Green Bay
5	319.60	158.59	315.09	177.08	Grassy and Cat Islands

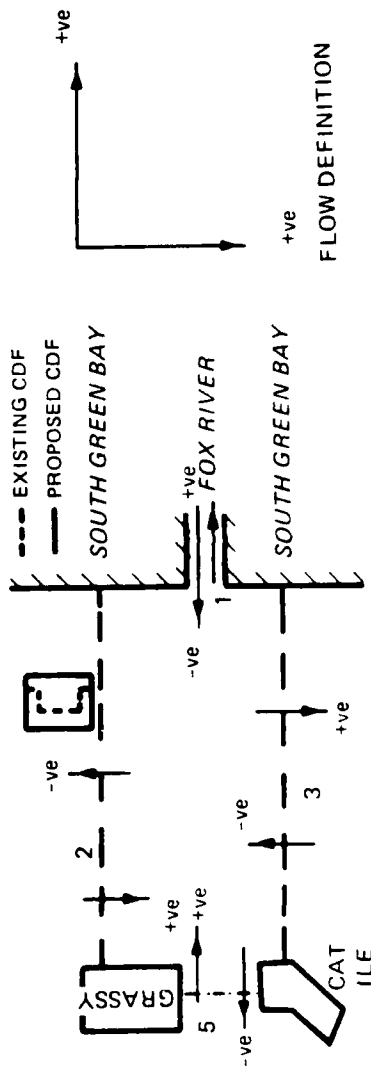


Note: Test conditions: Fox River flow = 1,000 cfs; seiche magnitude = 0.64 ft; mean wind speed = 7.60 knots (constant); wind direction = 210 deg (constant); simulation period = 36 hr. Each number should be multiplied by 10⁶ as shown.

Table 4

Lower Green Bay Numerical Study, Range Computations, 2,000 cfs

Range No.	Results				Item
	Existing		Proposed		
	+ve Flow * 10 ⁶ ft ³	-ve Flow * 10 ⁶ ft ³	+ve Flow * 10 ⁶ ft ³	-ve Flow * 10 ⁶ ft ³	
1	80.97	343.79	80.57	343.34	Mouth of Fox River
2	73.05	332.44	82.55	308.42	Grassy Island and South Green Bay
3	211.68	126.22	213.97	126.98	Cat Island and South Green Bay
5	206.82	135.52	194.92	155.54	Grassy and Cat Islands

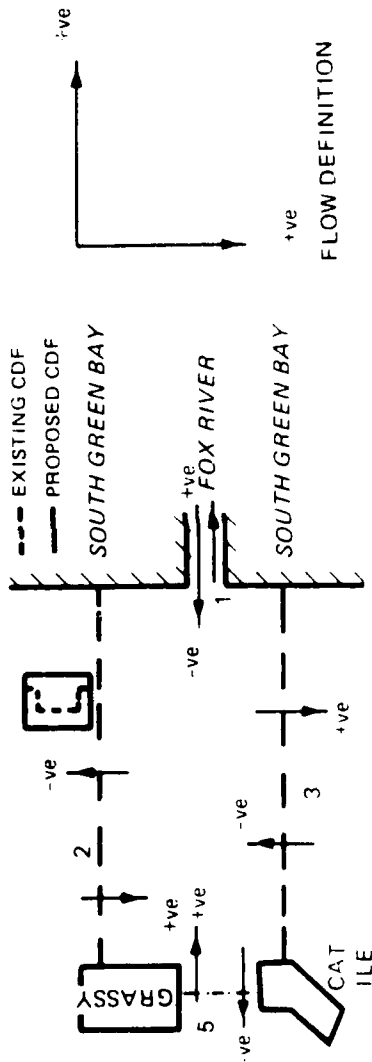


Note: Test conditions: Fox River flow = 2,000 cfs; seiche magnitude = 0.46 ft; mean wind speed = 6.04 knots (constant); wind direction = 210 deg (constant); simulation period = 36 hr. Each number should be multiplied by 10⁶ as shown.

Table 5

Lower Green Bay Numerical Study, Range Computations, 4,000 cfs

Range No.	Results				Item
	Existing		Proposed		
	+ve Flow * 10 ⁶ ft ³	-ve Flow * 10 ⁶ ft ³	+ve Flow * 10 ⁶ ft ³	-ve Flow * 10 ⁶ ft ³	
1	49.37	567.09	60.52	577.98	Mouth of Fox River
2	84.18	479.33	107.25	441.04	Grassy Island and South Green Bay
3	290.52	161.59	282.55	156.73	Cat Island and South Green Bay
5	219.87	227.49	208.23	281.07	Grassy and Cat Islands



Note: Test conditions: Fox River flow = 4,000 cfs; seiche magnitude = 0.60 ft; mean wind speed = 8.04 knots (constant); wind direction = 210 deg (constant); simulation period = 36 hr. Each number should be multiplied by 10⁶ as shown.

Table 6
Percentage Change in Flow Distribution Between Bay Regions
and the Region Near Mouth of Fox River

<u>Bay</u>	<u>Discharge Rate, cfs</u>		
	<u>1,000</u>	<u>2,000</u>	<u>4,000</u>
Lower East 2	-6	-10	-13
Middle 5	14	22	27
Peat Lake 3	0	1	-1

Note: A (-) indicates a reduction in discharge toward Bay region.
A discussion of results presented in the above table is as follows:
Flow exchange differences caused by the existing and proposed CDF with Peat Lake Bay are insignificant. Results for Middle or Lower East Bays indicate CDF expansion simply redistributes flow by increasing discharge via the main channel to Middle Bay. Consequently, discharge through the small cross section between Grassy Island and the expanded CDF is reduced.

Table 7
Time Averaged Concentrations for Existing
and Proposed CDF

Coordinate N, M	Average Concentration mg/l		Coordinate N, M	Average Concentration mg/l	
	Existing	Proposed		Existing	Proposed
44, 30	2.96	3.28	46, 37	3.78	3.48
44, 31	3.28	3.92	46, 38	3.27	3.25
44, 32	3.15	4.03	46, 39	1.50	1.64
44, 33	3.44	3.74	46, 40	1.42	1.55
44, 34	3.63	3.85	46, 41	1.57	1.68
44, 35	3.31	3.59	46, 42	1.31	1.49
44, 36	3.53	3.69	46, 43	1.54	1.70
44, 37	2.47	1.66	46, 44	1.44	1.64
44, 38	1.75	1.72	46, 45	1.67	1.83
44, 39	0.76	0.84	46, 46	1.72	1.87
44, 40	0.69	0.91	47, 30	4.05	3.89
44, 41	0.71	0.89	47, 31	3.94	3.85
44, 42	0.77	0.95	47, 32	4.22	4.07
44, 43	0.76	0.92	47, 33	4.46	4.26
44, 44	0.89	1.00	47, 34	4.68	4.43
44, 45	0.76	0.95	47, 35	4.65	4.42
44, 46	0.90	1.14	47, 36	4.57	4.31
45, 30	3.83	4.39	47, 37	4.32	4.17
45, 31	4.35	4.25	47, 38	3.67	3.56
45, 32	4.39	4.22	47, 39	1.25	1.36
45, 33	4.32	3.96	47, 40	1.38	1.50
45, 34	4.06	3.65	47, 41	1.99	2.20
45, 35	3.72	3.31	47, 42	1.90	2.01
45, 36	3.27	3.00	47, 43	2.12	2.13
45, 37	2.75	2.60	47, 44	1.76	1.93
45, 38	2.69	2.60	47, 45	2.04	2.19
45, 39	0.79	1.01	48, 32	3.98	4.09
45, 40	0.78	1.02	48, 33	3.99	3.94
45, 41	0.78	1.04	48, 34	4.38	4.17
45, 42	0.81	1.06	48, 35	4.66	4.47
45, 43	0.82	1.08	48, 36	4.63	4.54
45, 44	0.92	1.17	48, 37	4.60	4.46
45, 45	0.87	1.14	48, 38	4.60	4.32
45, 46	1.11	1.37	48, 39	1.99	2.13
46, 30	3.92	3.42	48, 40	2.89	2.97
46, 31	4.30	3.96	48, 41	3.46	3.60
46, 32	4.76	4.61	49, 37	4.71	4.56
46, 33	4.73	4.55	49, 38	4.67	4.66
46, 34	4.63	4.39	49, 39	2.54	2.58
46, 35	4.39	4.10	49, 40	3.05	3.19
46, 36	4.16	3.86			

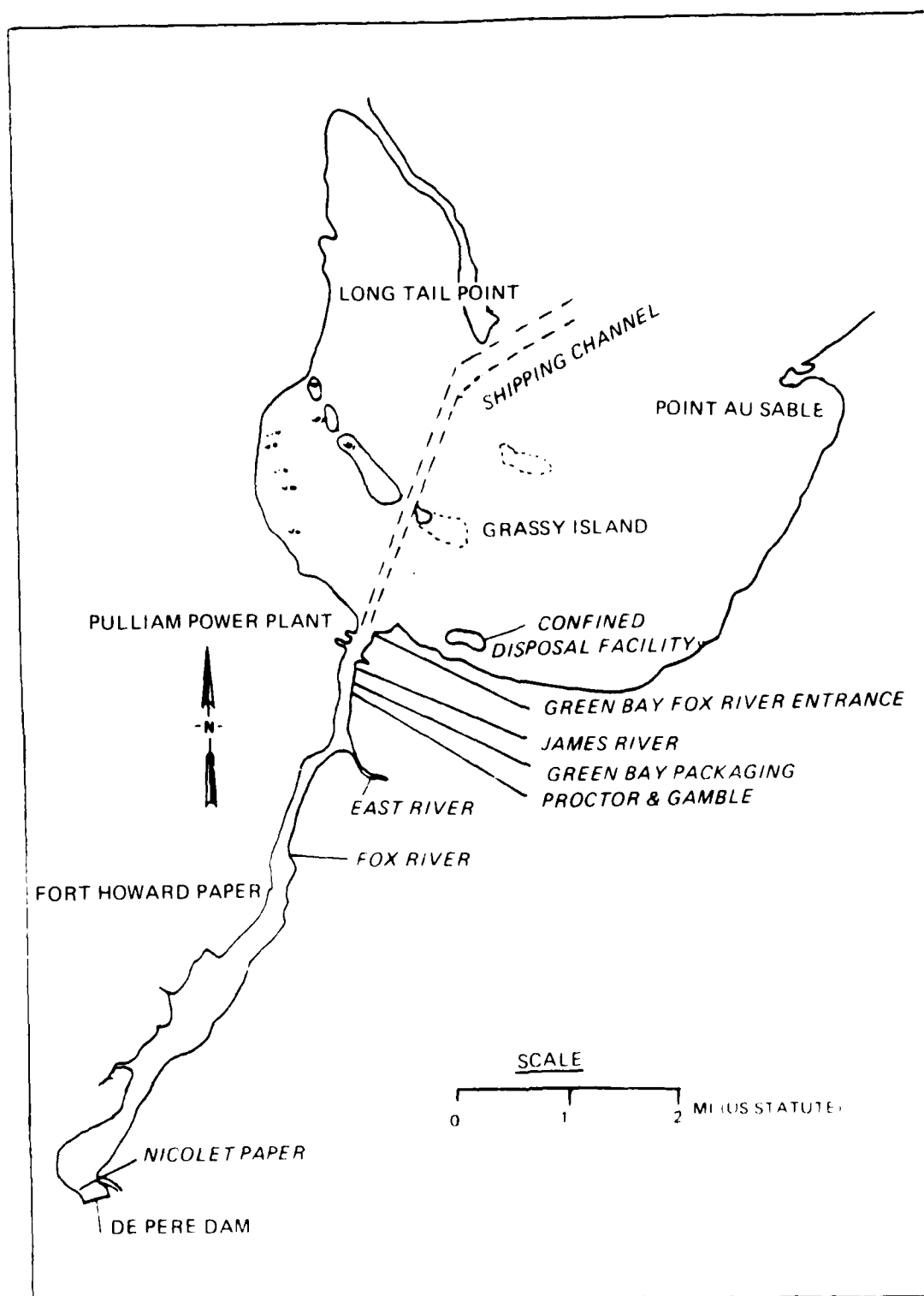


Figure 1. Lower Green Bay location map

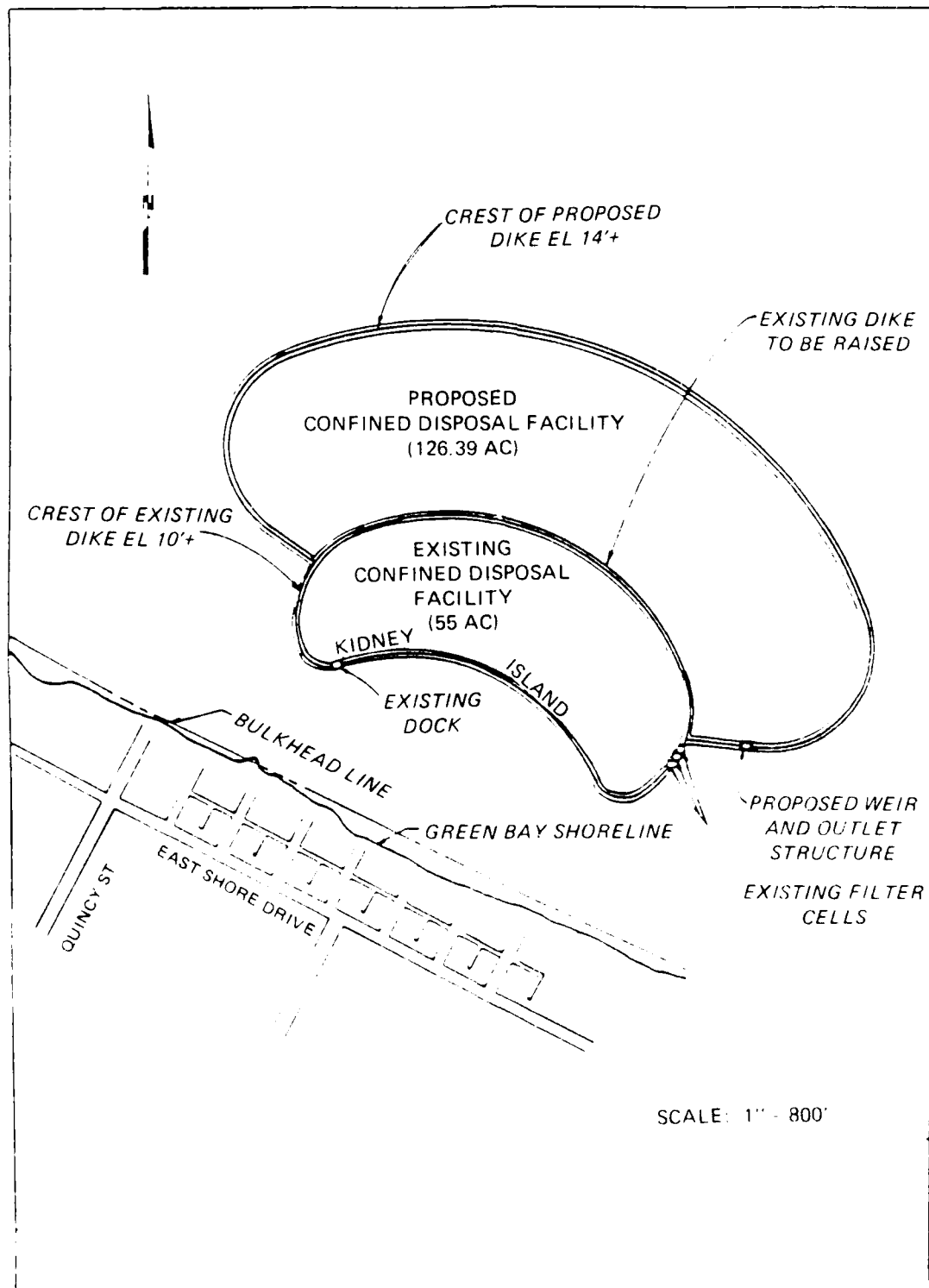


Figure 2. Green Bay Harbor Confined Disposal Facility configuration

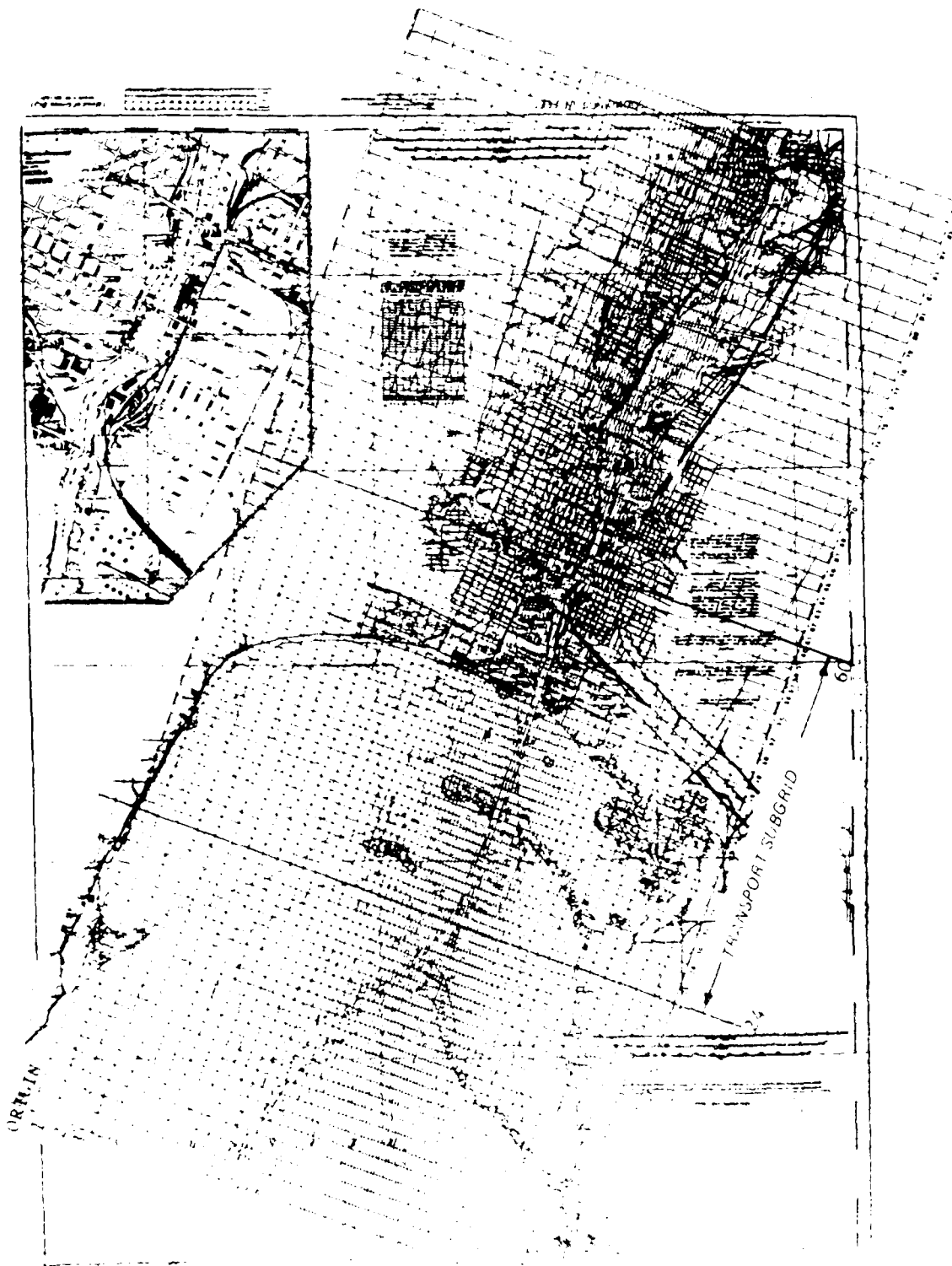


Figure 3. Hydrodynamic numerical grid and transport subgrid laid over NOAA Chart 14918

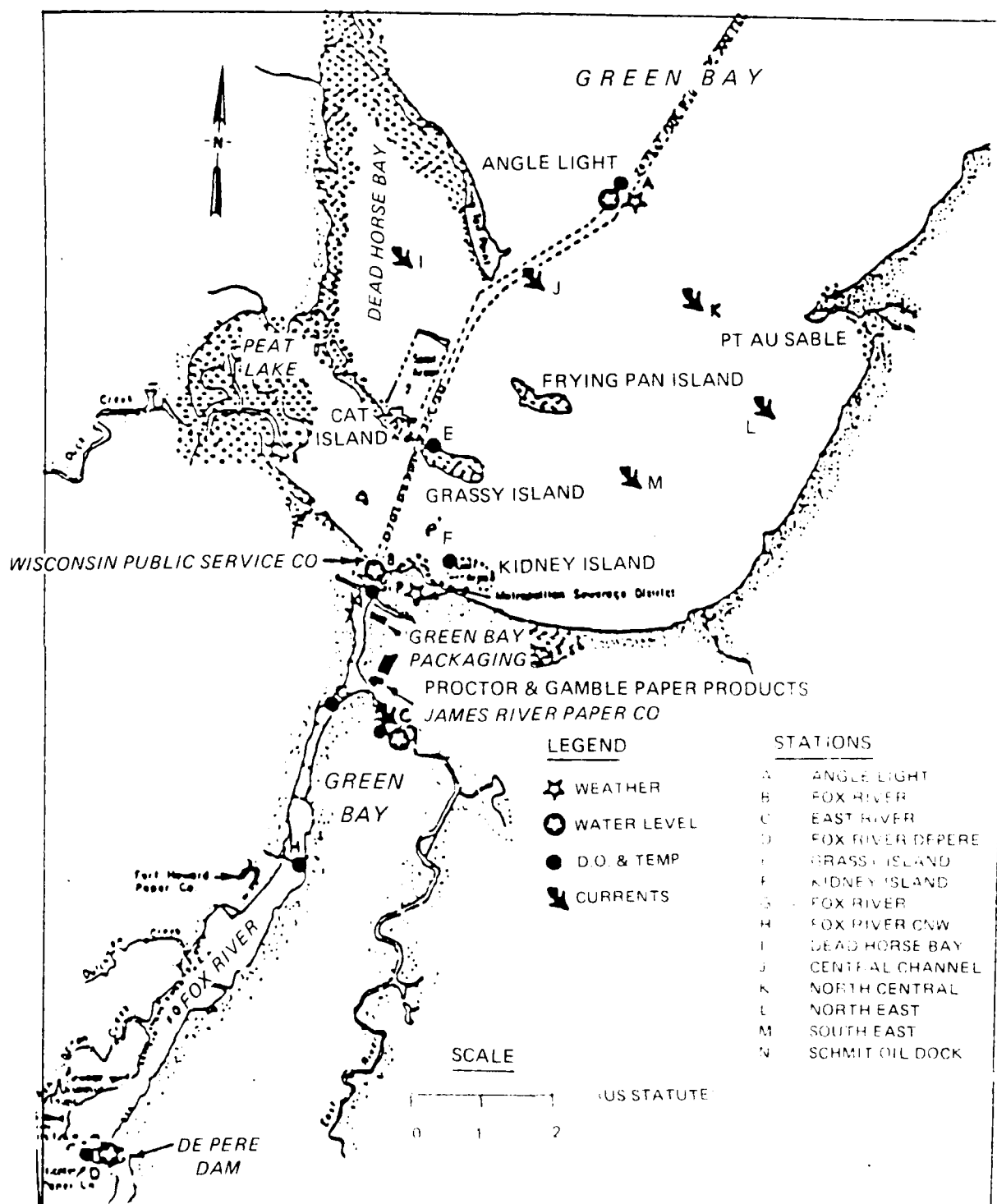


Figure 4. Water surface elevation and current stations

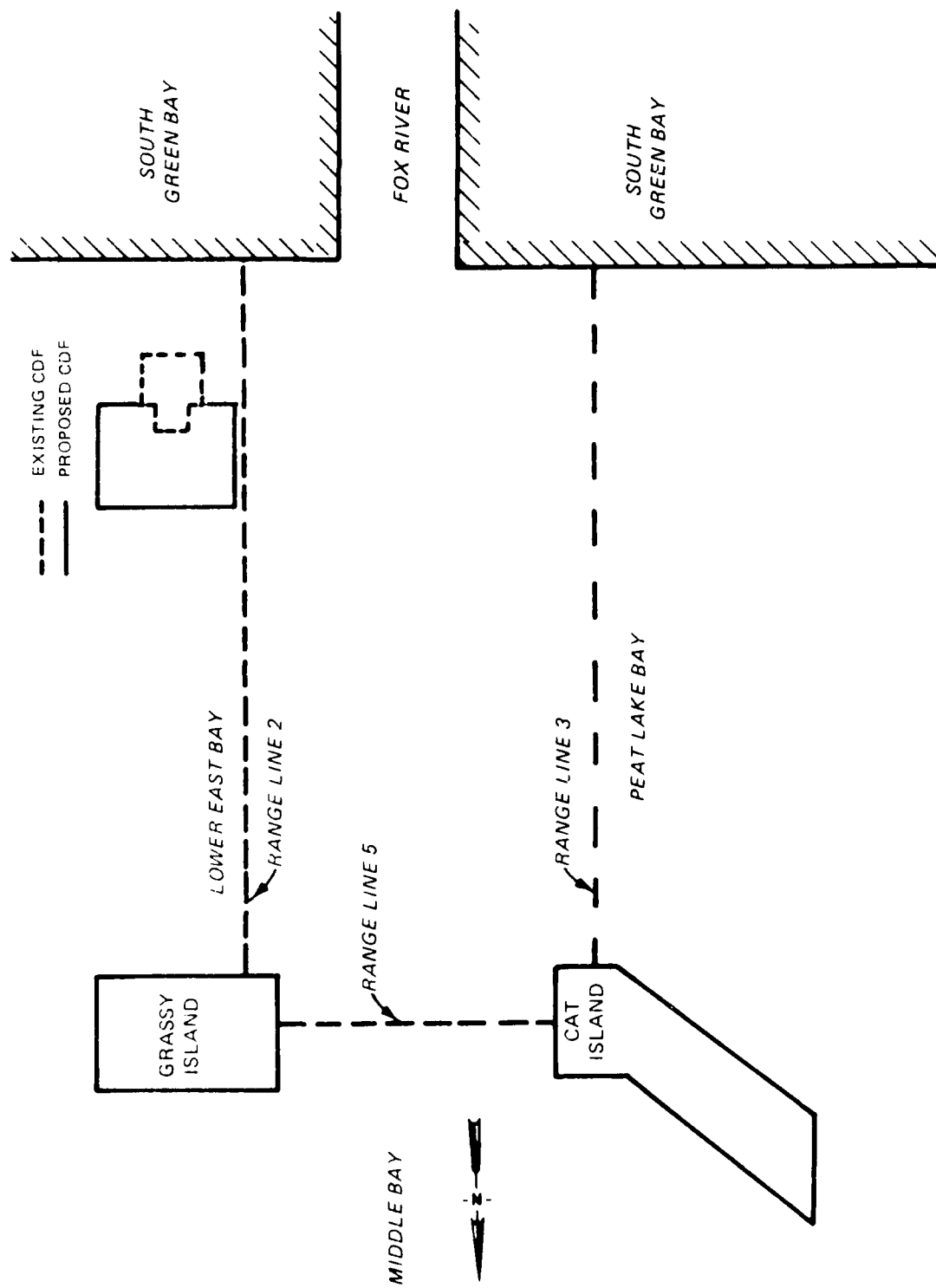


Figure 5. Flow distribution test configuration

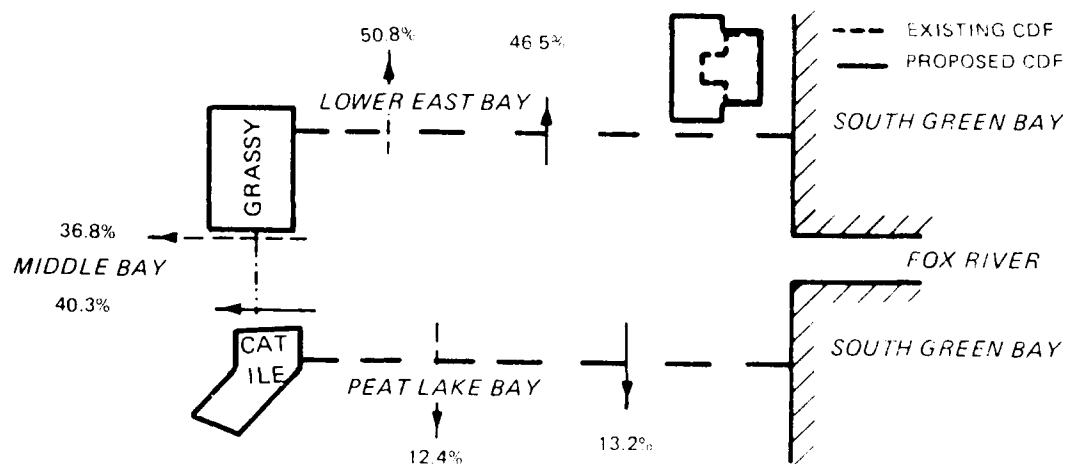


Figure 6. Results of Fox River flow distribution test, flow = 2,000 cfs (no other boundary conditions)

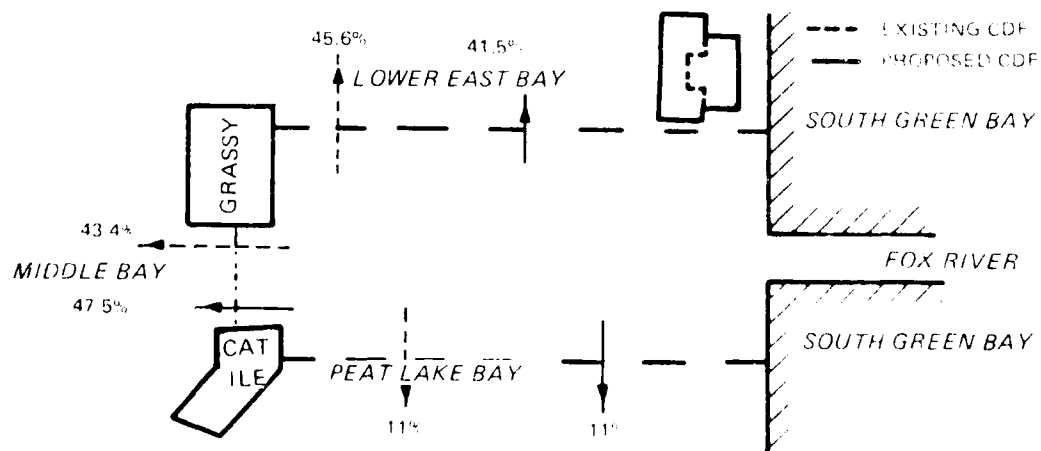
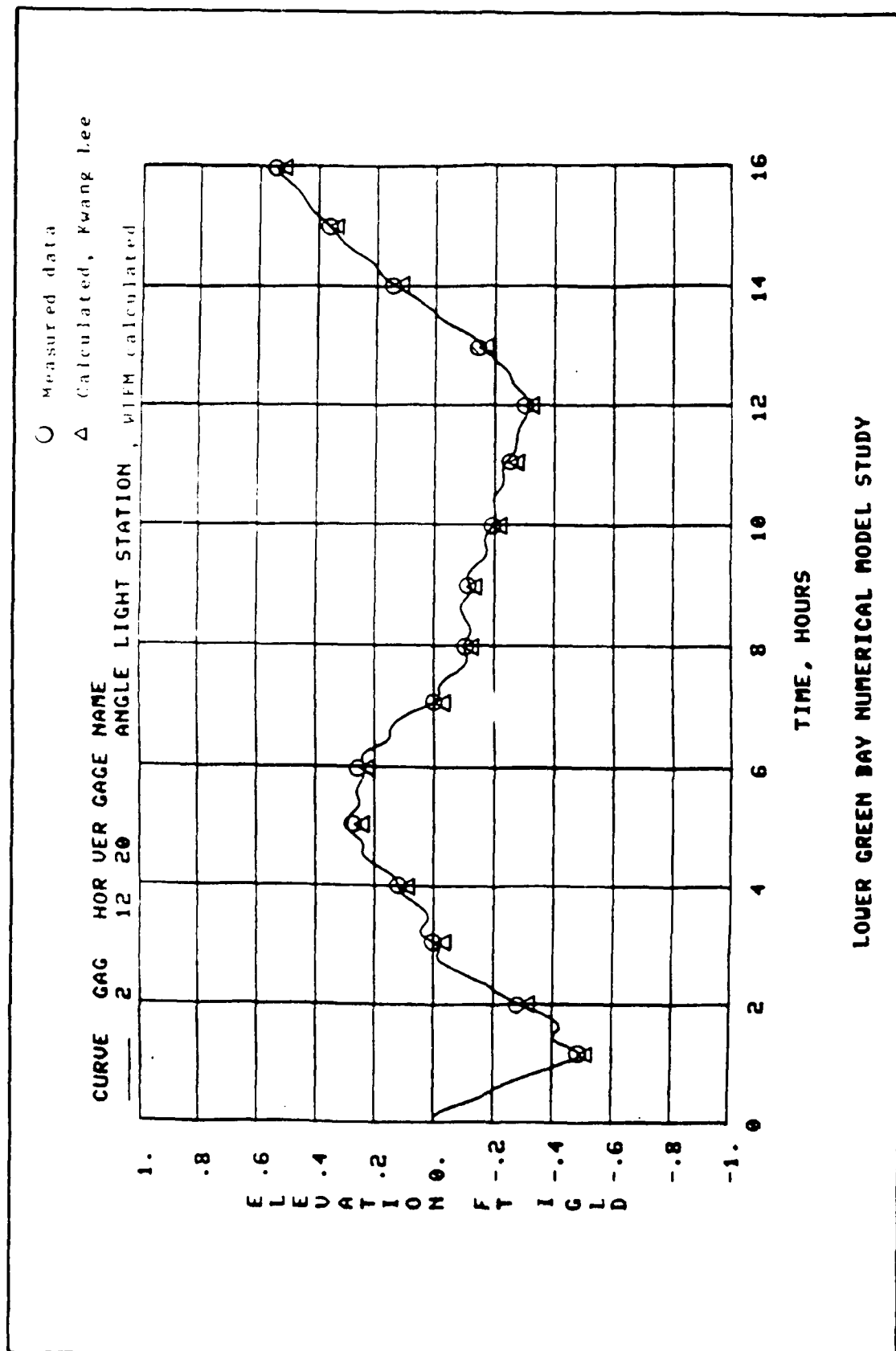
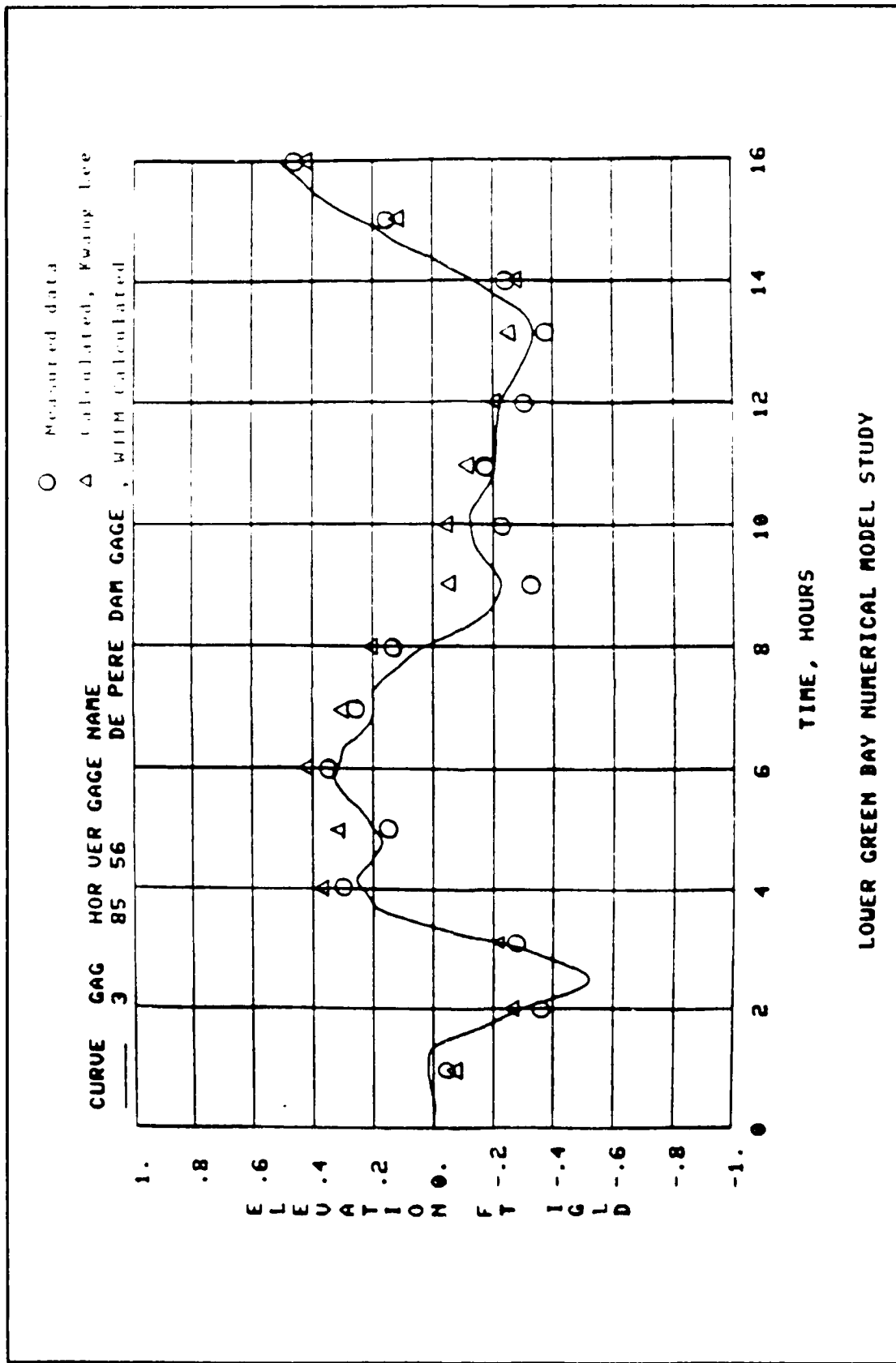
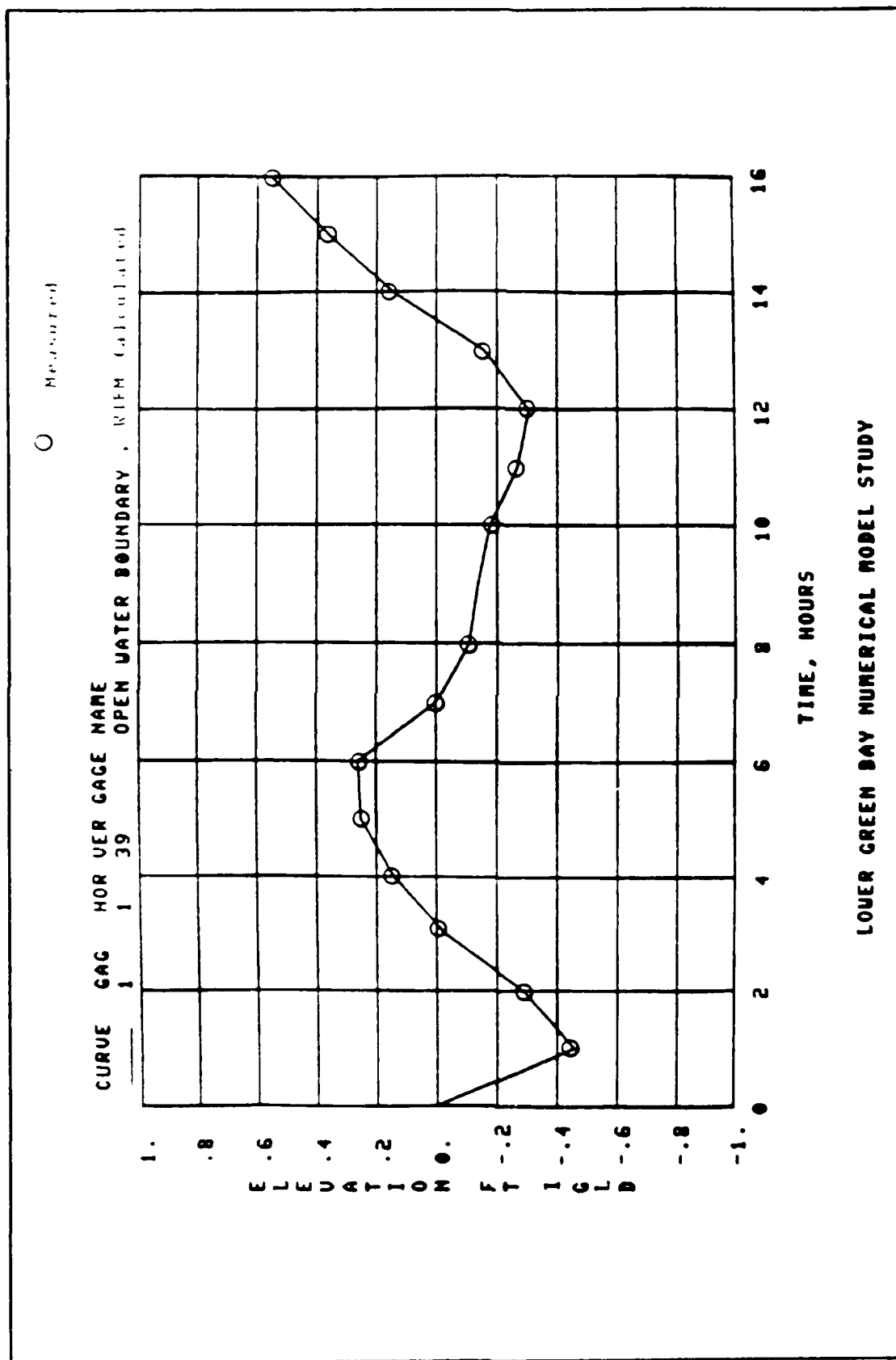
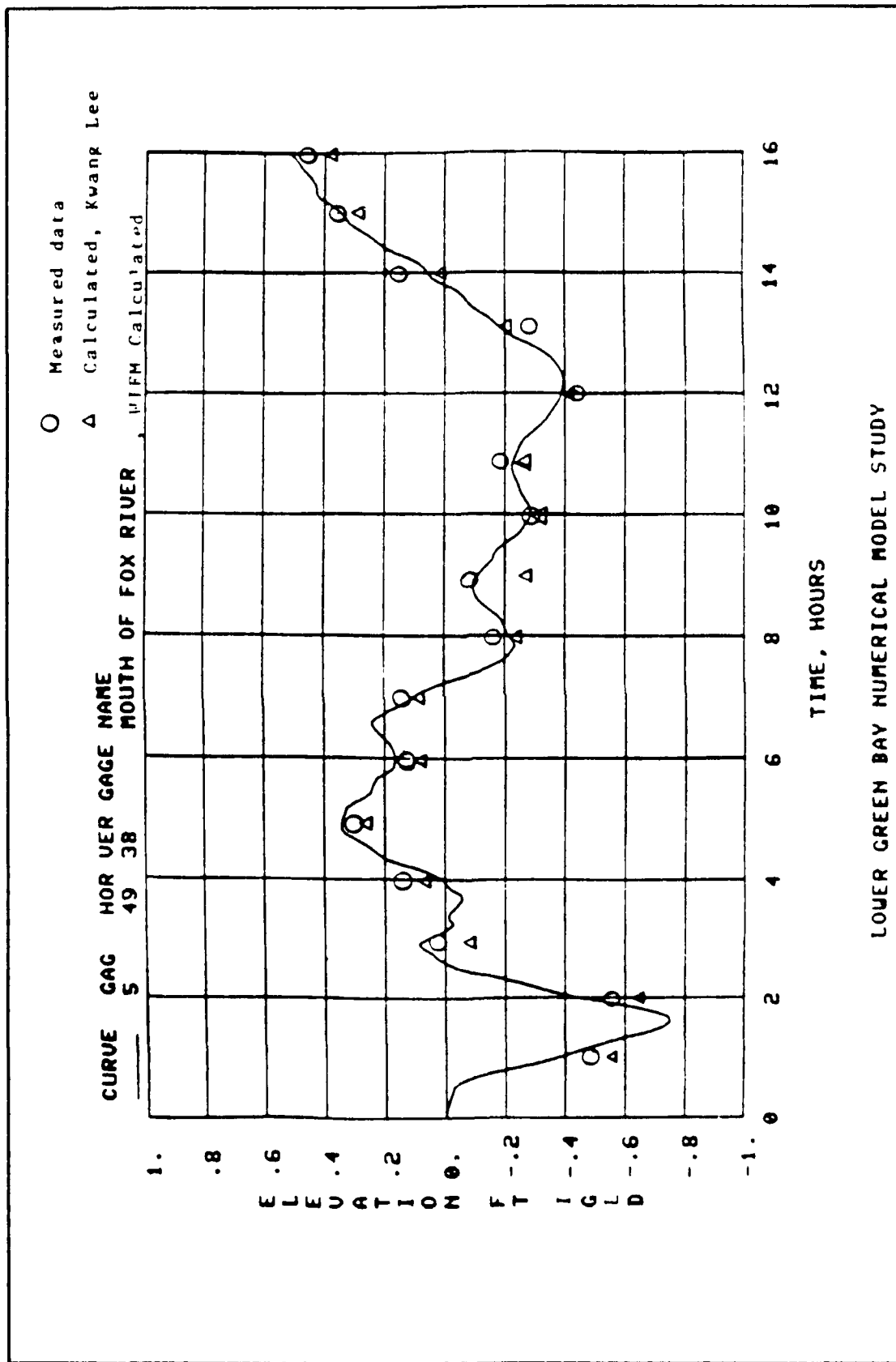


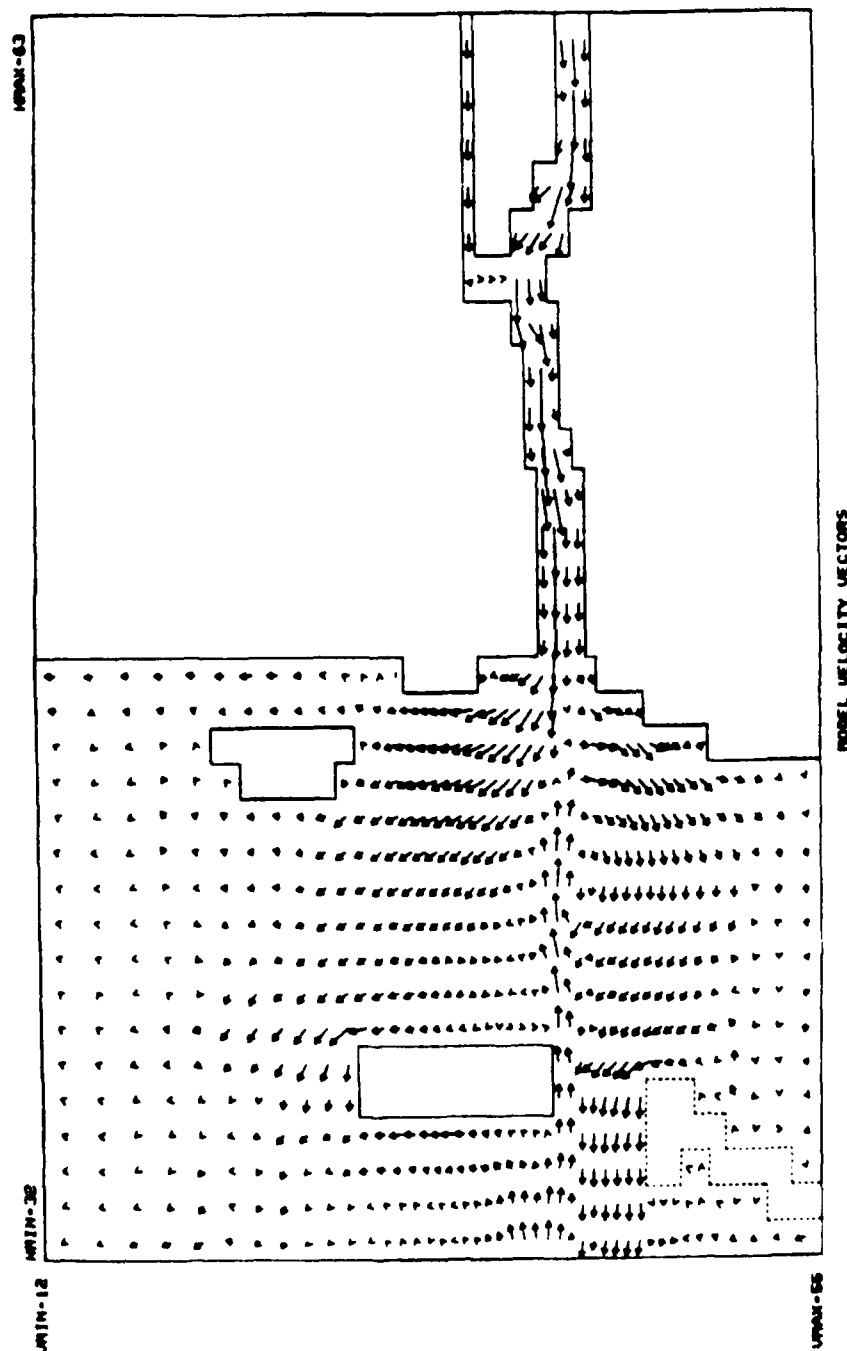
Figure 7. Results of Fox River flow distribution test, flow = 4,000 cfs (no other boundary conditions)



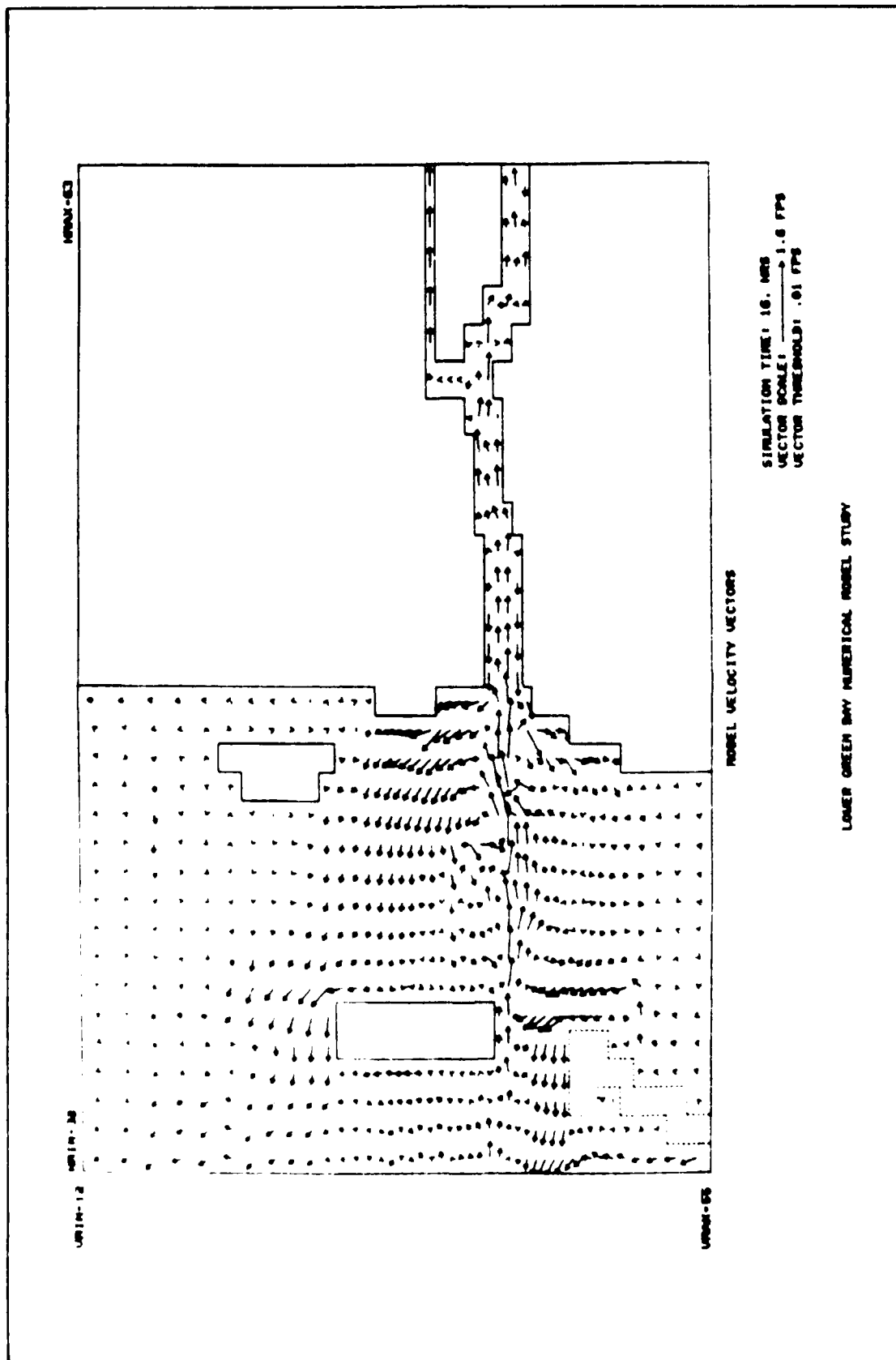


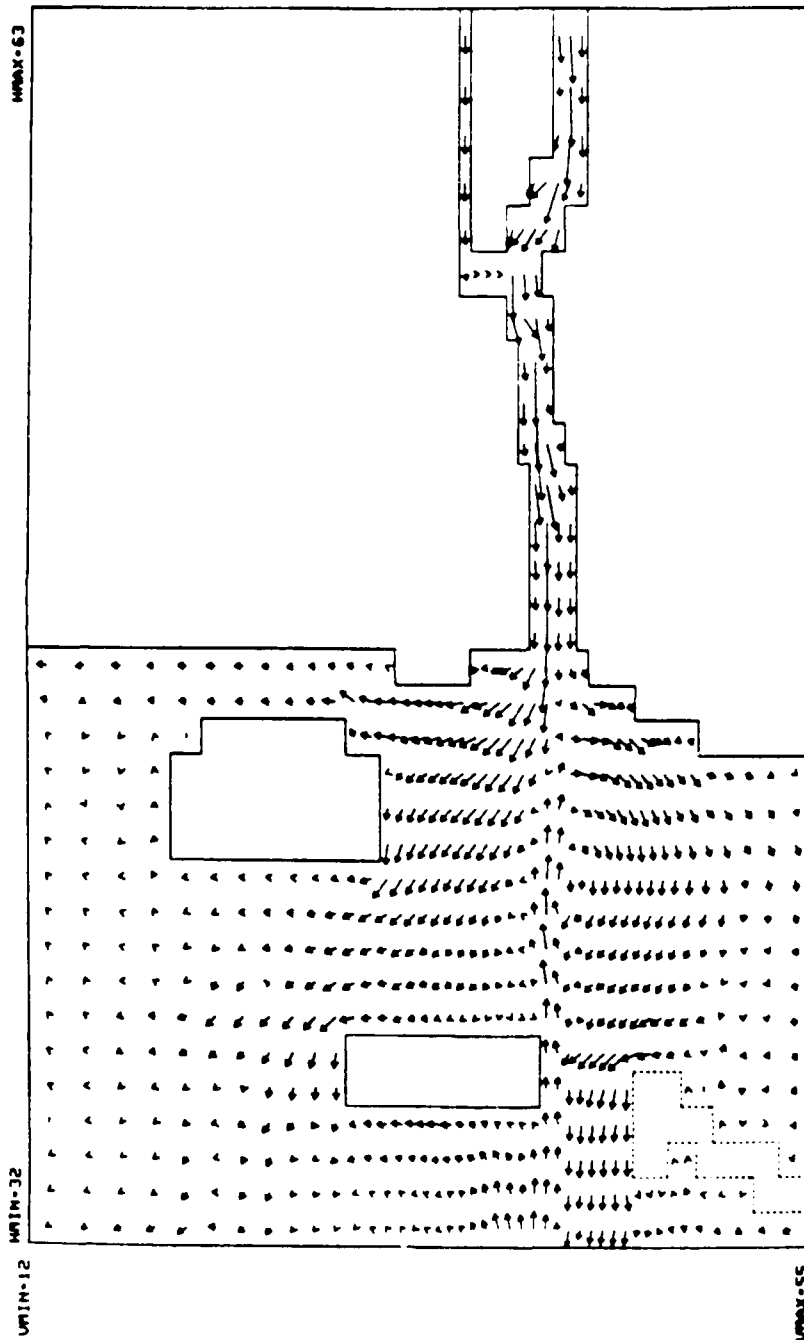






LOWER GREEN BAY NUMERICAL MODEL STUDY





LOWER GREEN BAY NUMERICAL MODEL STUDY

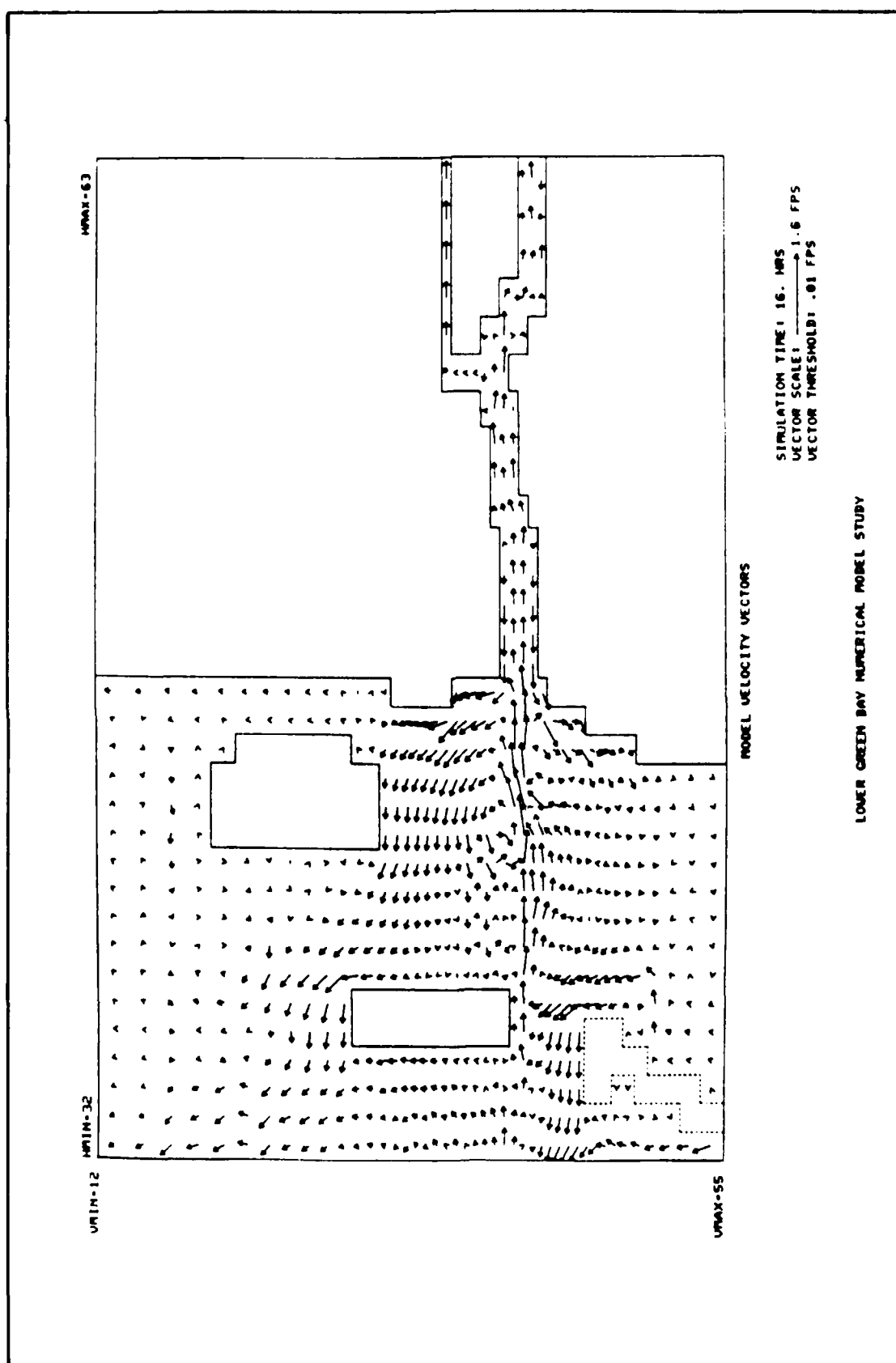
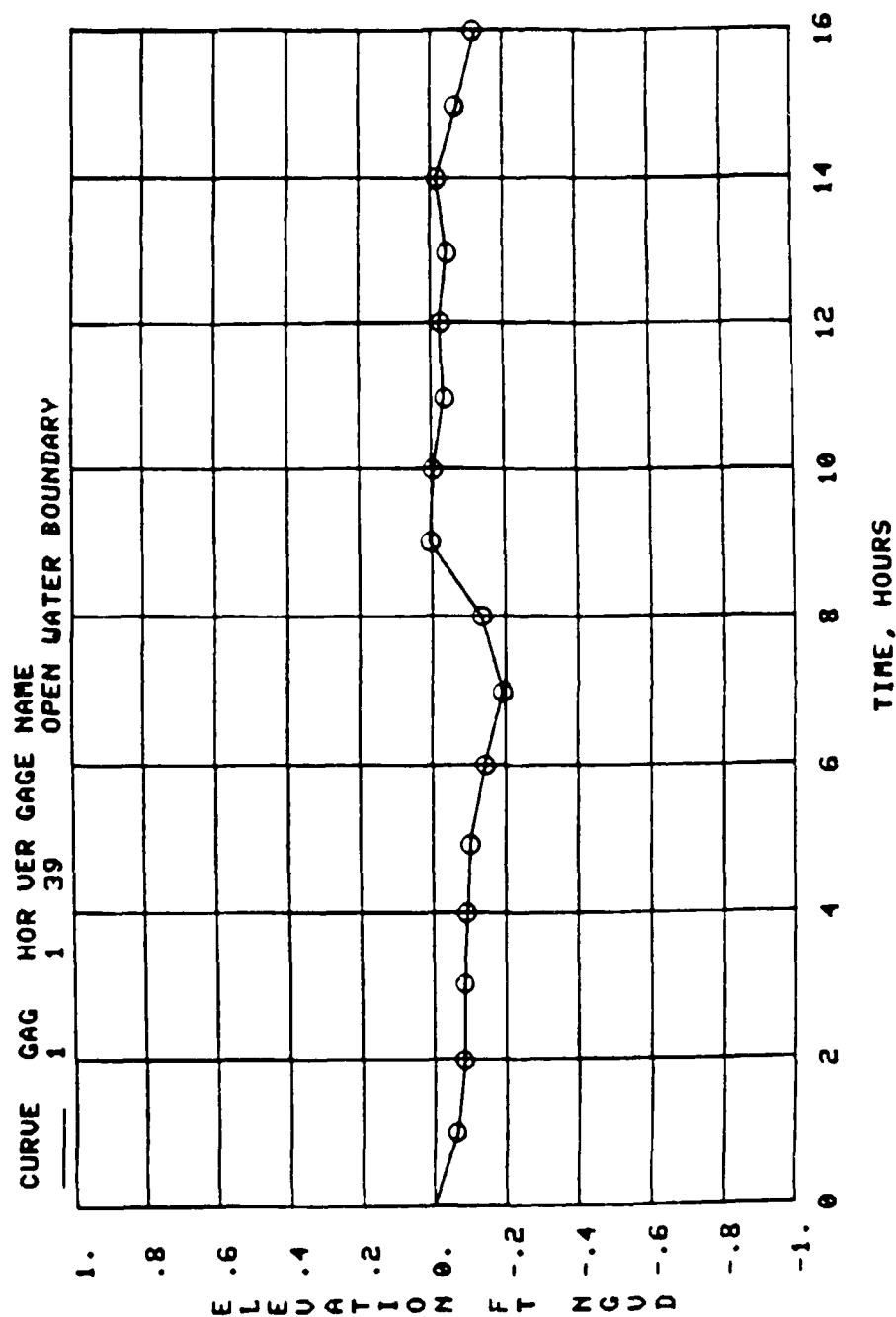
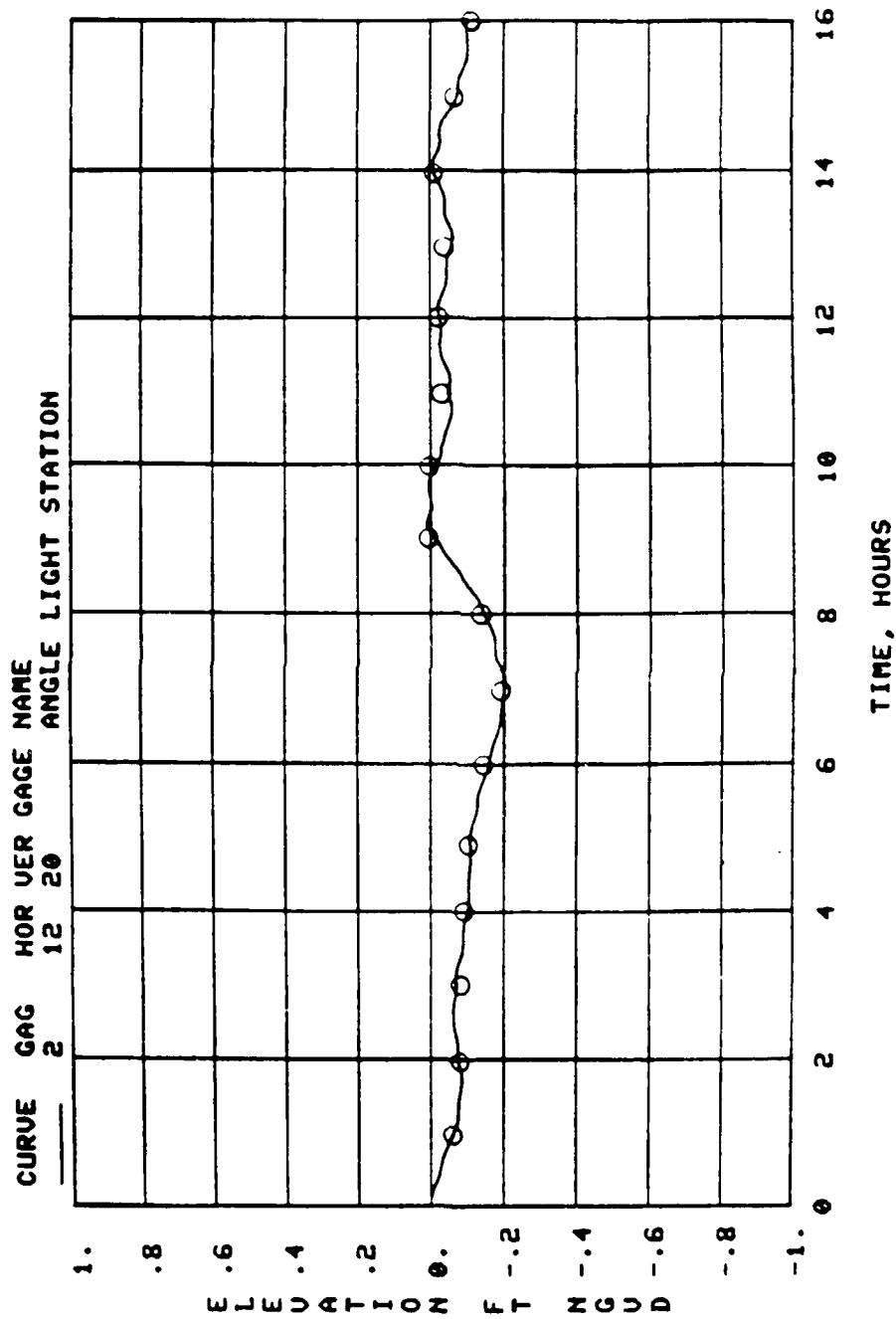


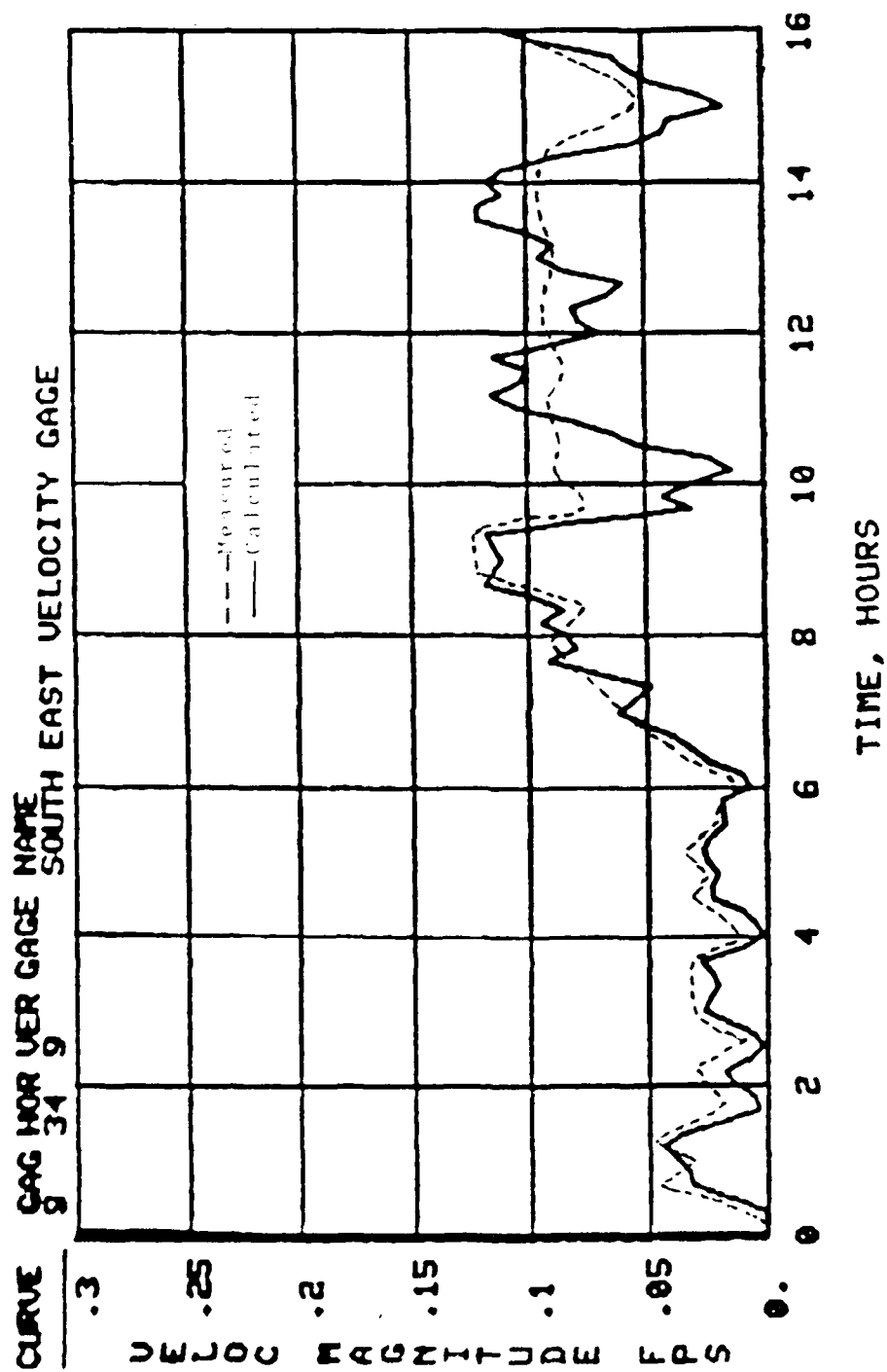
PLATE 8

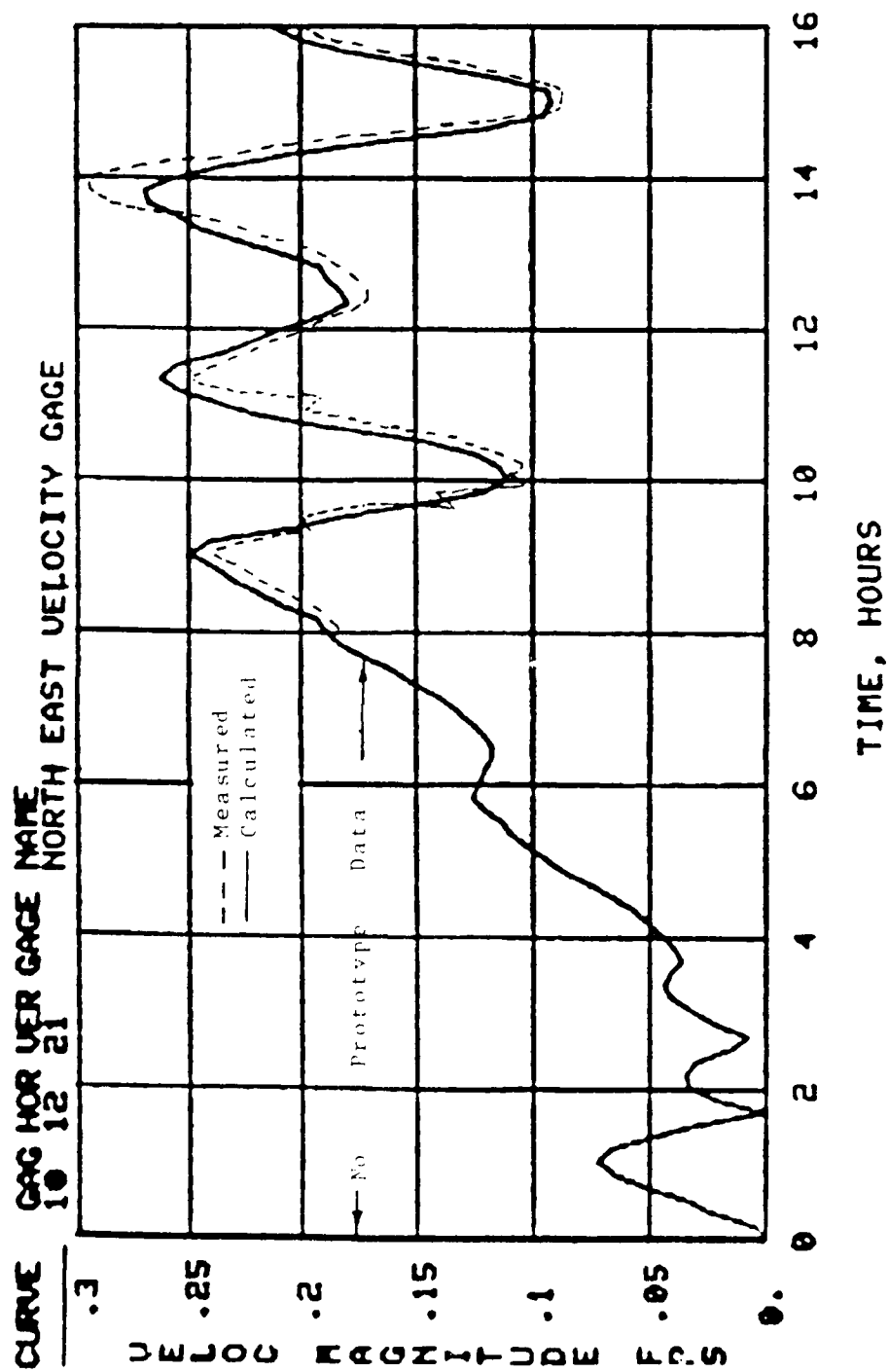


LOWER GREEN BAY NUMERICAL MODEL STUDY

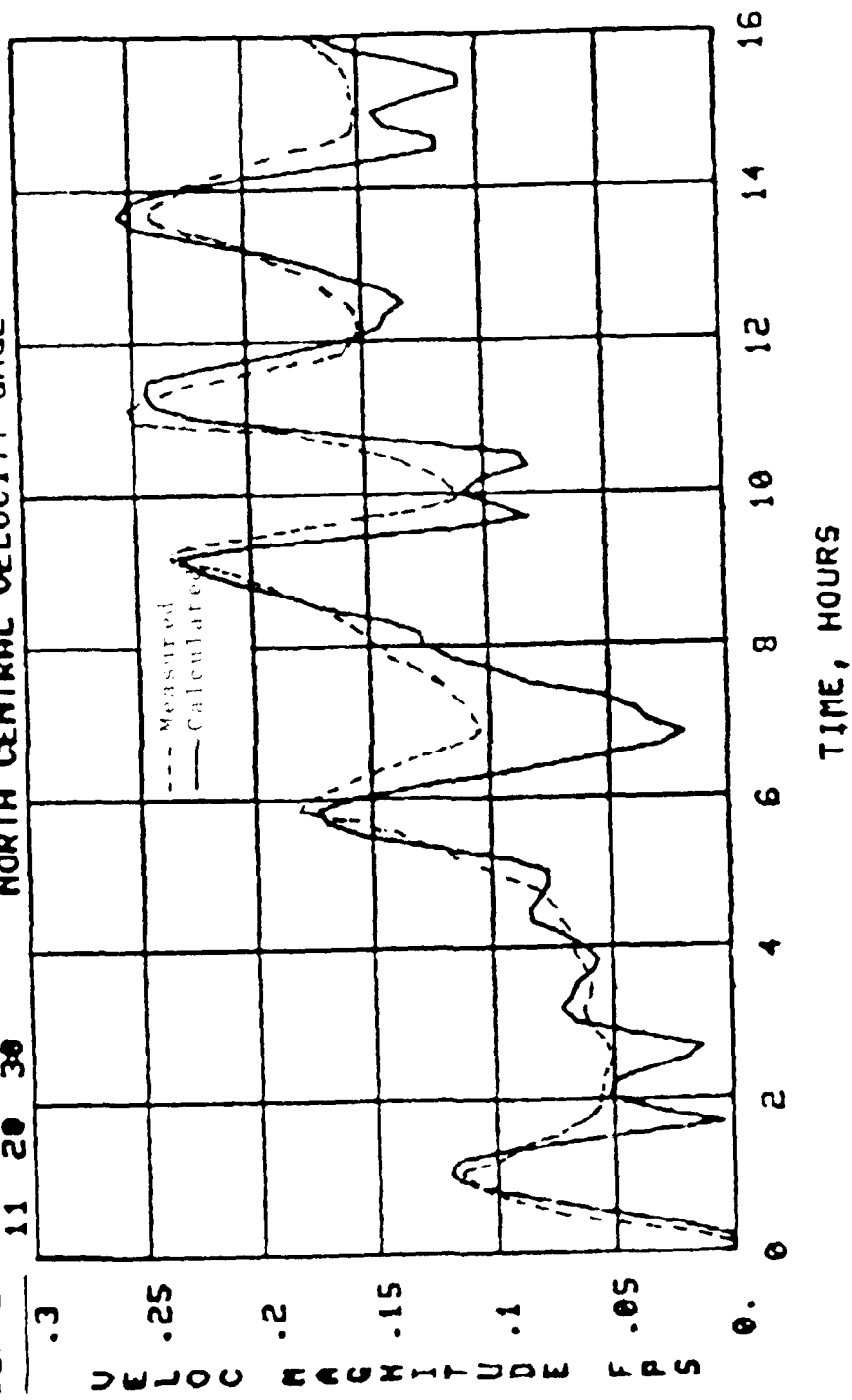


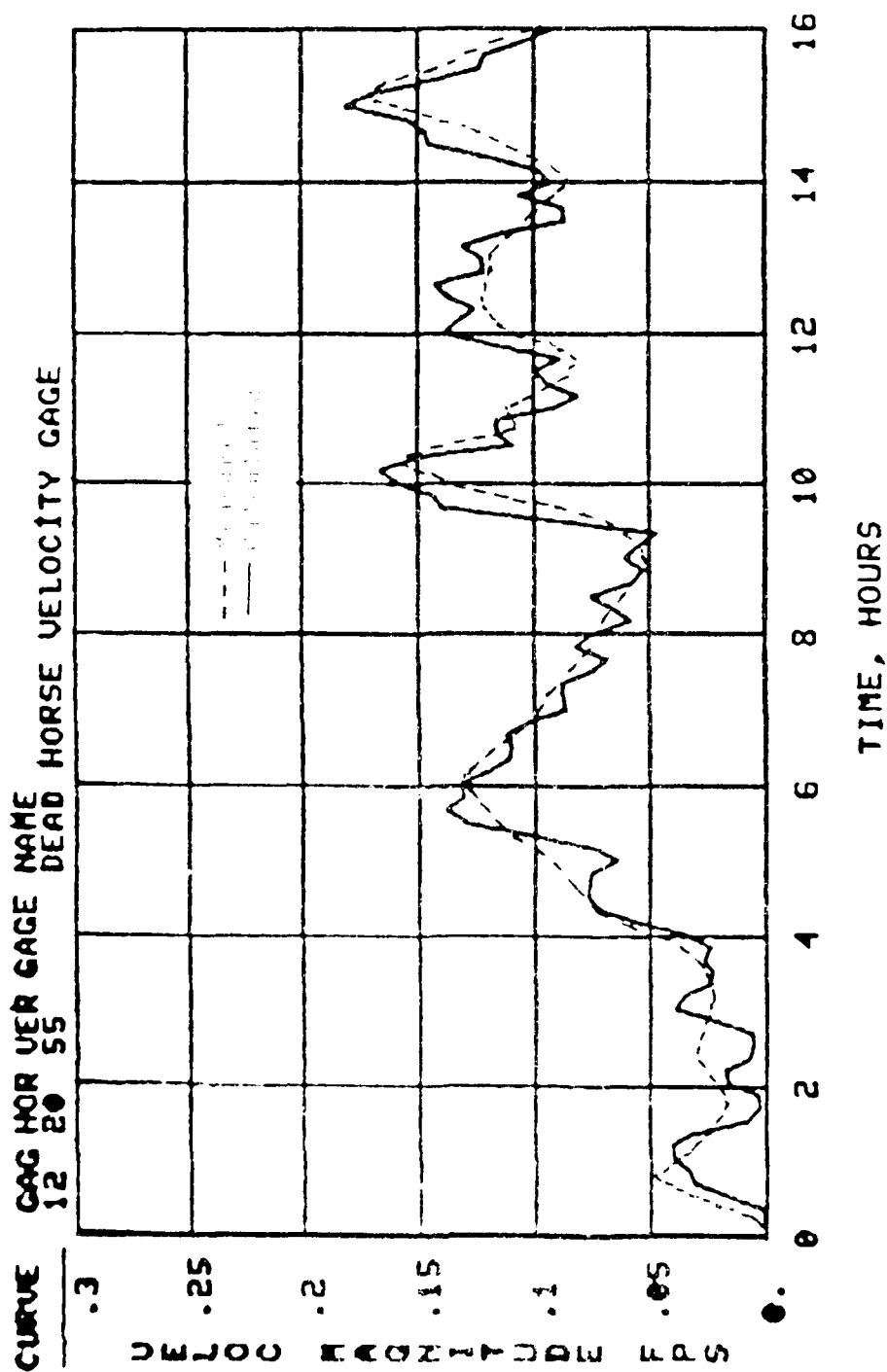
LOWER GREEN BAY NUMERICAL MODEL STUDY



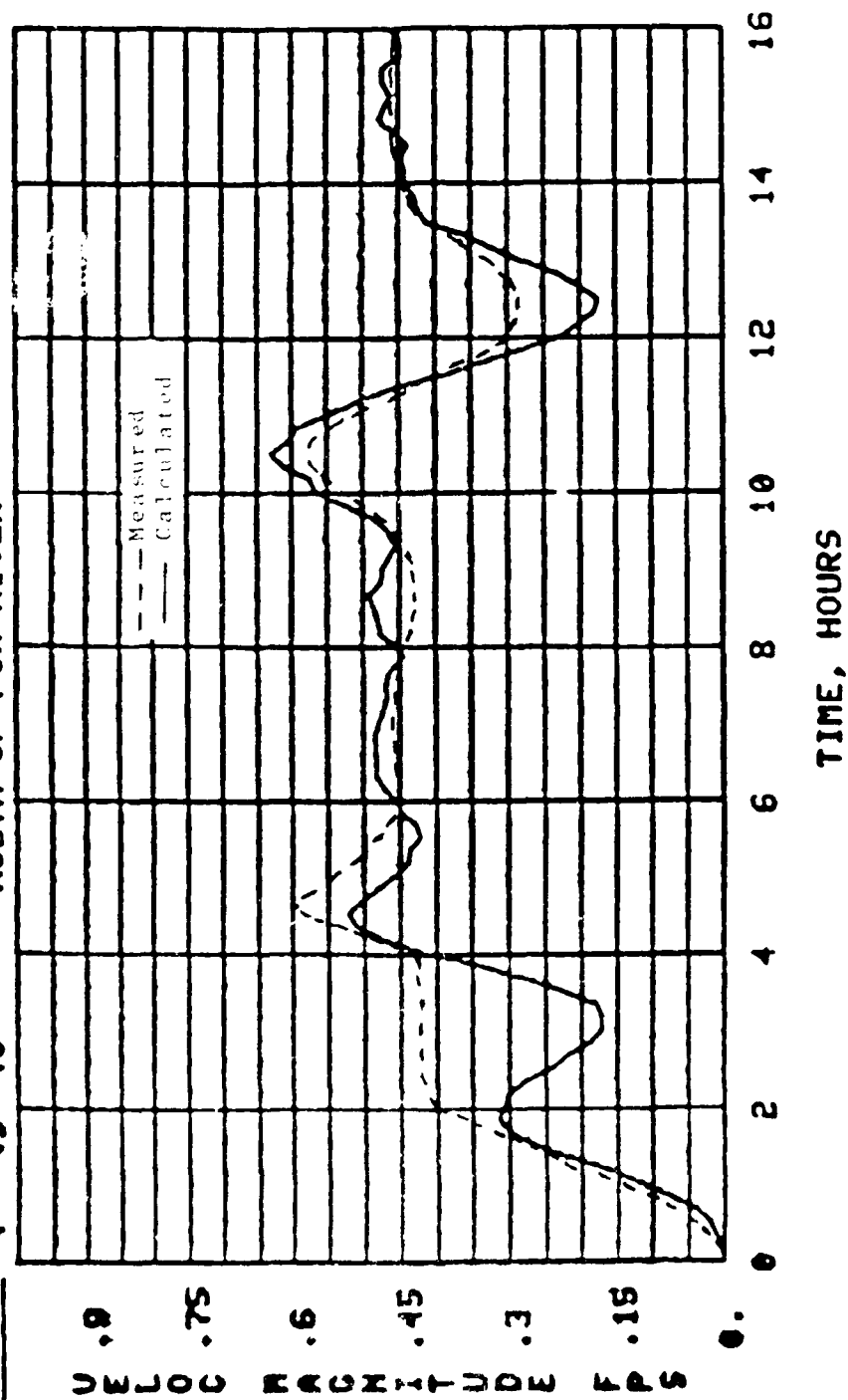


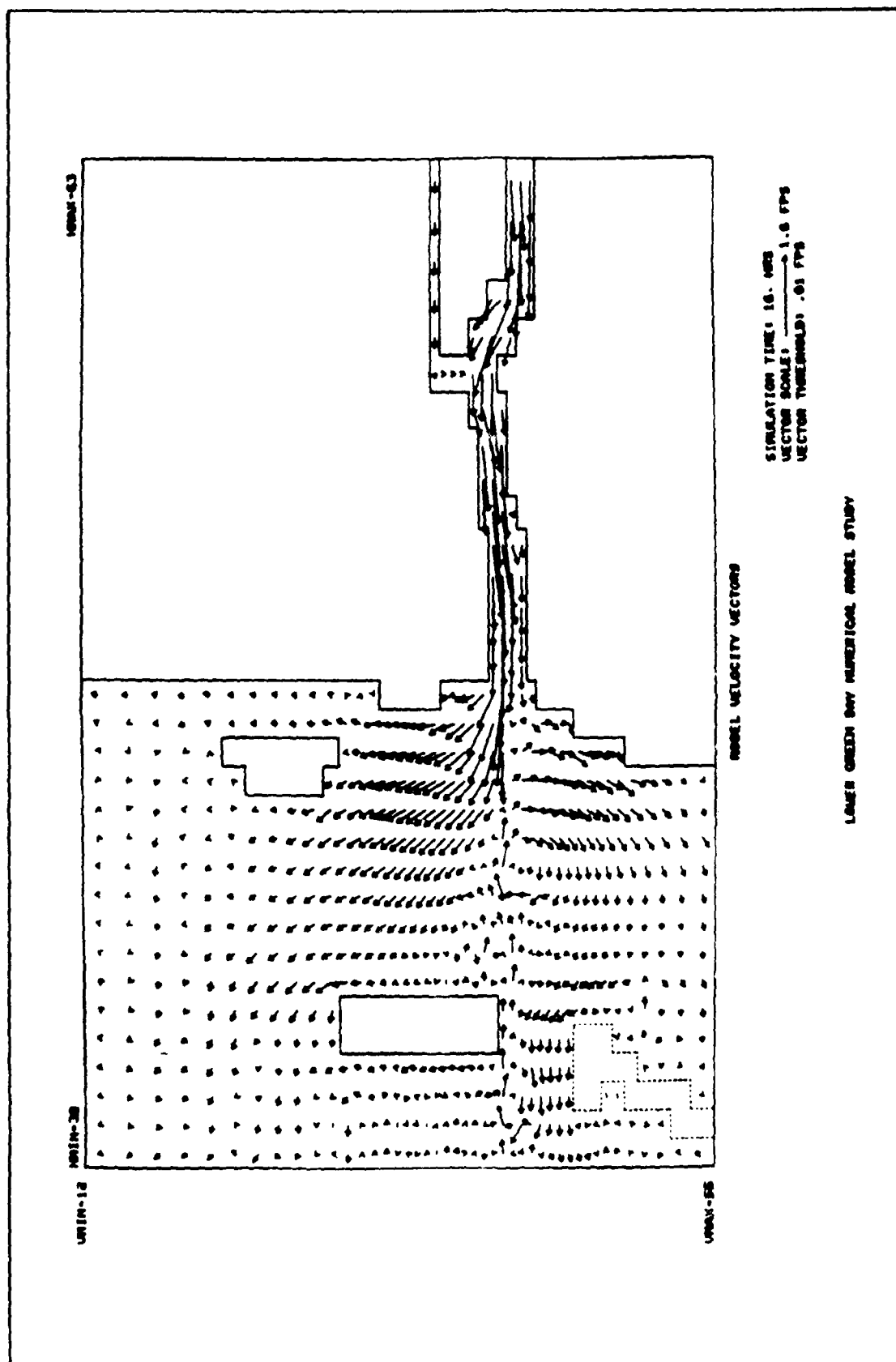
CURVE 11 20 30 GAG HOR VER GAGE NAME NORTH CENTRAL VELOCITY GAGE





CURVE 4 49 40 GAGE HOR UER GAGE NAME MOUTH OF FOX RIVER





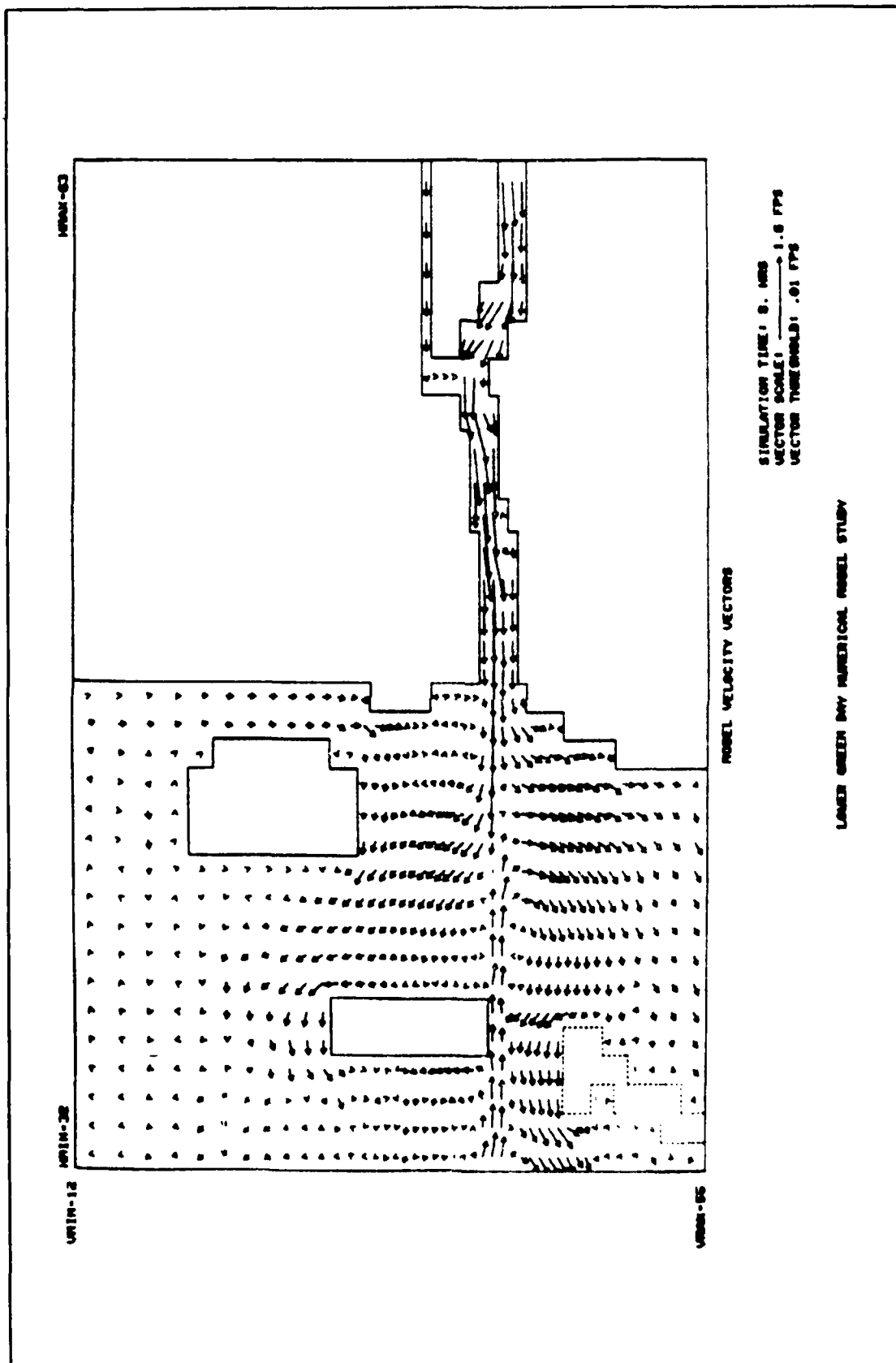
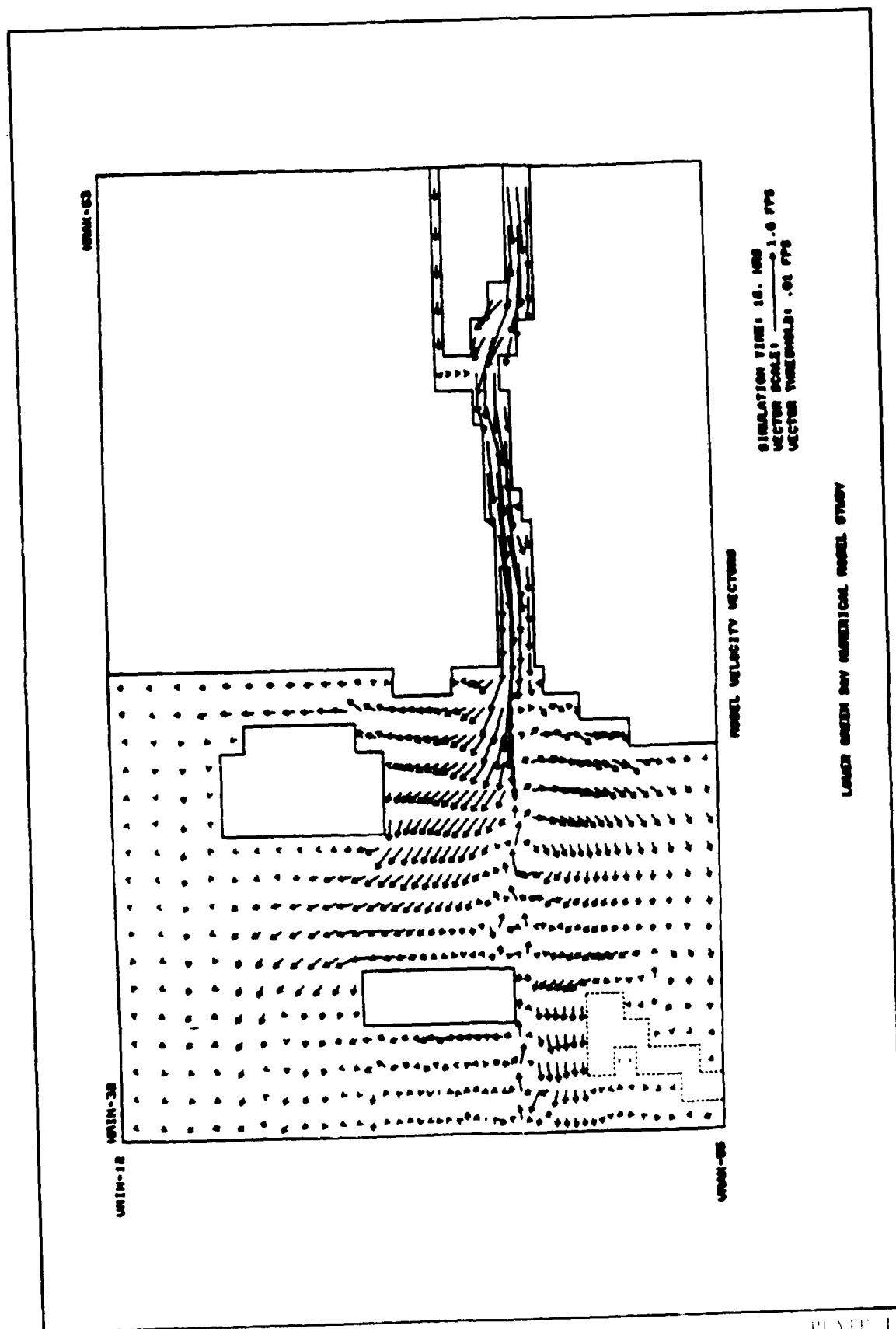
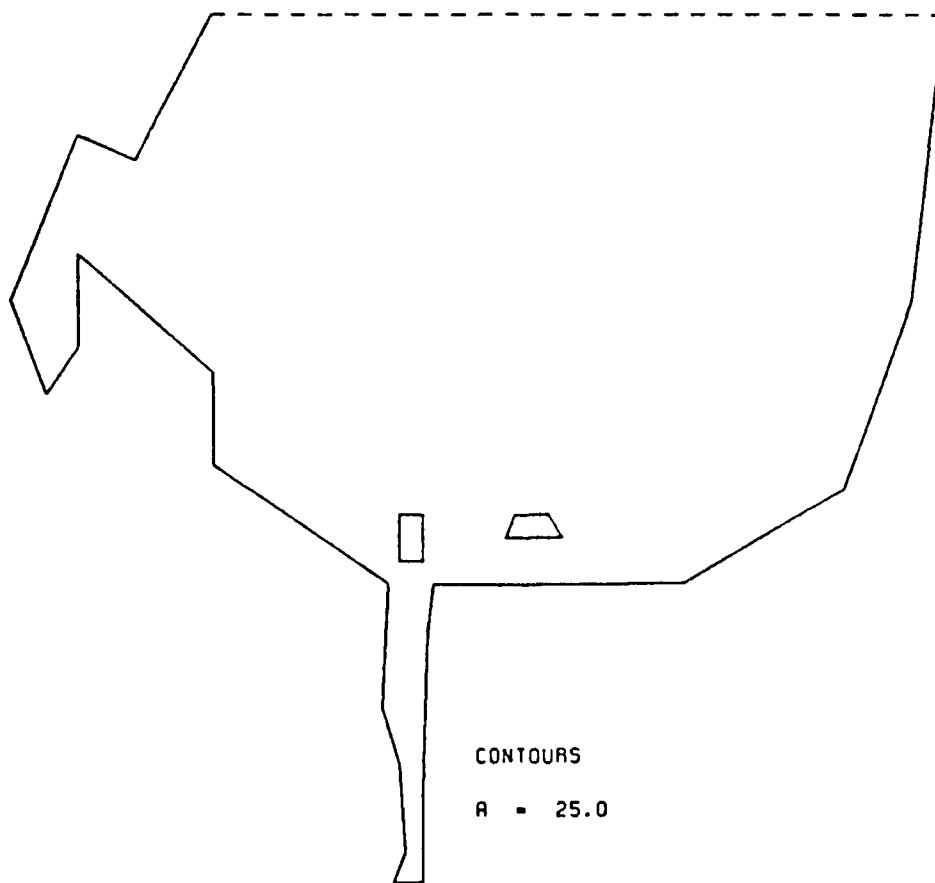


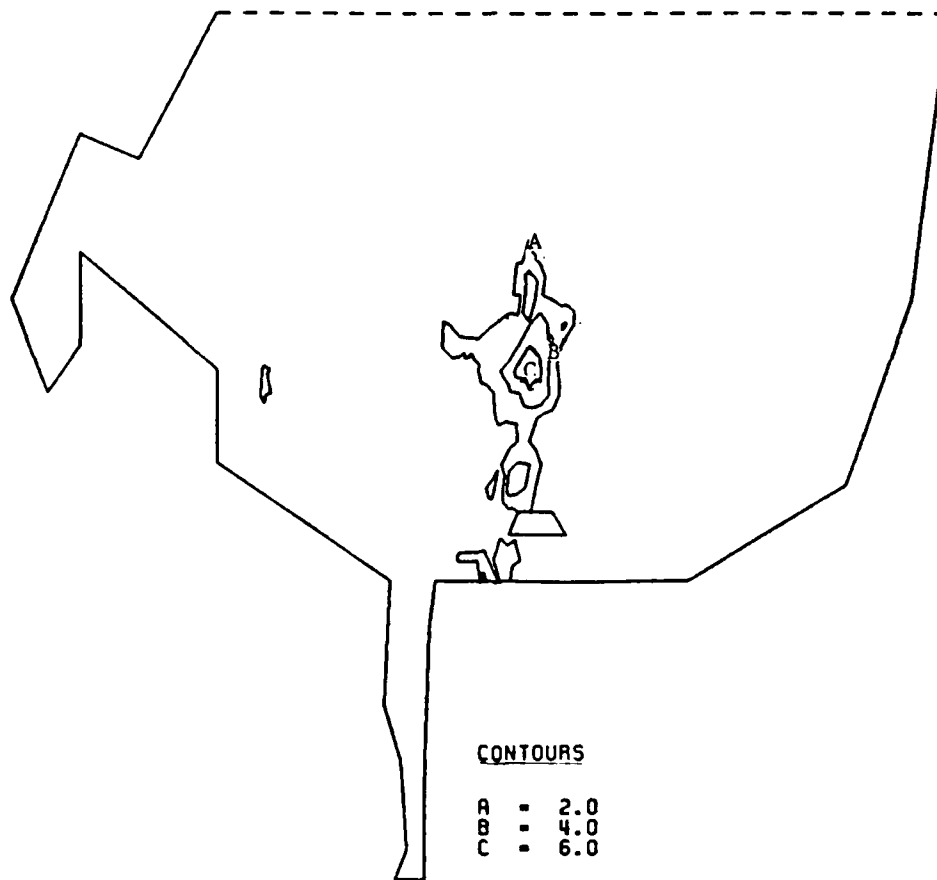
PLATE 18



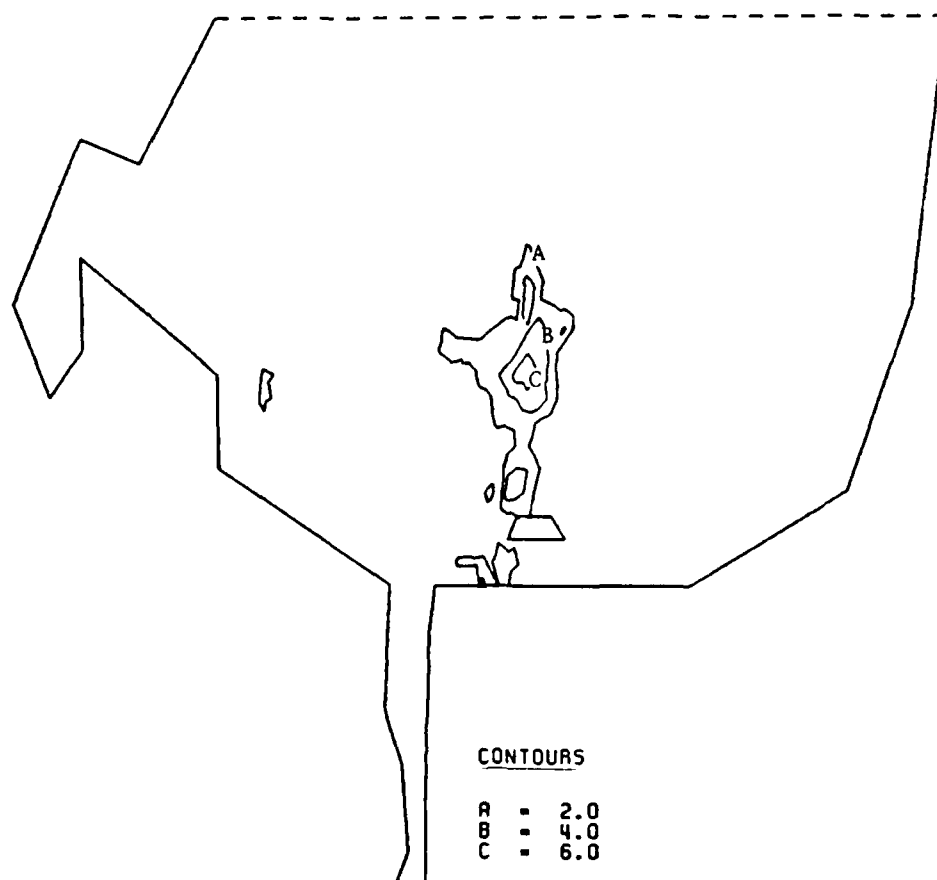
LOW FLOW, EXISTING CDF, KD=6.
INITIAL



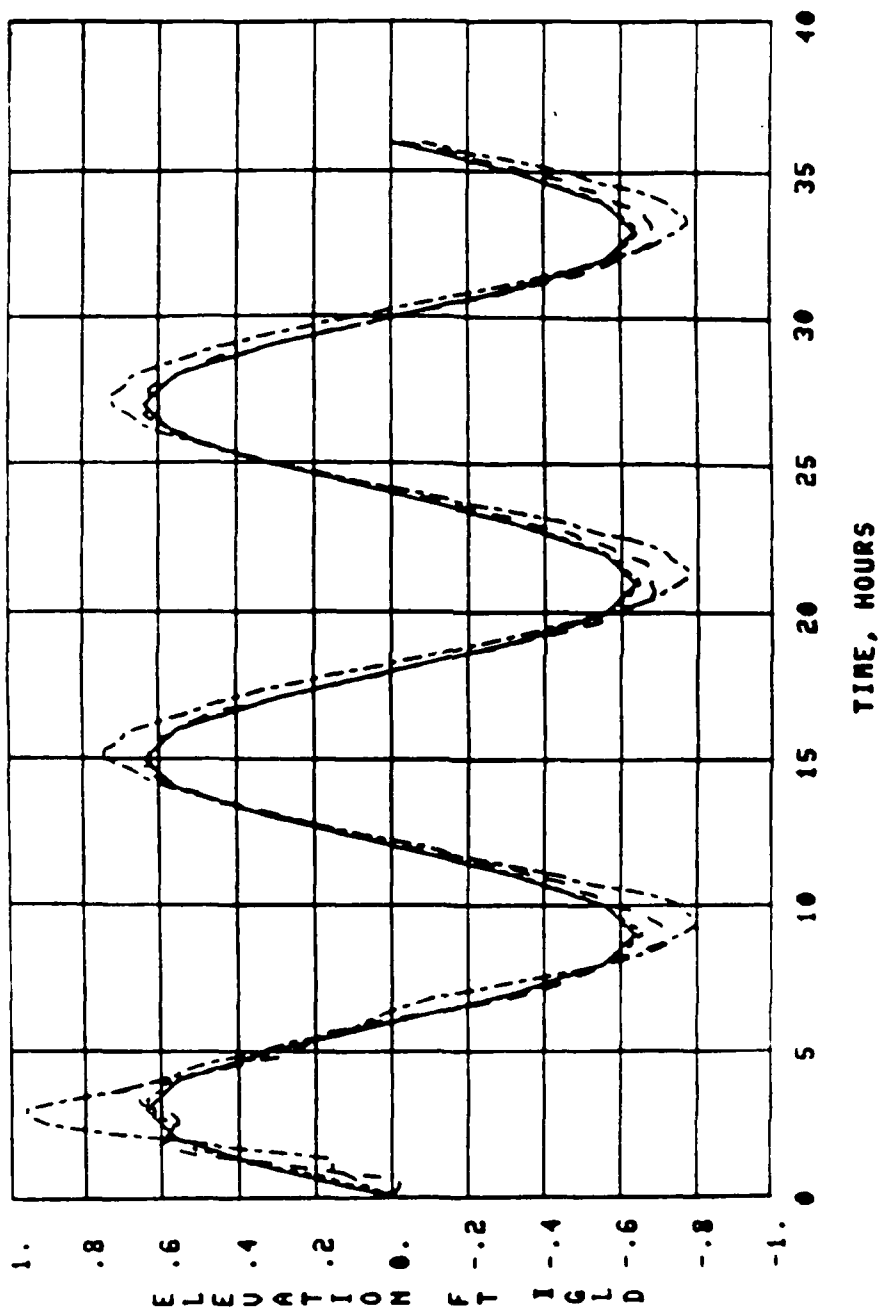
LOW FLOW, EXISTING CDF, KD=1.
TIME = 24 HR, ITIME=1440



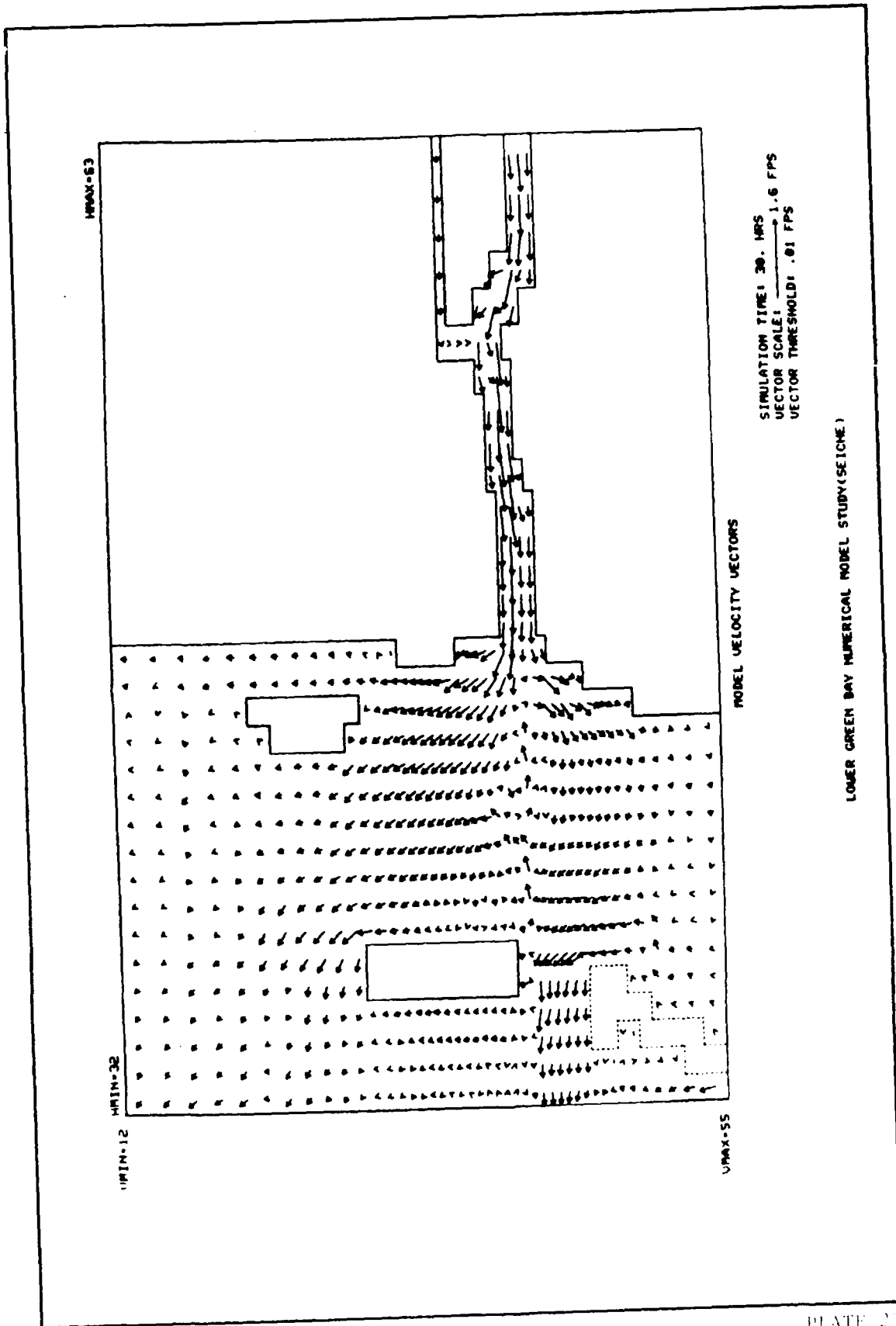
LOW FLOW, EXISTING CDF, KD=10.
TIME = 24 HR, ITIME=1440

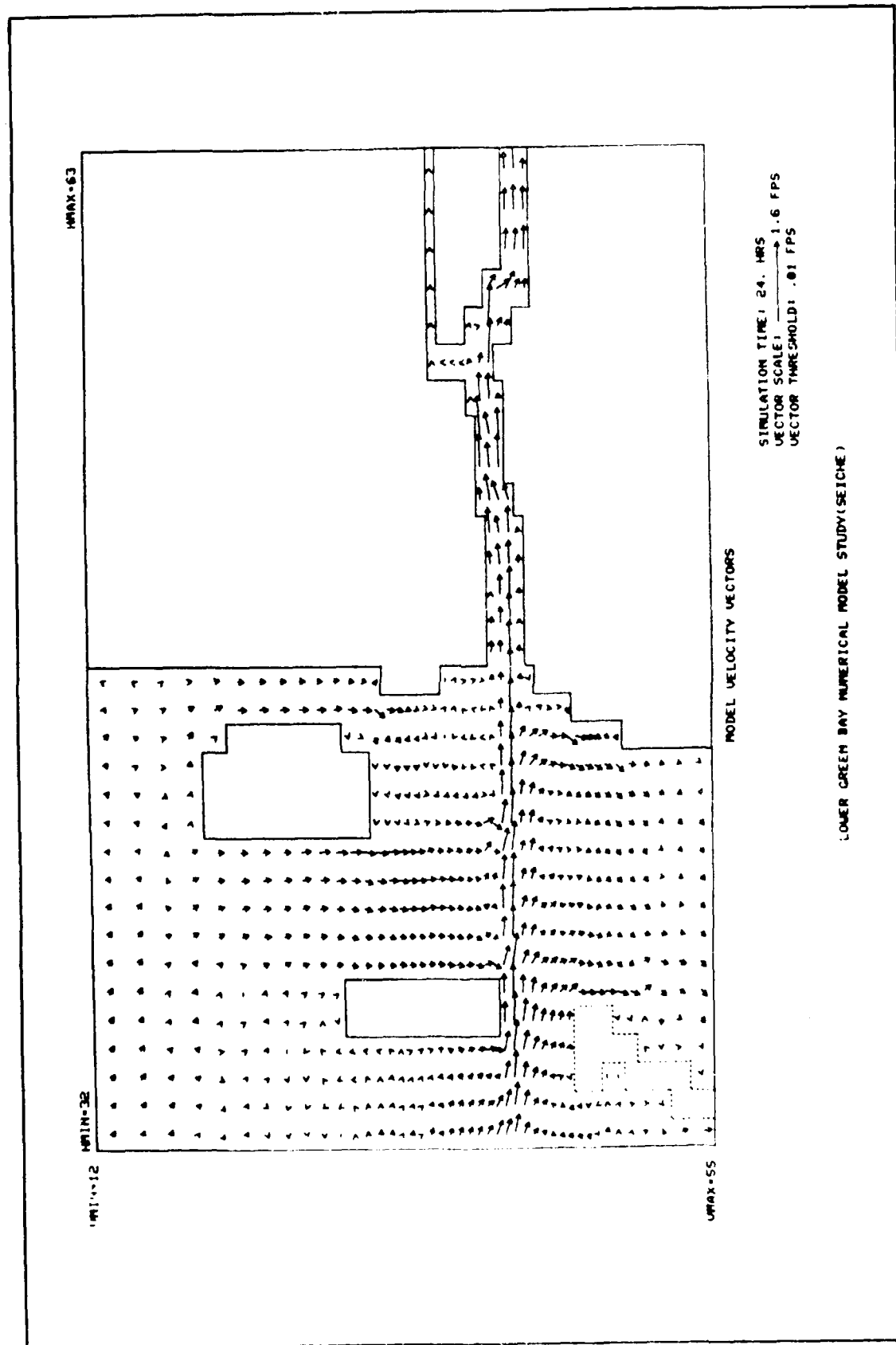


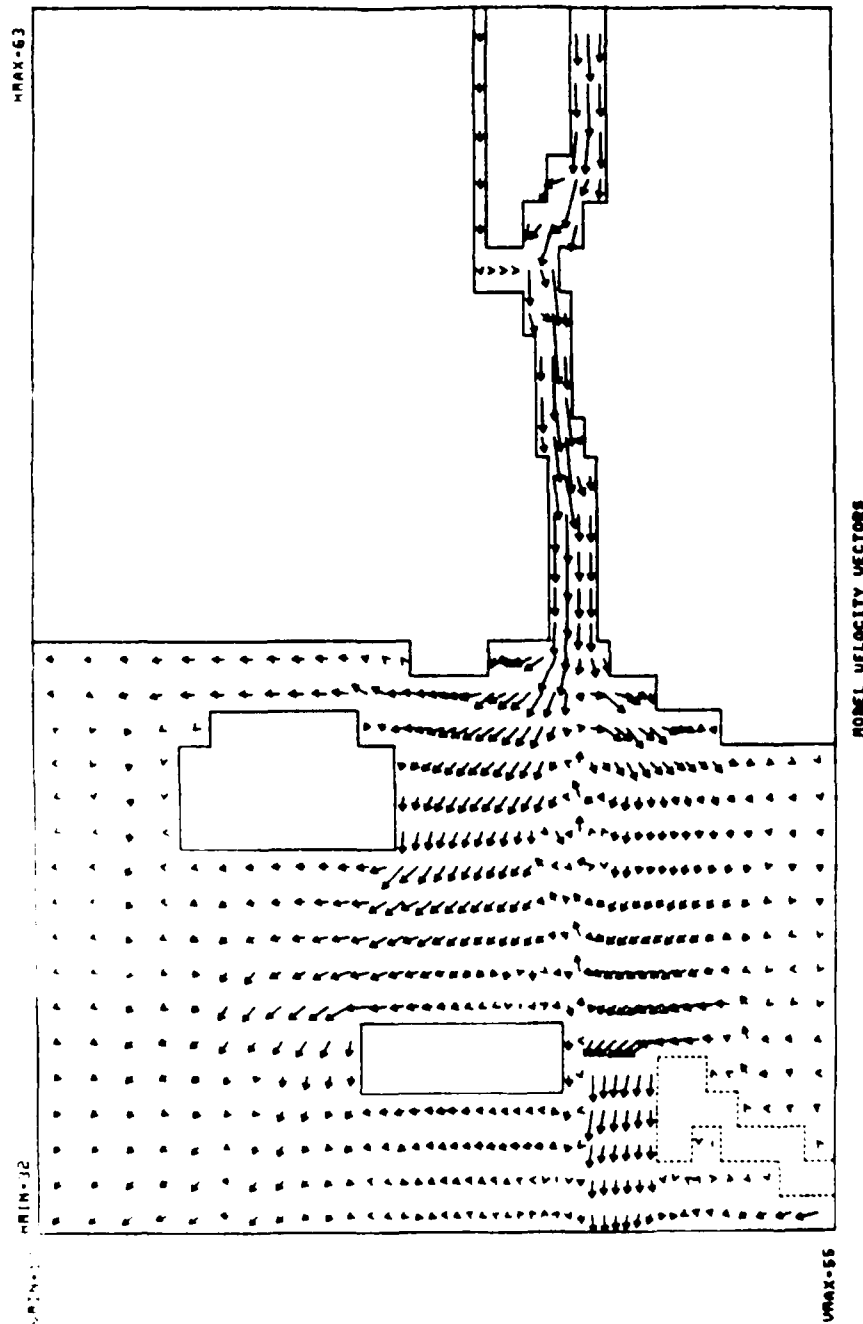
CURVE	GAG	HOR	UER	GAGE	NAME
1	1	39			OPEN WATER BOUNDARY
2	2	12	20		ANGLE LIGHT STATION
3	3	85	56		DE PERE DAM GAGE
4	4	49	40		MOUTH OF FOX RIVER



LOWER GREEN BAY NUMERICAL MODEL STUDY(SEICHE)

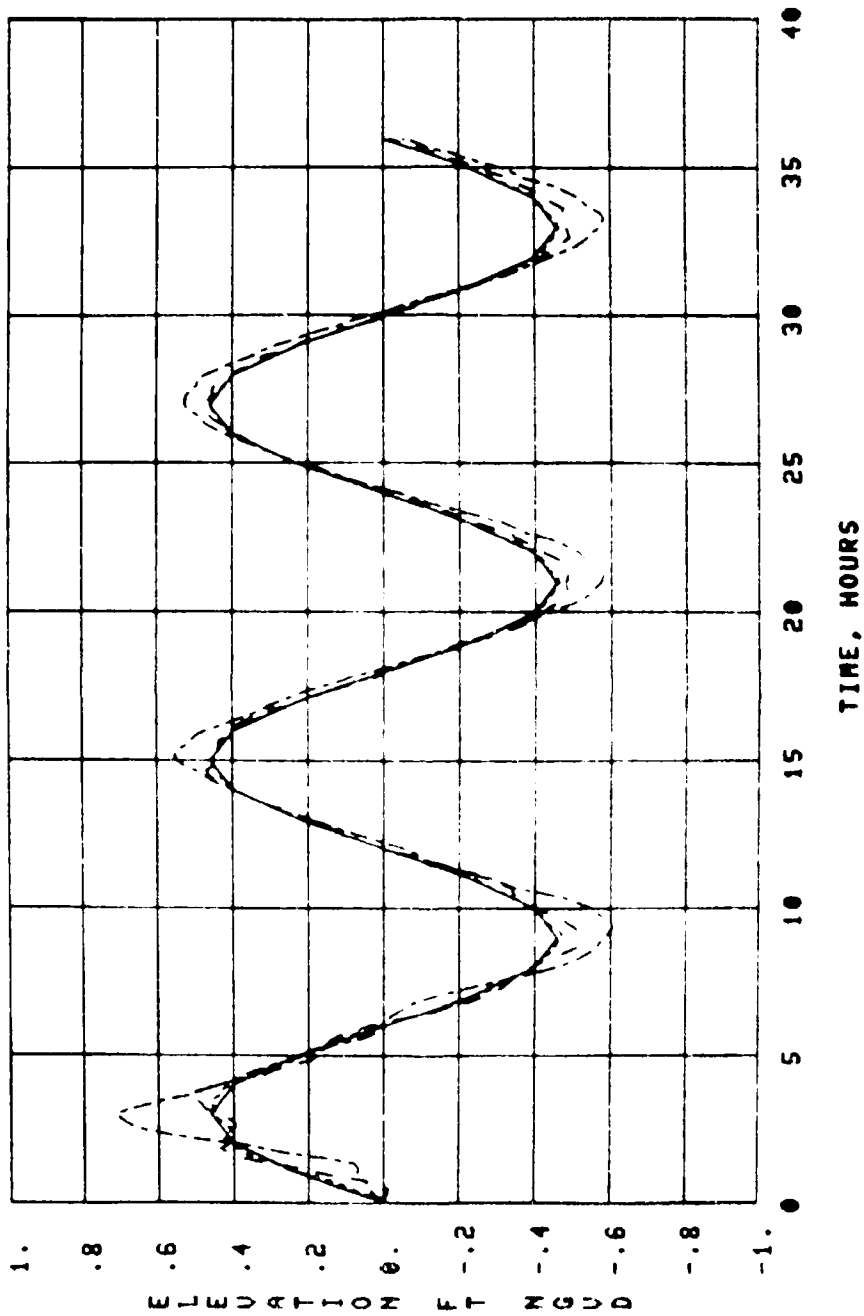




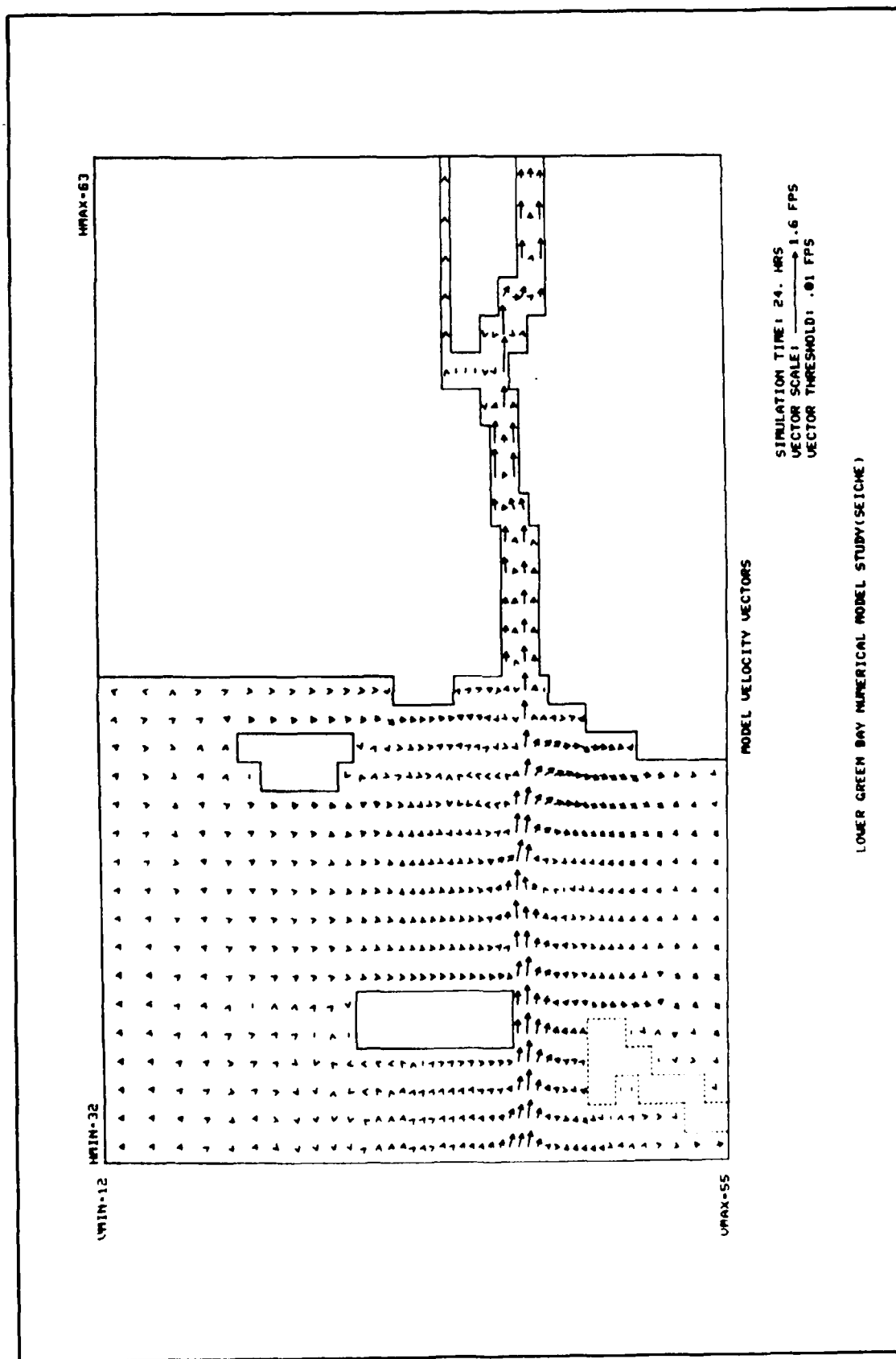


LOWER GREEN BAY NUMERICAL MODEL STUDY (DEICKE)

CURVE	GAG	HOR	VER	GAGE	NAME	OPEN	WATER	BOUNDARY
---	1	1	39			ANGLE	LIGHT	STATION
---	2	12	20			DE PERE	DAM	GAGE
---	3	85	56			MOUTH	OF	FOX RIVER
---	4	49	40					



LOWER GREEN BAY NUMERICAL MODEL STUDY (SEICHE)



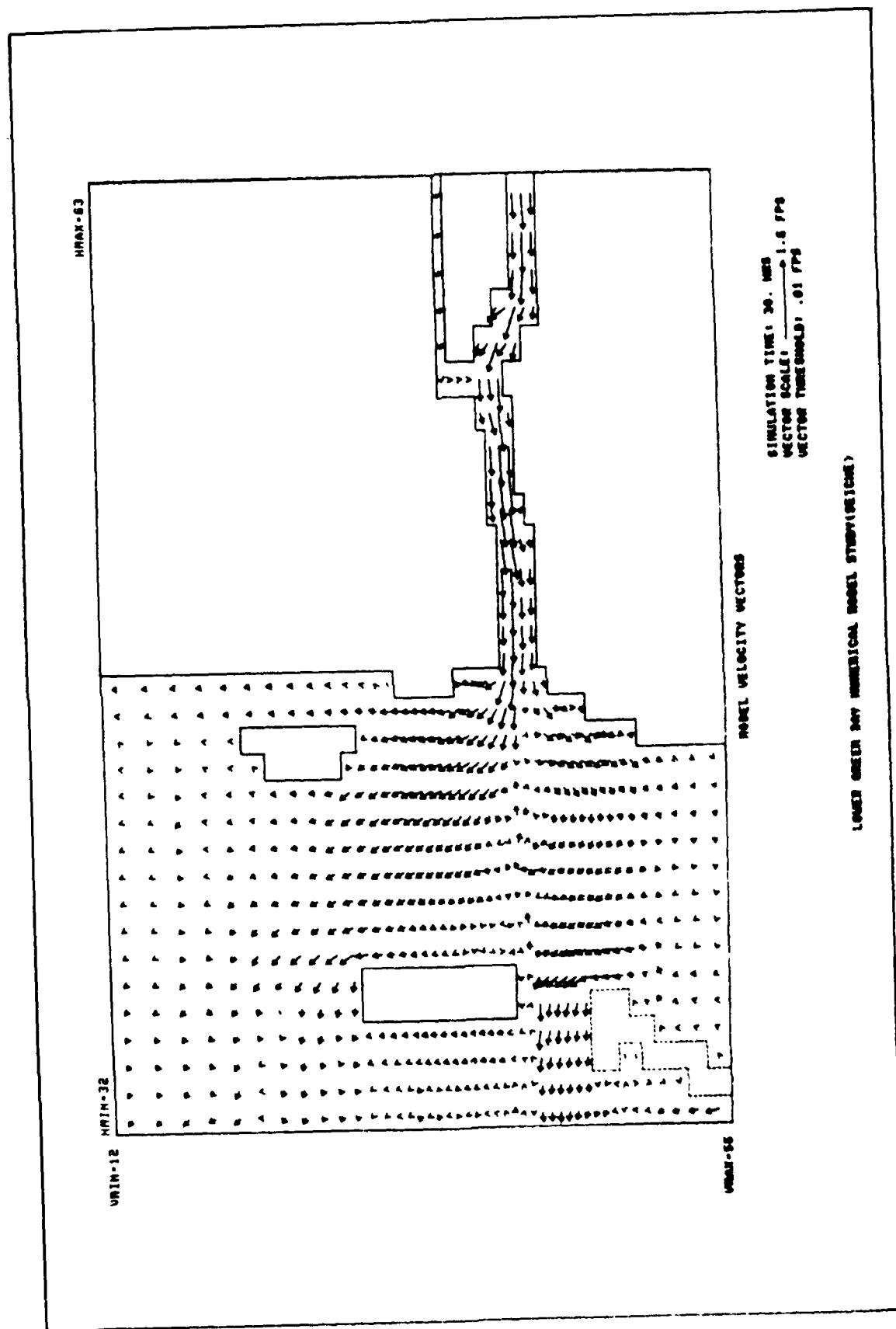
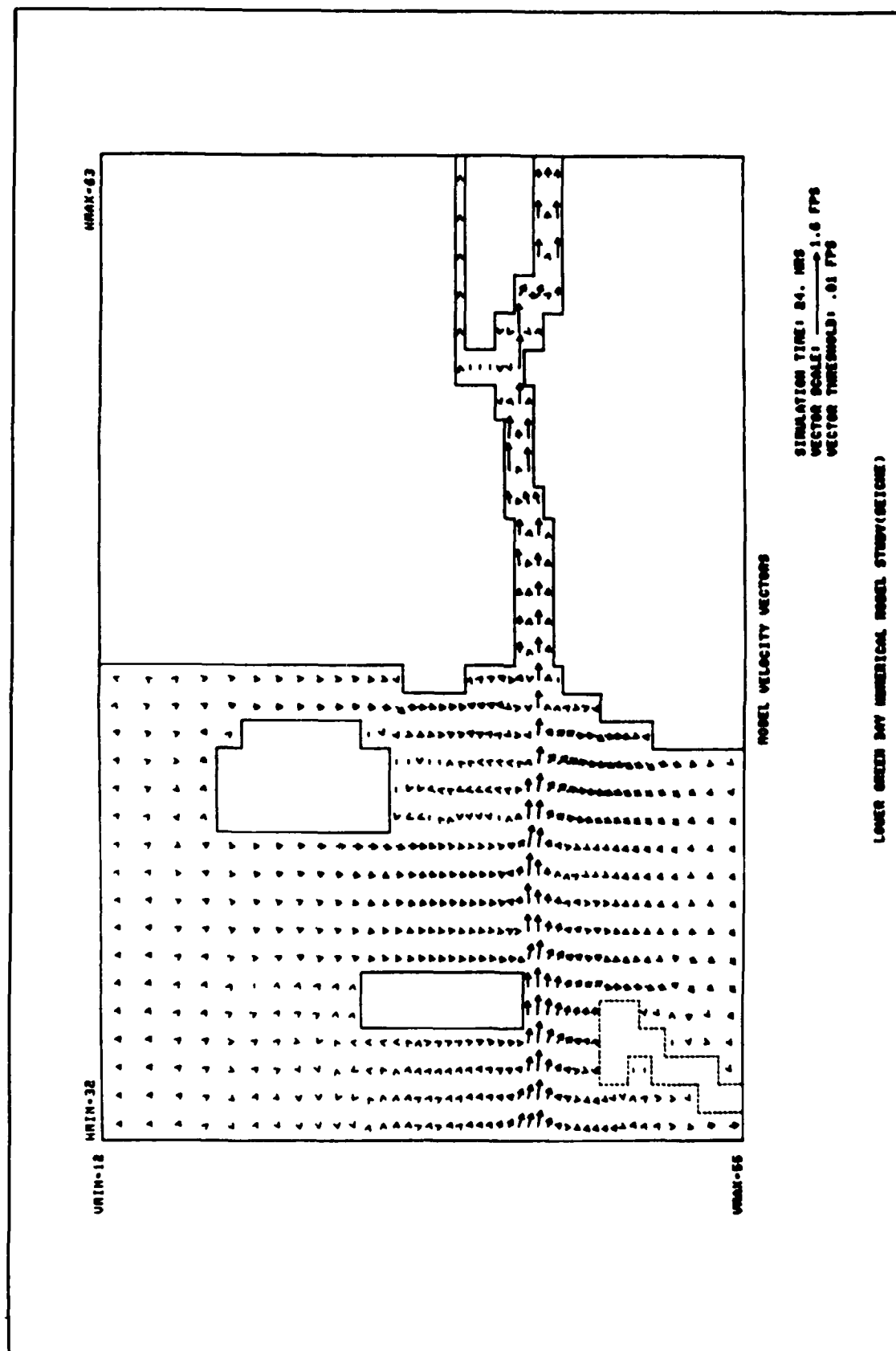


PLATE 30



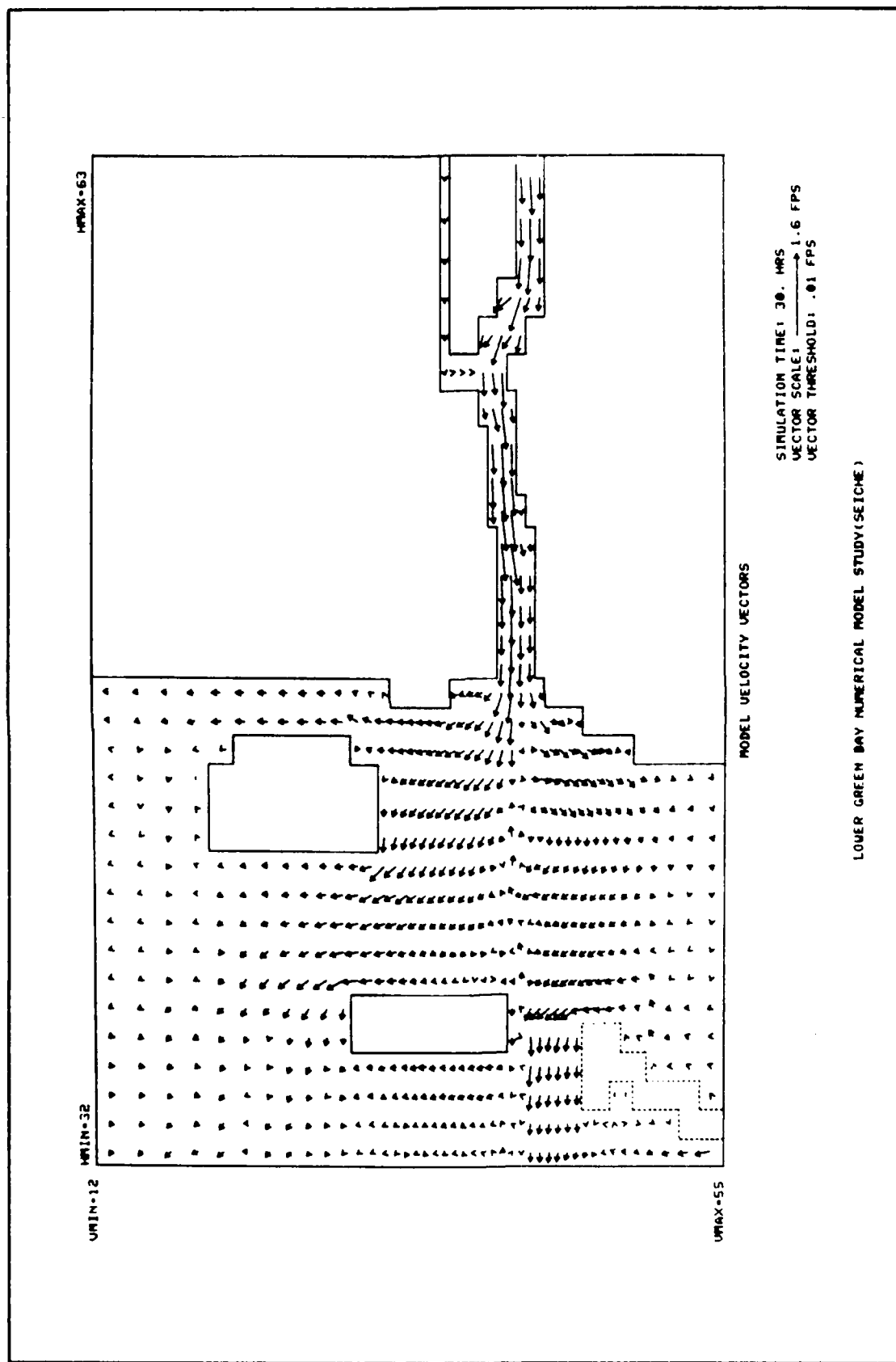
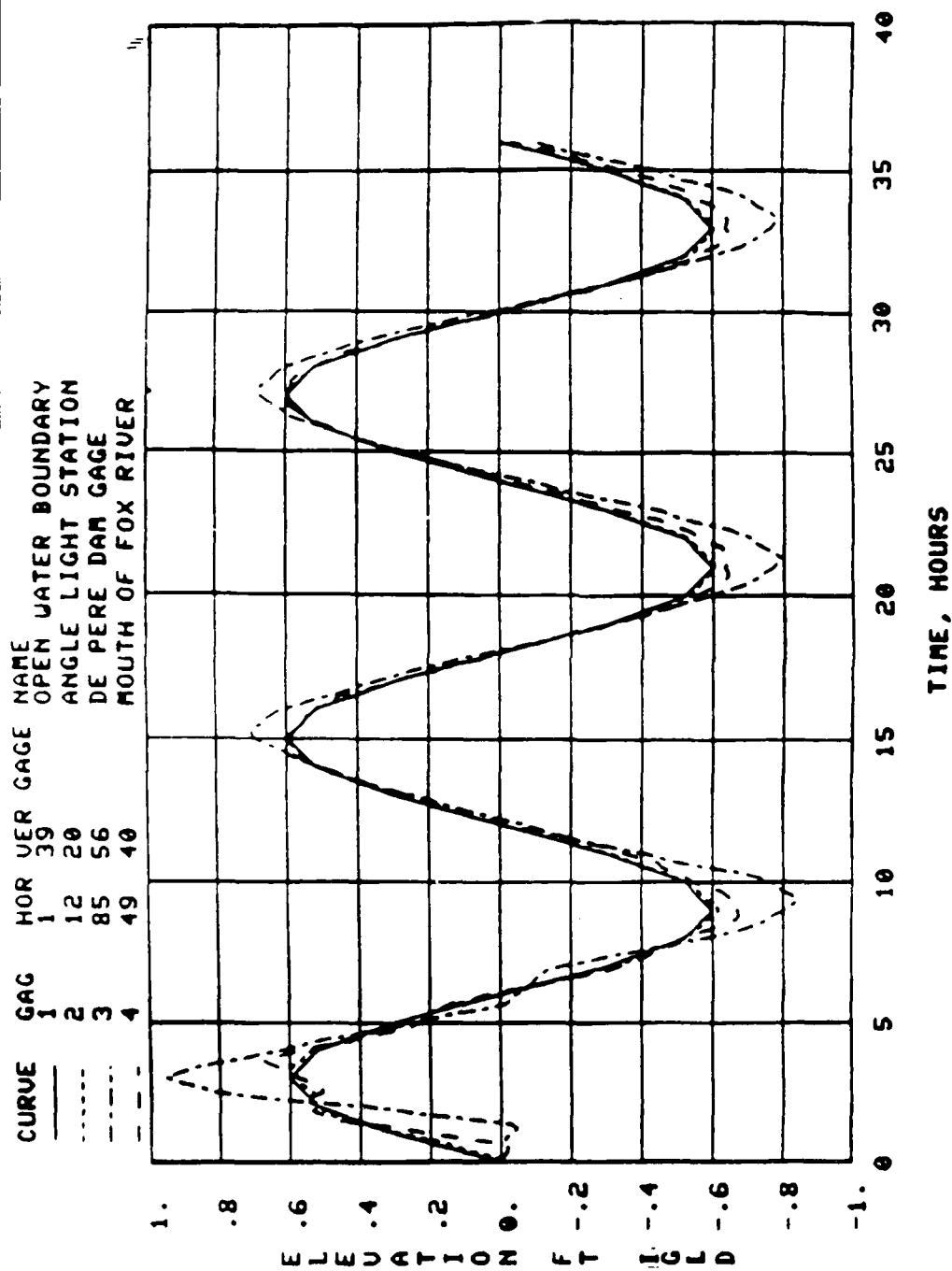
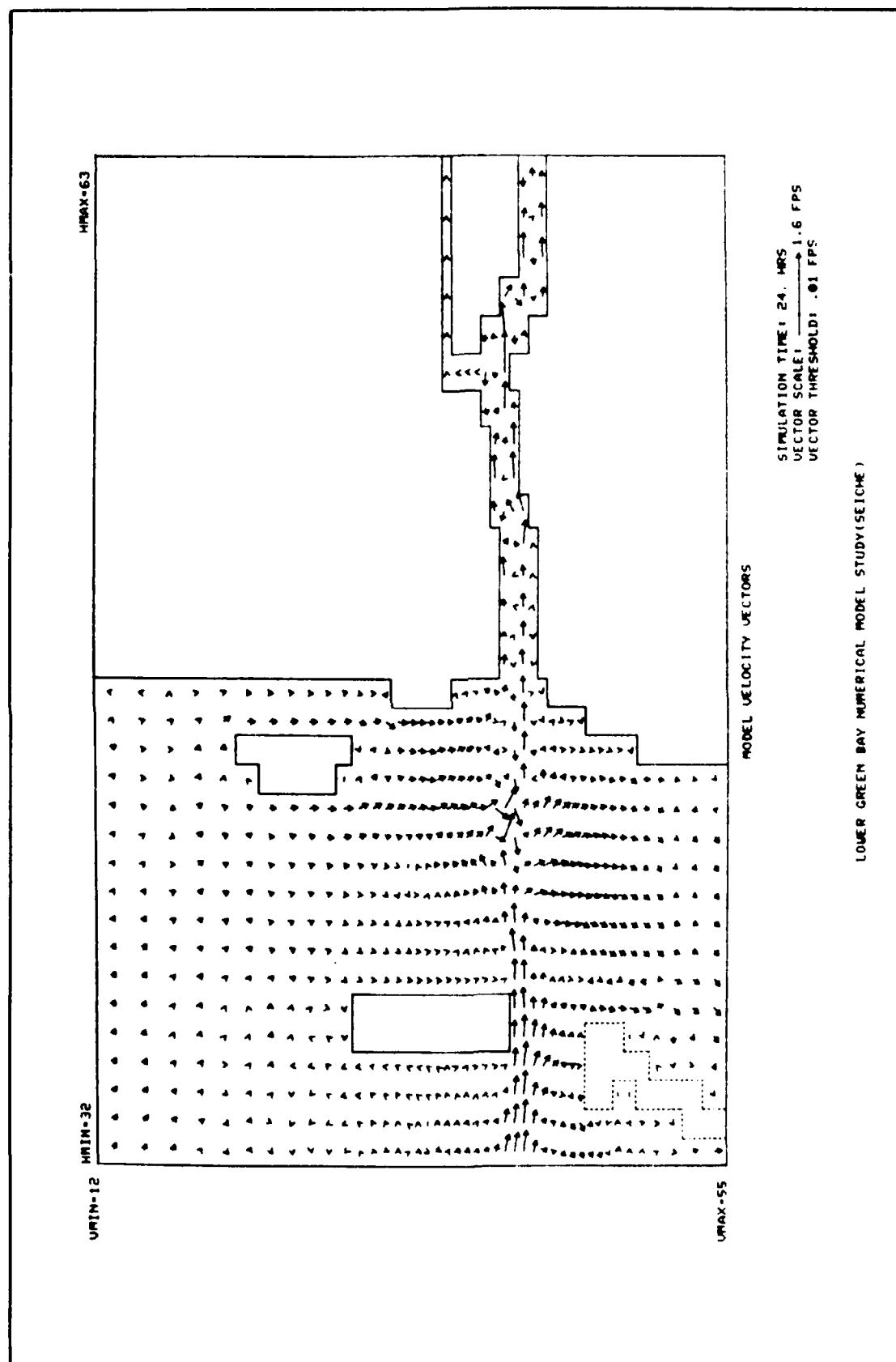
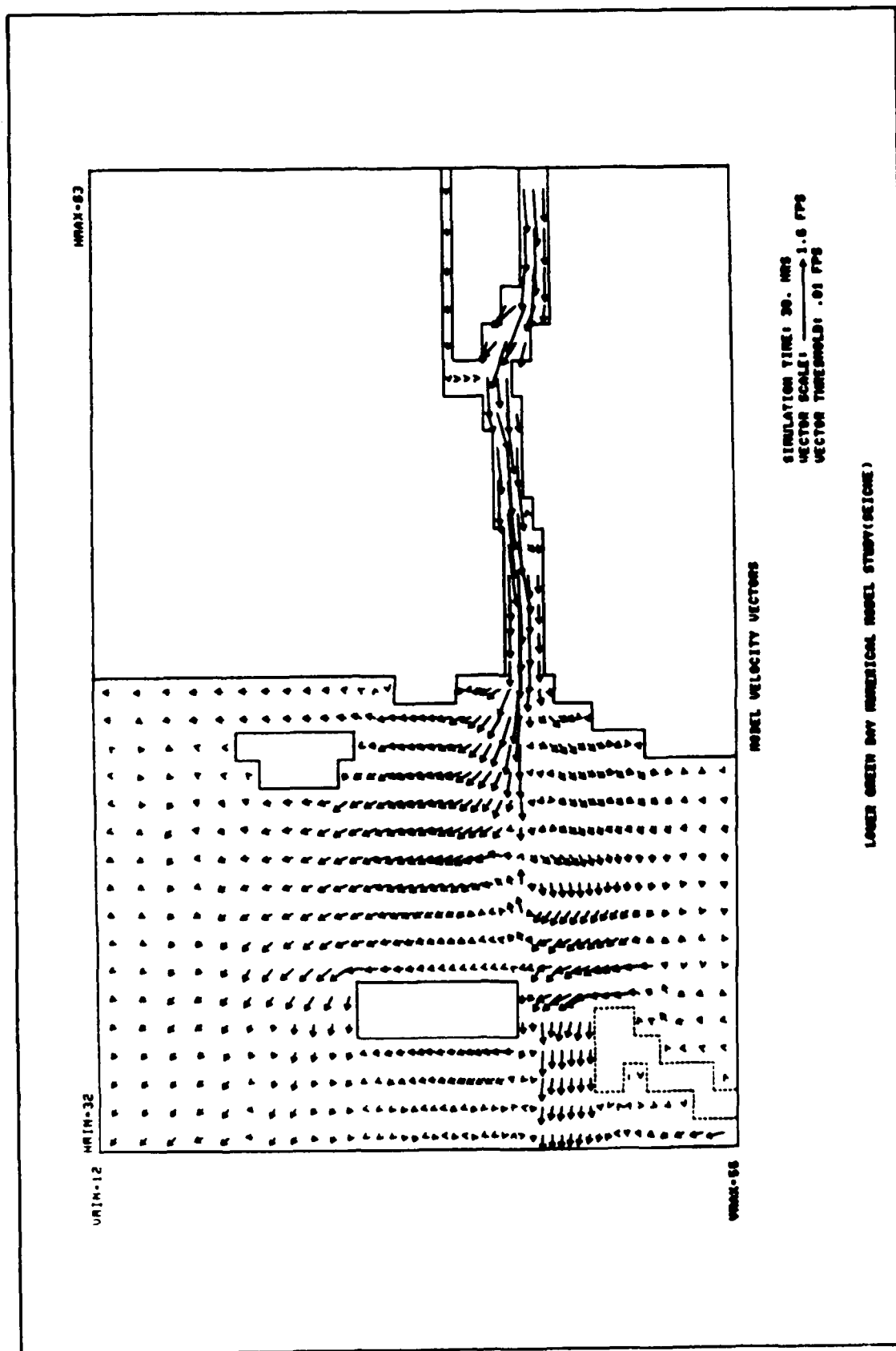


PLATE 32



LOWER GREEN BAY NUMERICAL MODEL STUDY (SEICHE)





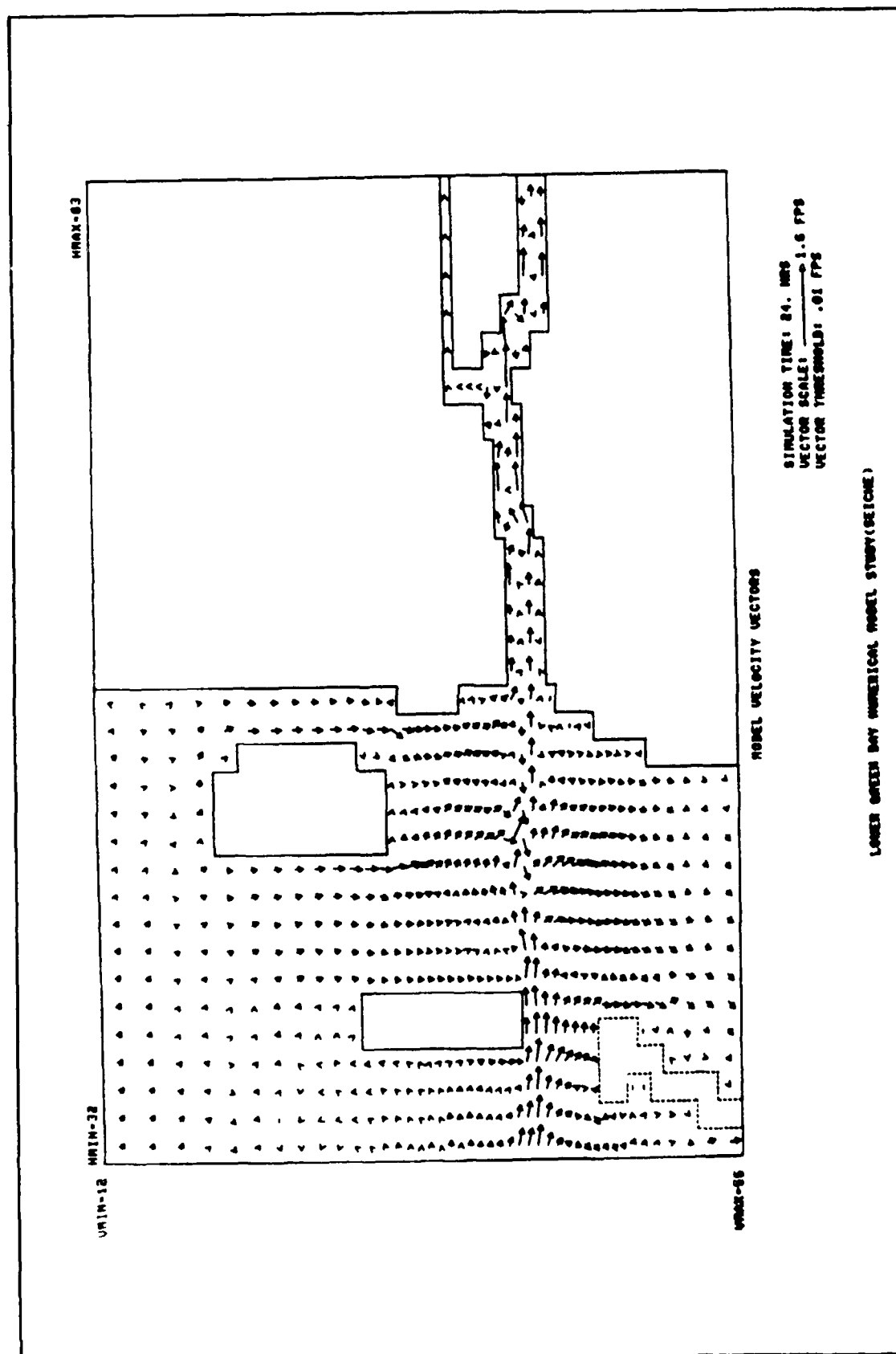
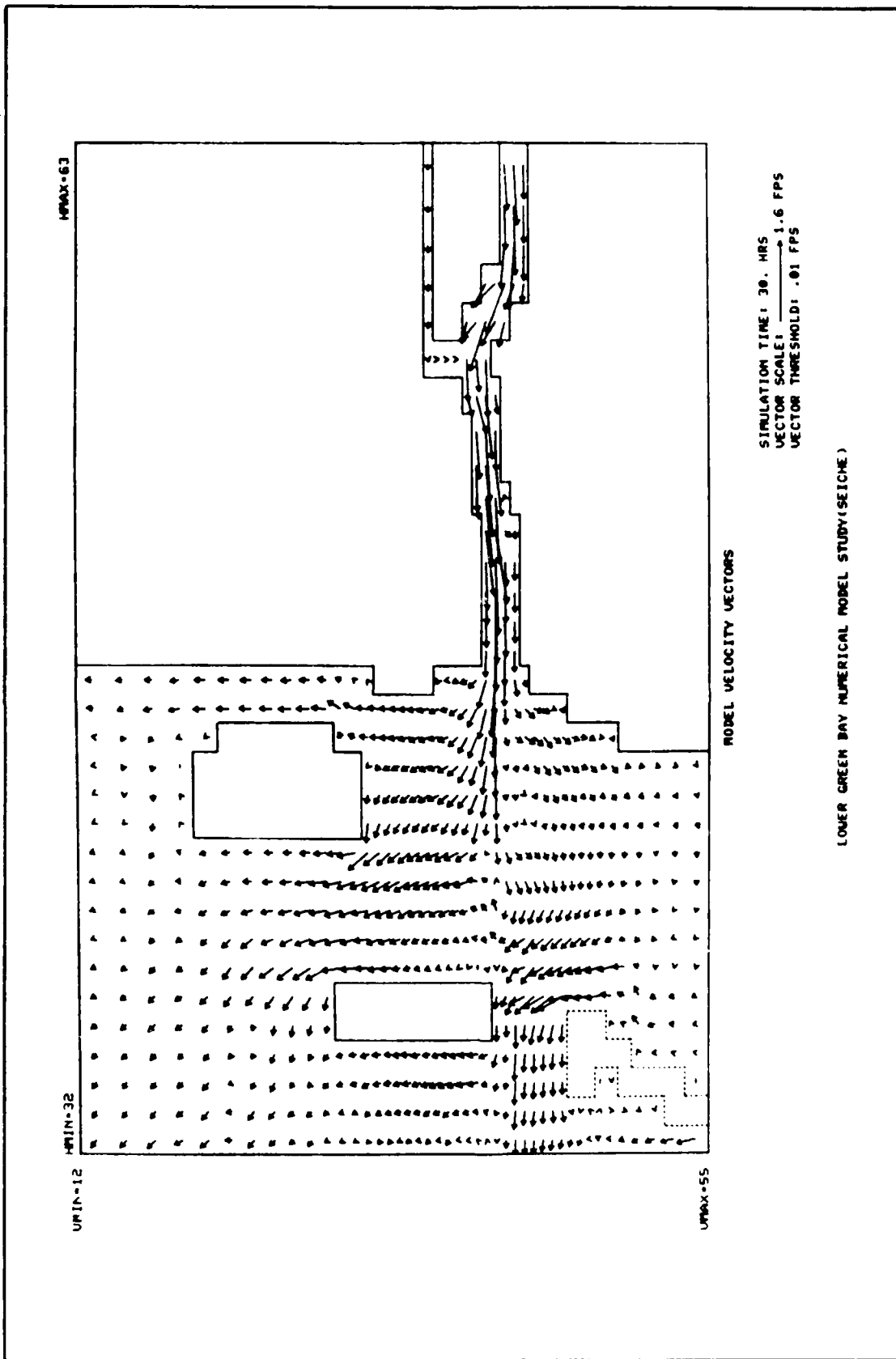
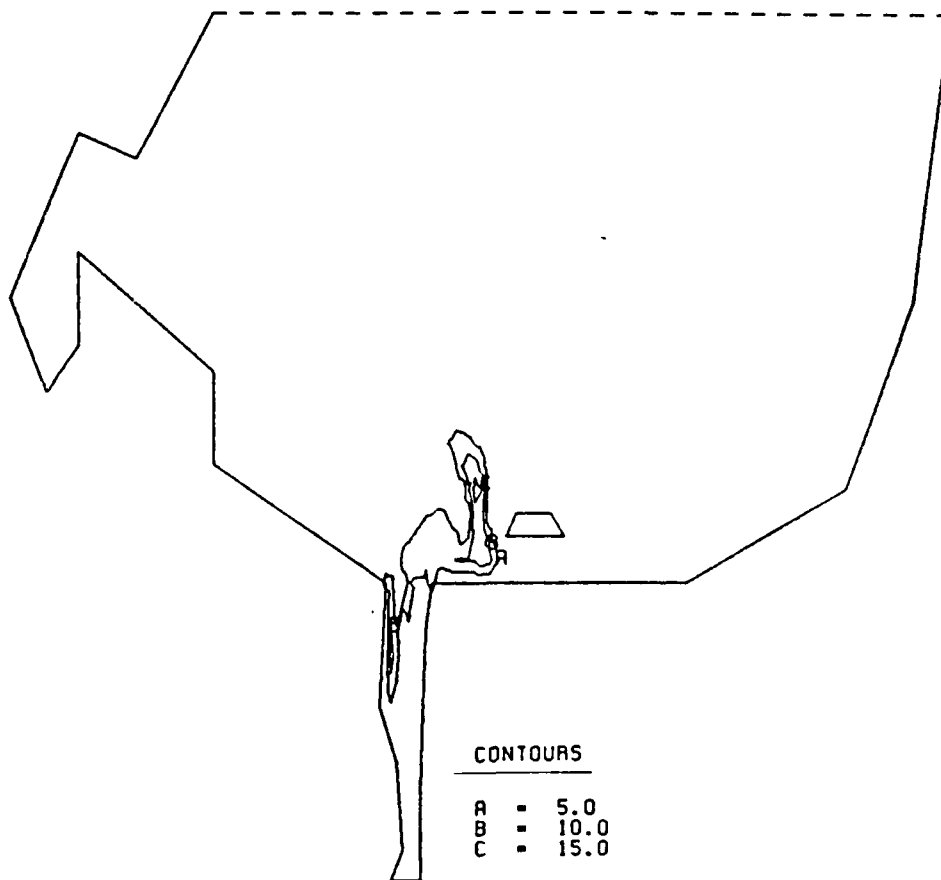


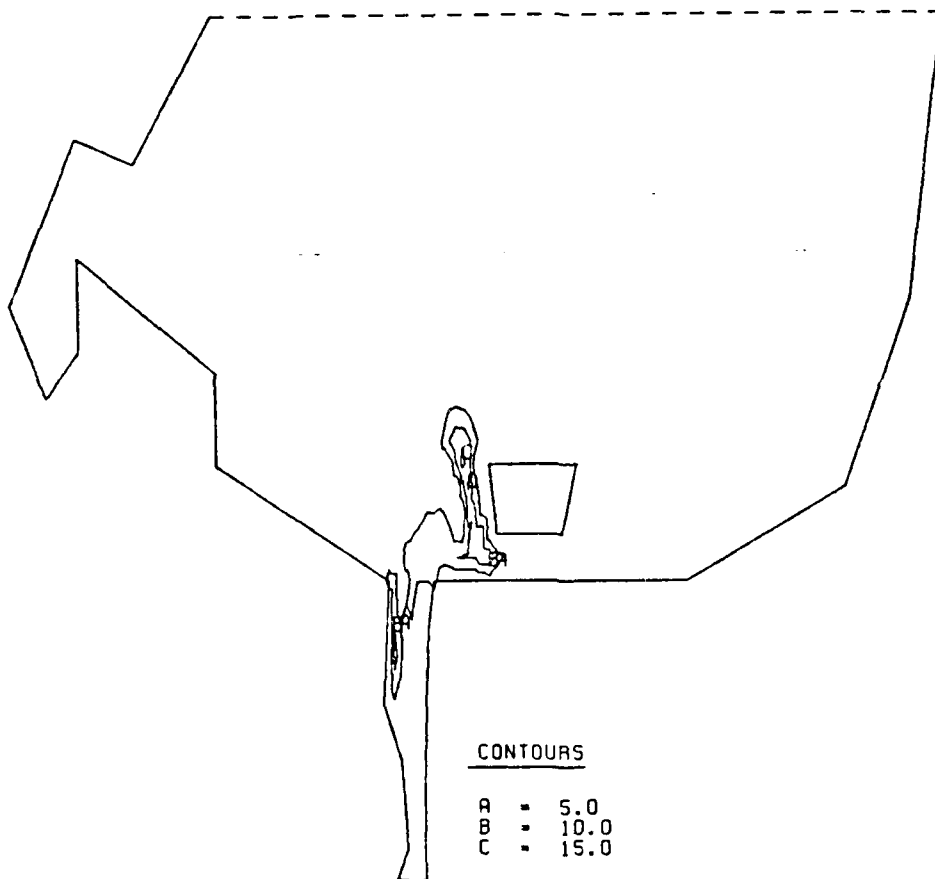
PLATE 36



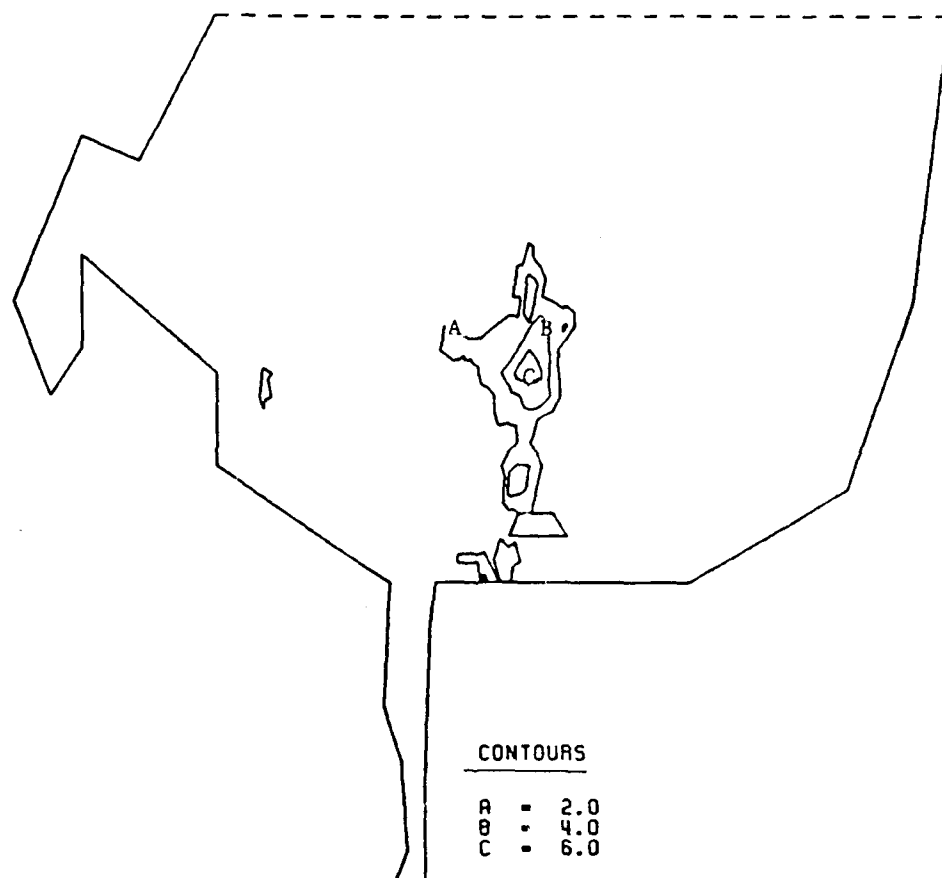
LOW FLOW, EXISTING CDF, KD=6.
TIME = 6 HR, ITIME=360



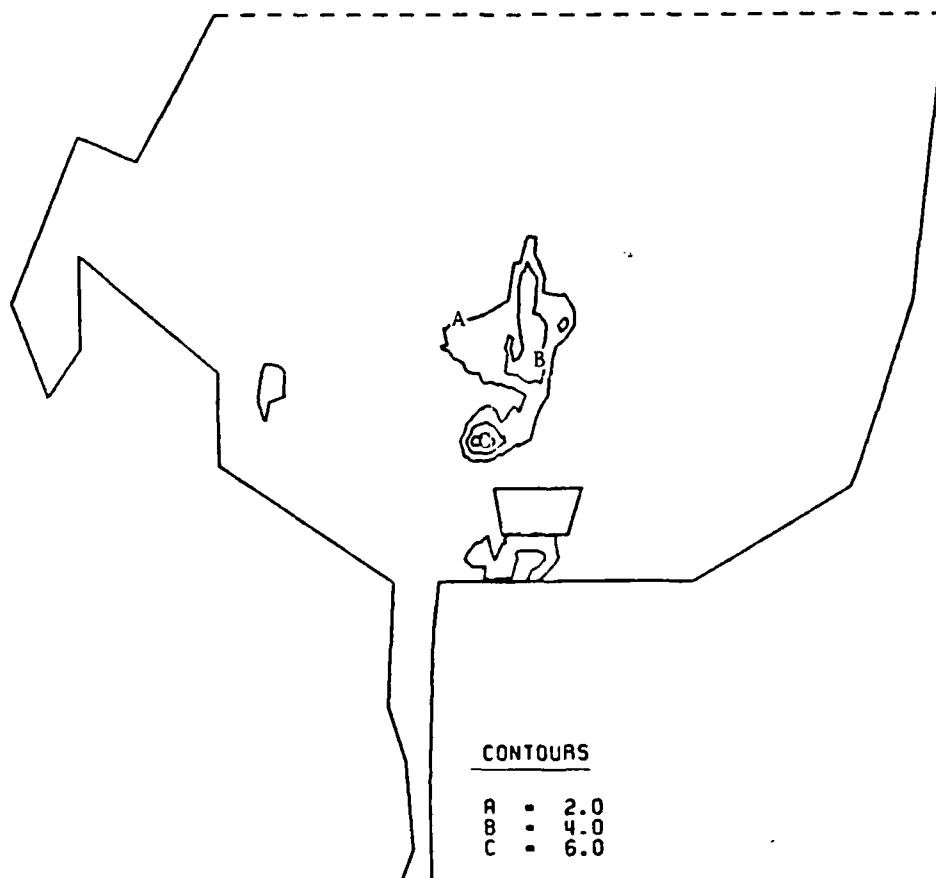
LOW FLOW, PROPOSED CDF, KD=6.
TIME = 6 HR, ITIME=360



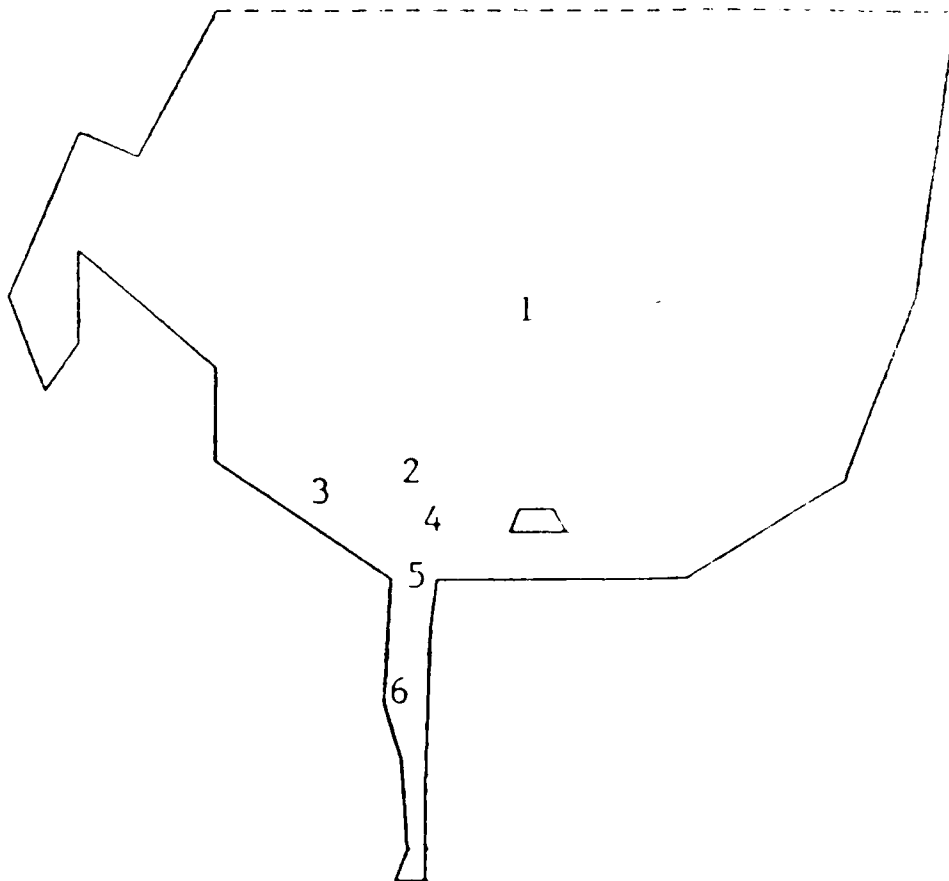
LOW FLOW, EXISTING CDF, KD=6.
TIME = 24 HR, ITIME=2040



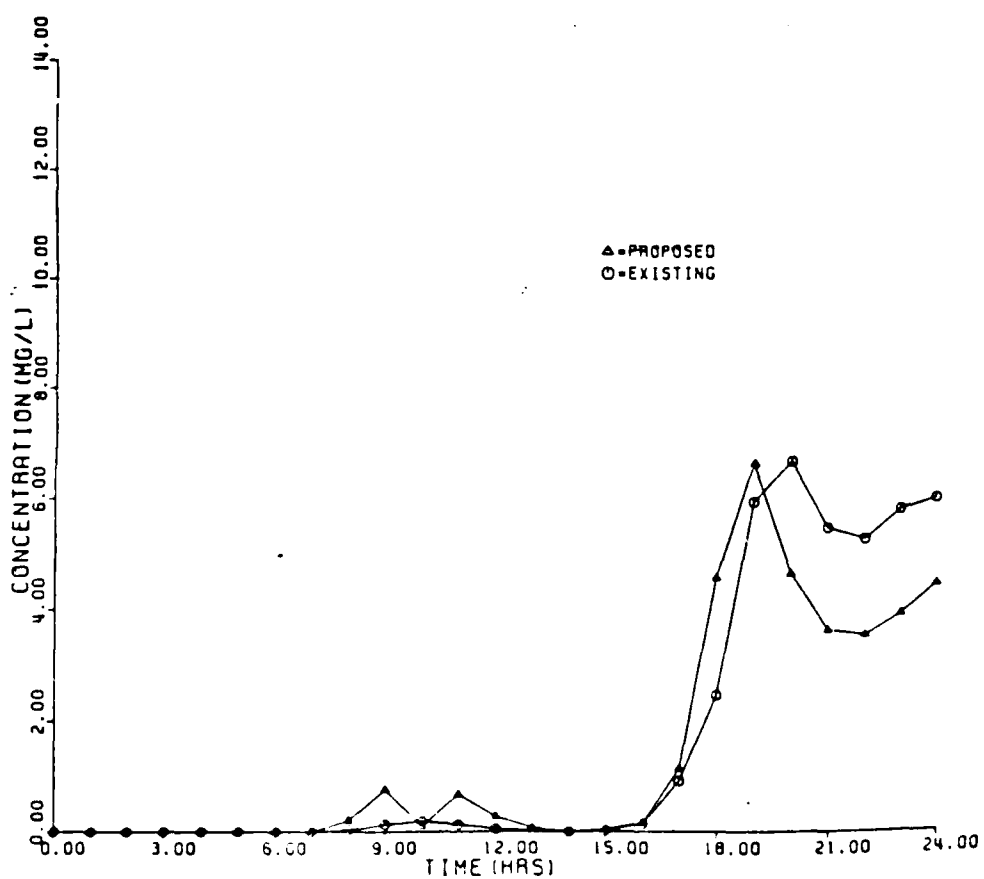
LOW FLOW, PROPOSED CDF, KD=6.
TIME = 24 HR, ITIME=1440



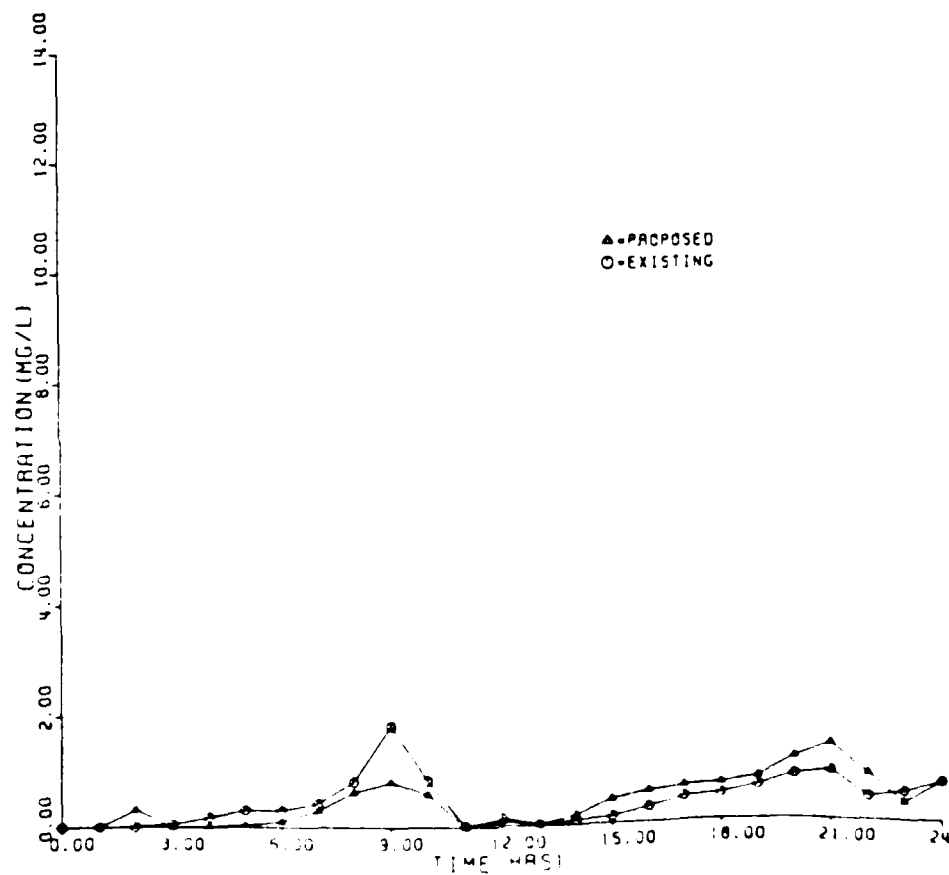
GAGE POINTS



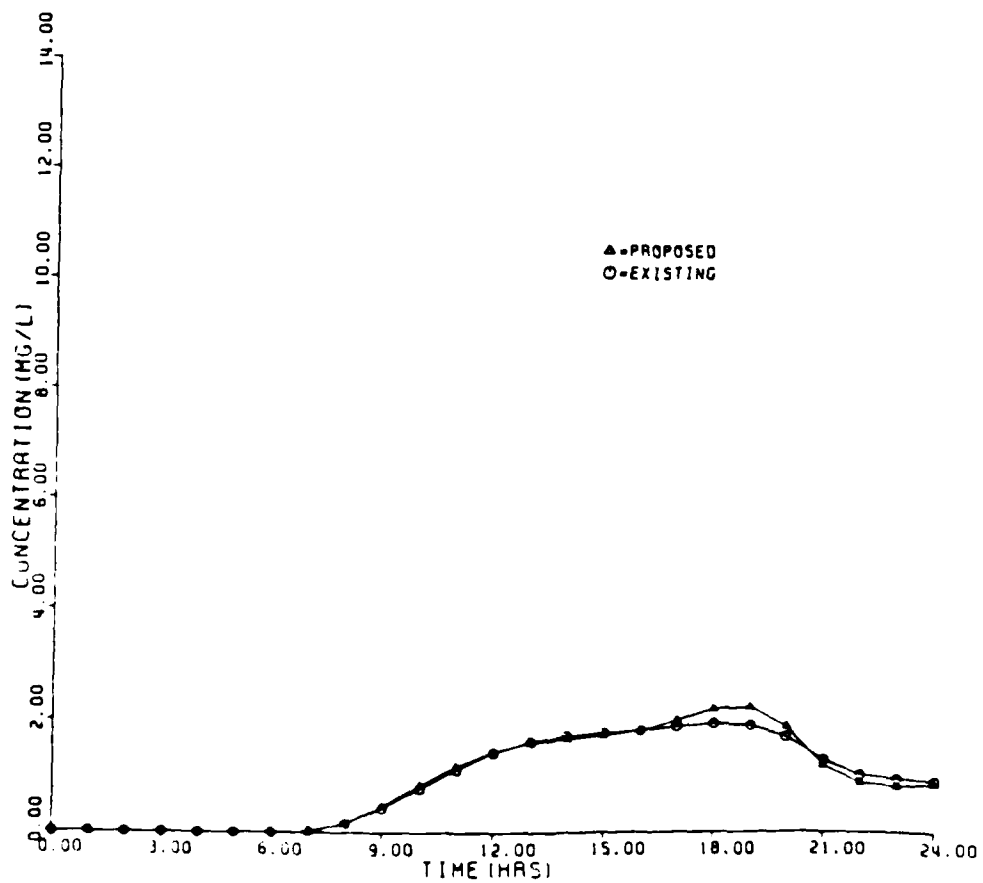
LOW FLOW - INSTANTANEOUS INJECTION
GAGE 1 SOUTHEAST OF GRASSY ISLAND
N=15, M=20



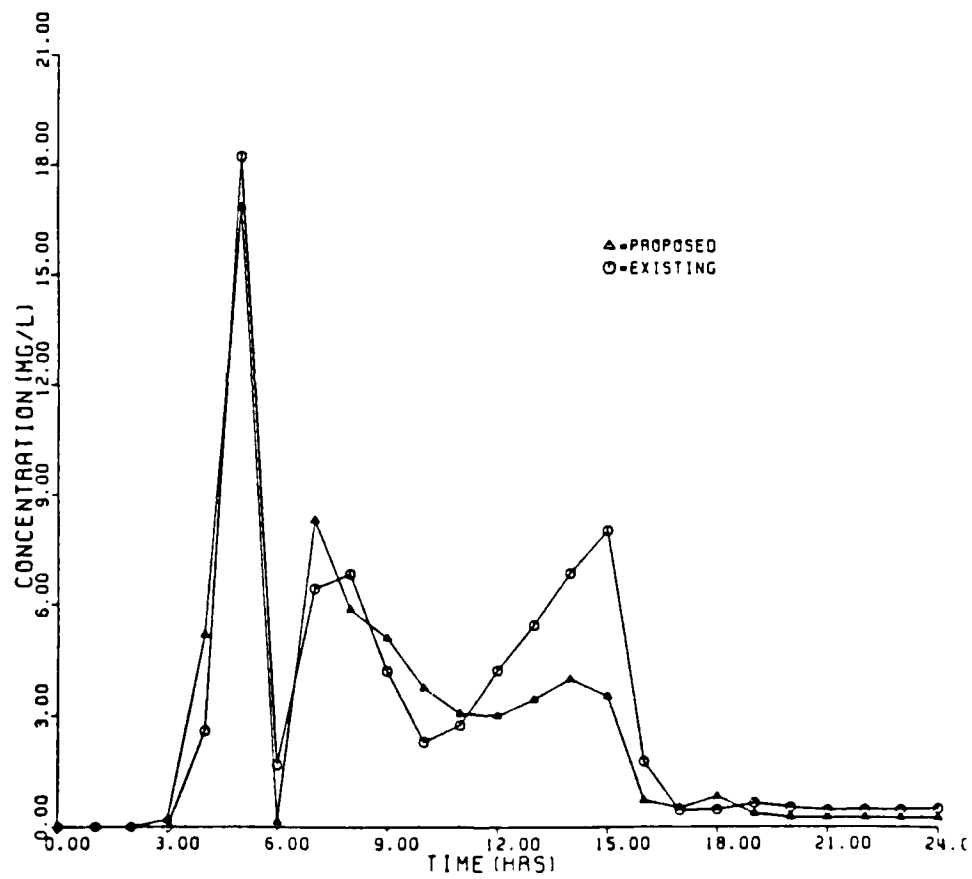
LOW FLOW - INSTANTANEOUS INJECTION
GAGE 2 MAIN CHANNEL
APP. 1/2 MI. NORTH OF FOX RIVER MOUTH



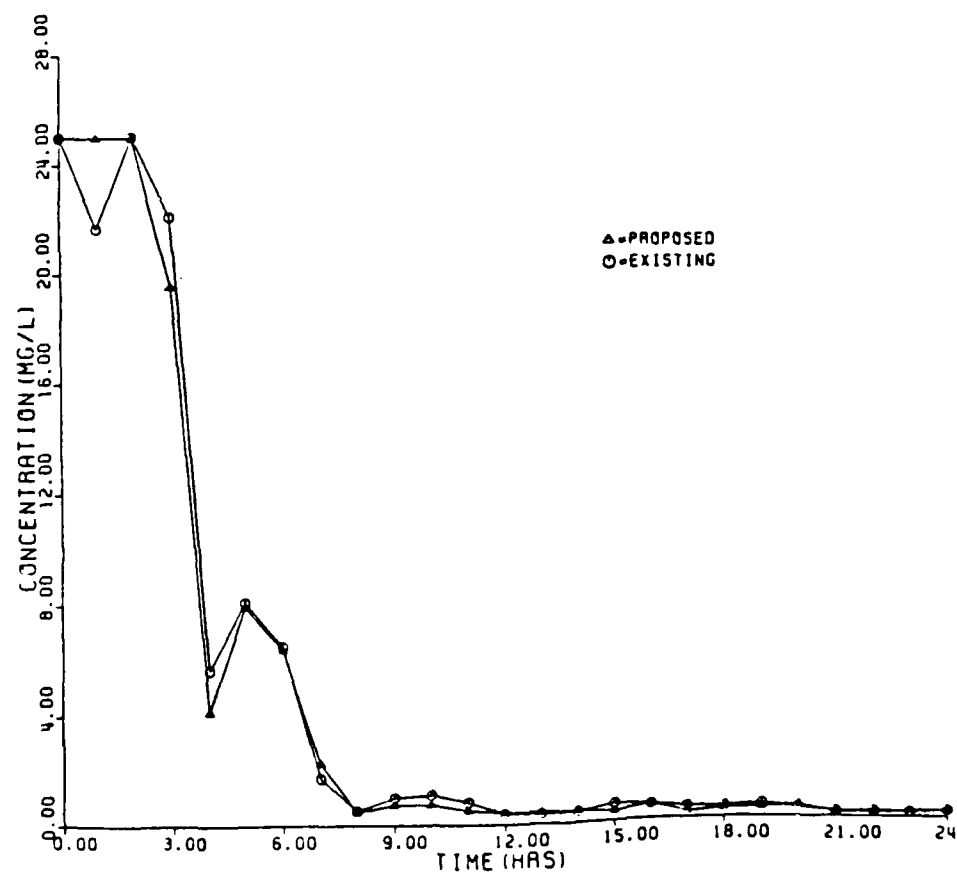
LOW FLOW - INSTANTANEOUS INJECTION
GAGE 3 WEST OF MAIN CHANNEL
N=20, M=55



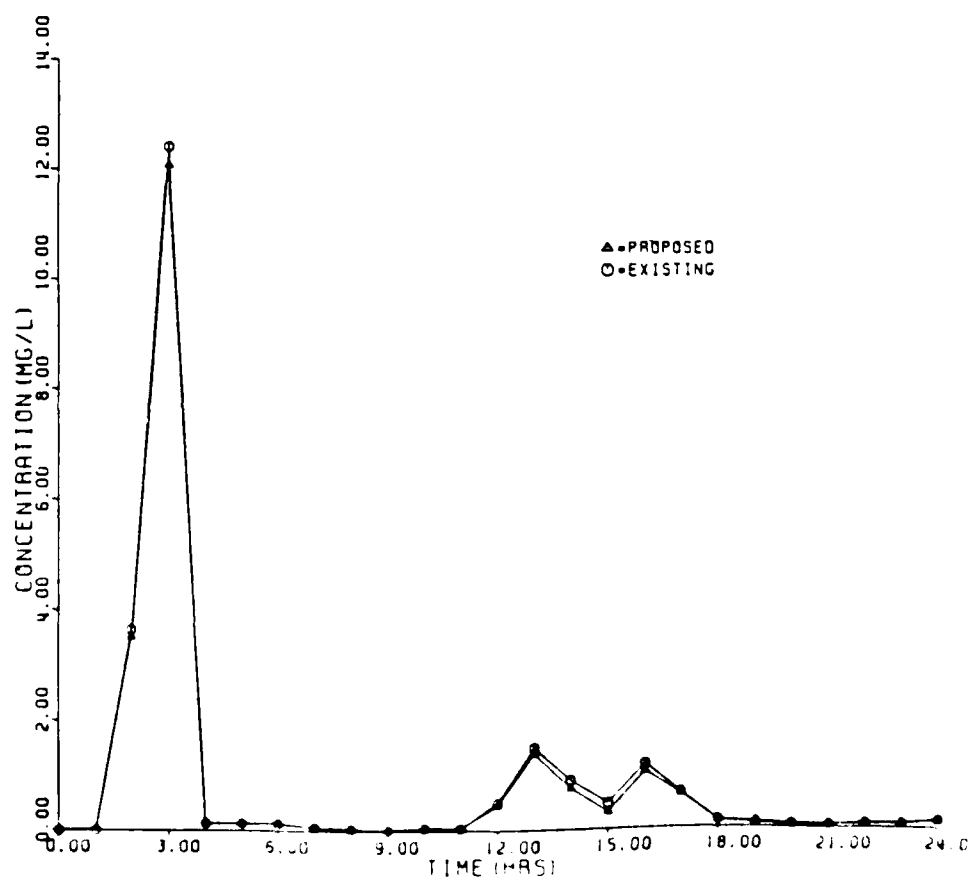
LOW FLOW - INSTANTANEOUS INJECTION
GAGE 4 APP. 1/4 MI. NO. OF FOX RIVER
N=22, M=29



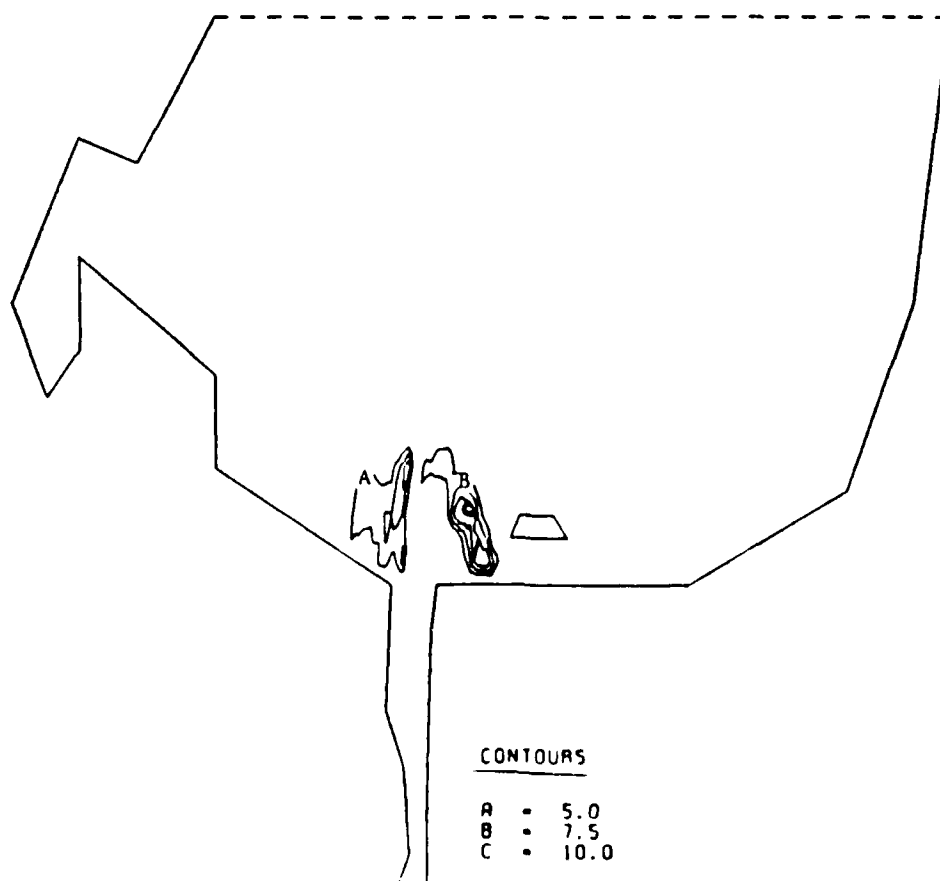
LOW FLOW - INSTANTANEOUS INJECTION
GAGE 5 MOUTH OF FOX RIVER
N=24,M=39



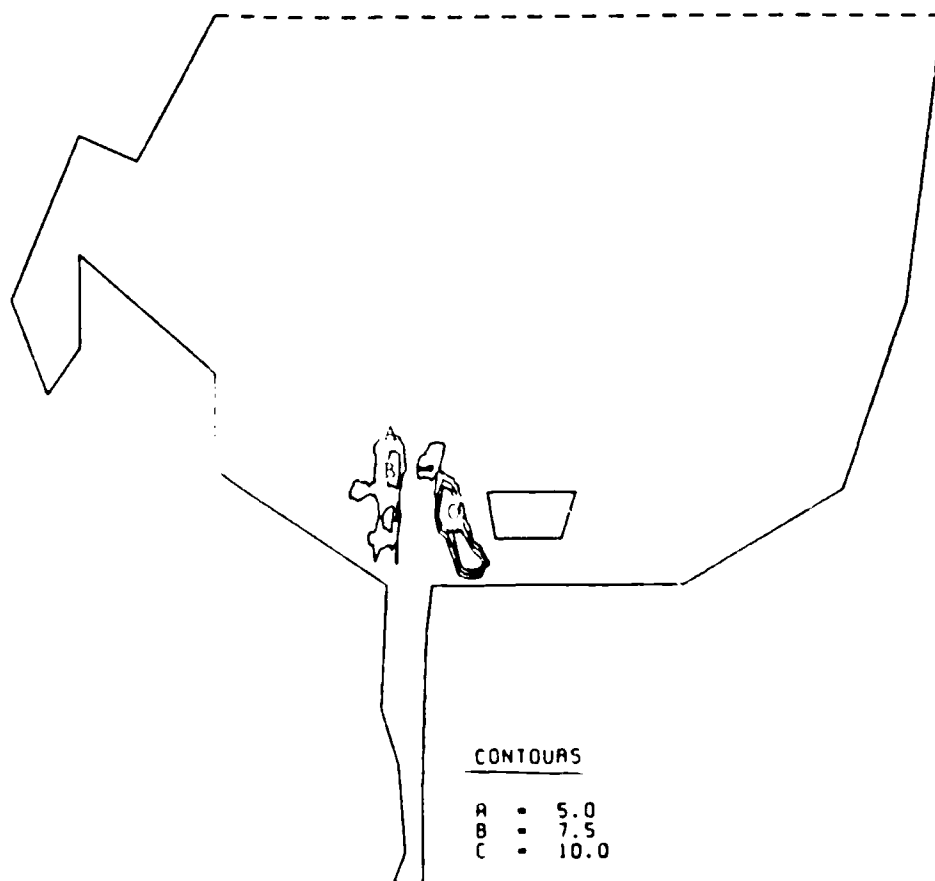
LOW FLOW - INSTANTANEOUS INJECTION
GAGE 6 FOX RIVER
N=32,M=38



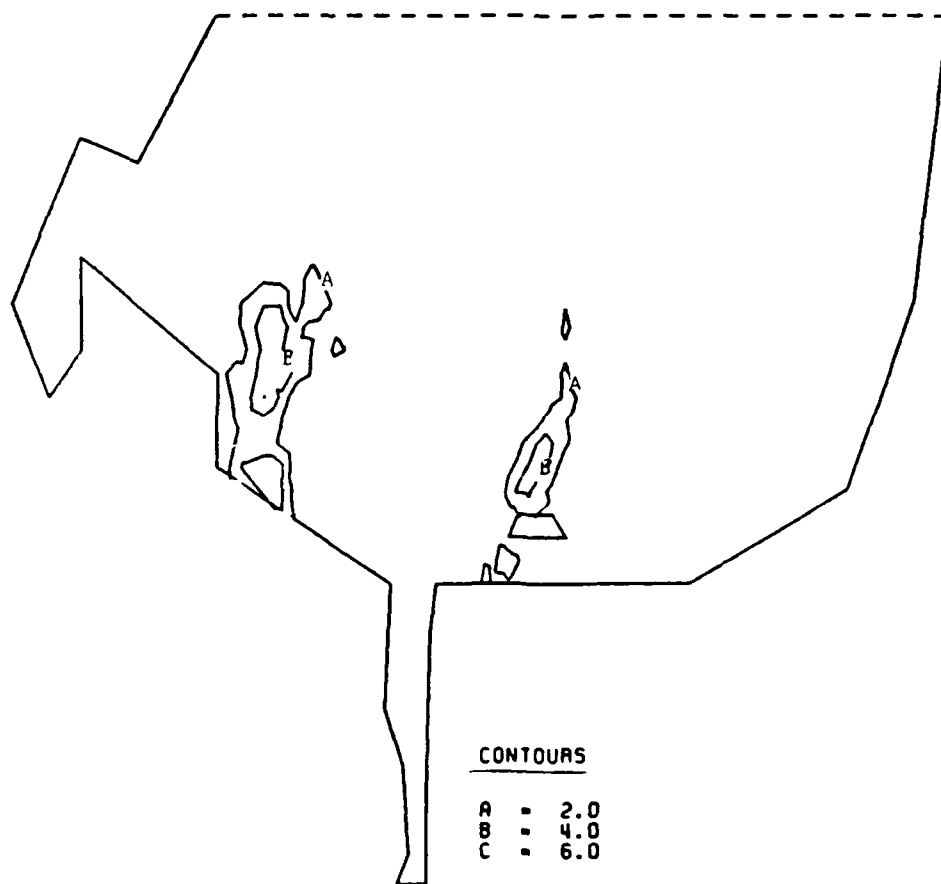
HIGH FLOW, EXISTING CDF, KD=6.
TIME = 6 HR, ITIME=360



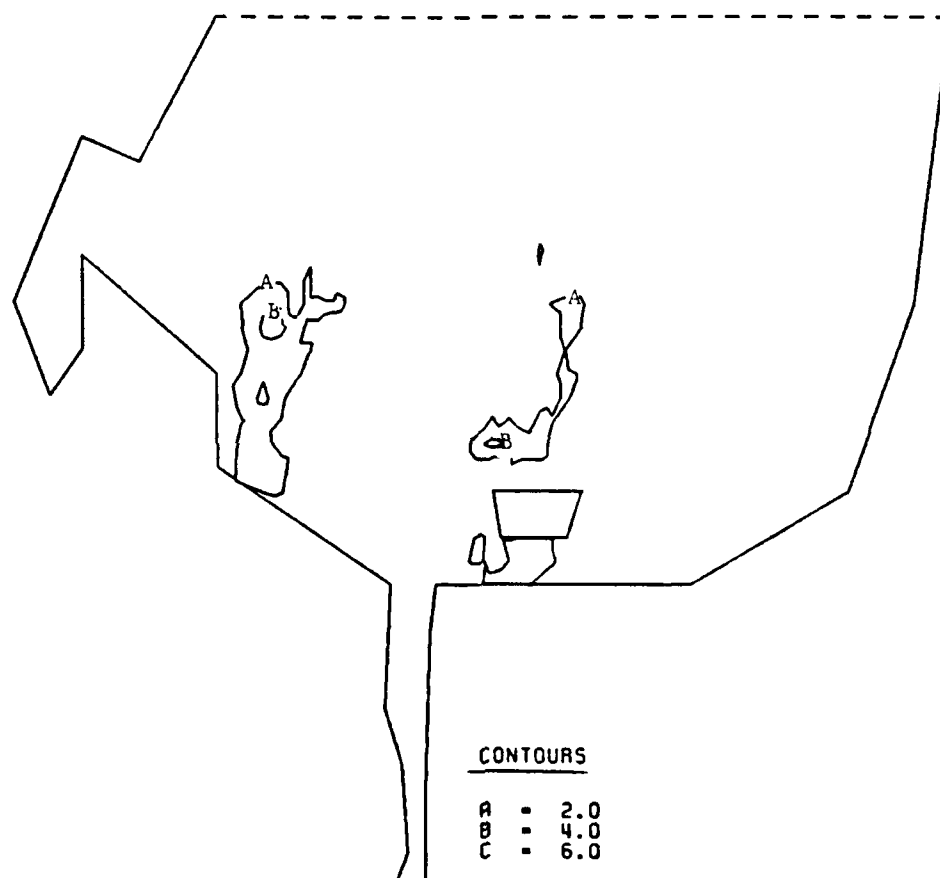
HIGH FLOW, PROPOSED CDF, KD=6.
TIME = 6 HR, ITIME=360



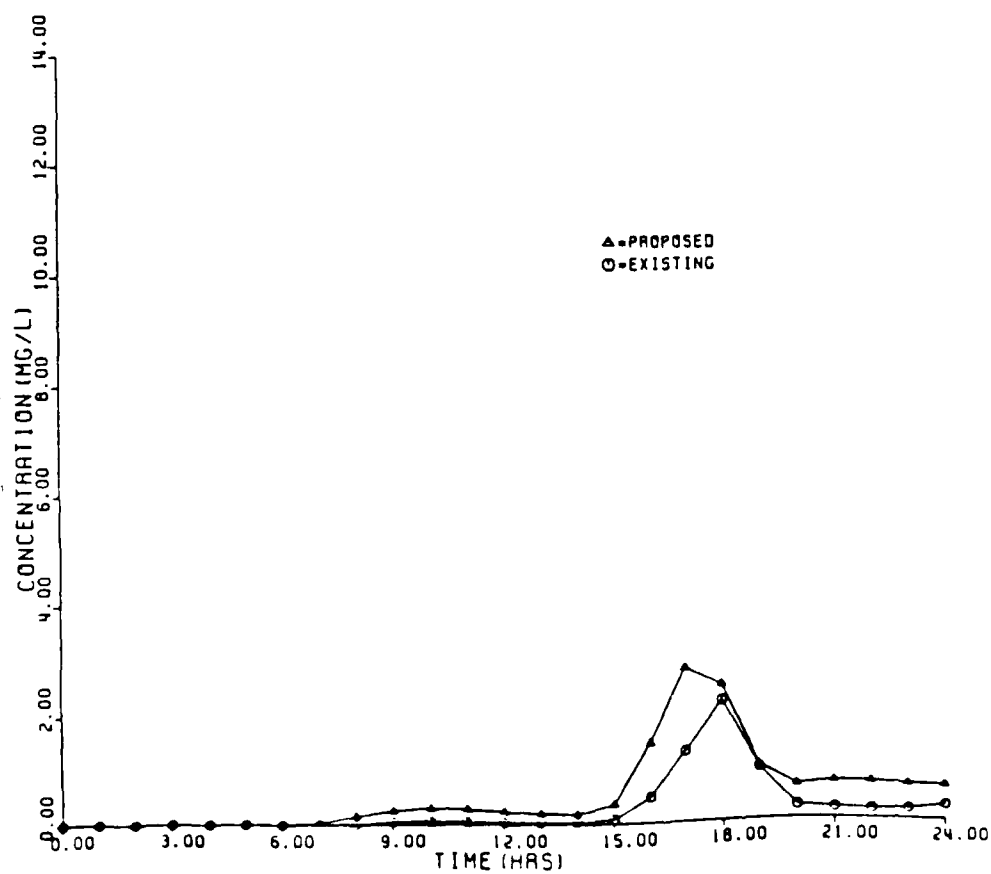
HIGH FLOW, EXISTING CDF, KD=6.
TIME = 24 HR, ITIME=1440



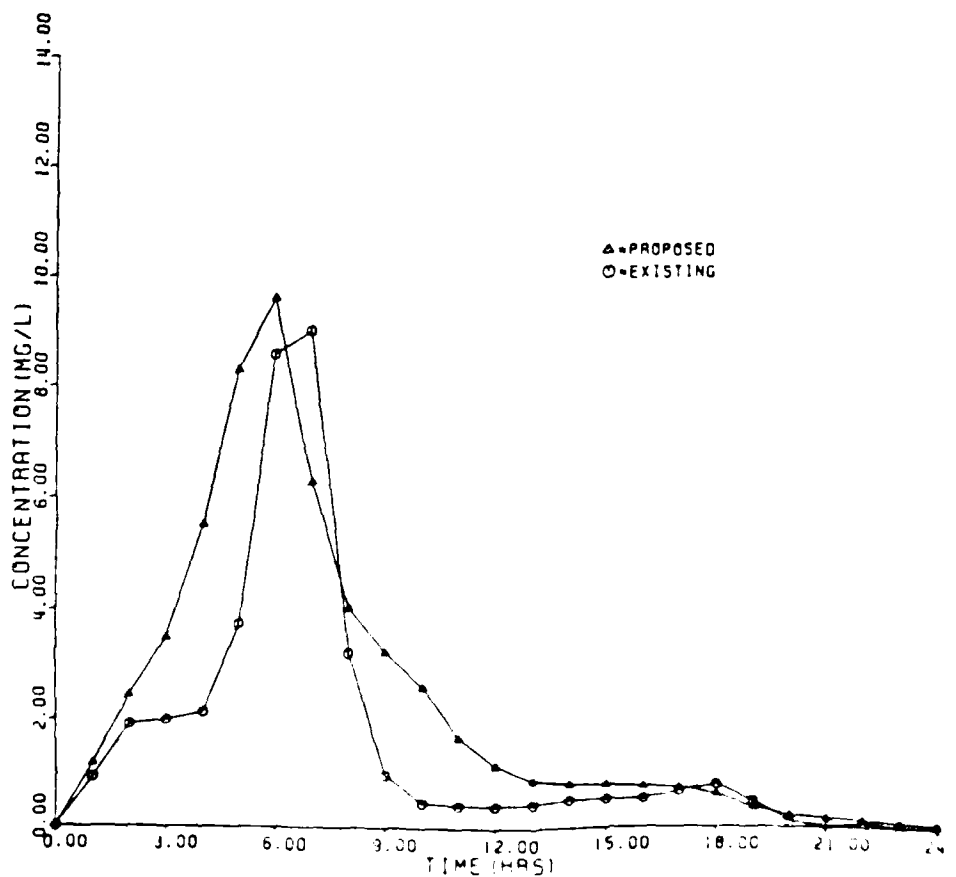
HIGH FLOW, PROPOSED CDF, KD=6.
TIME = 24 HR, ITIME=1440



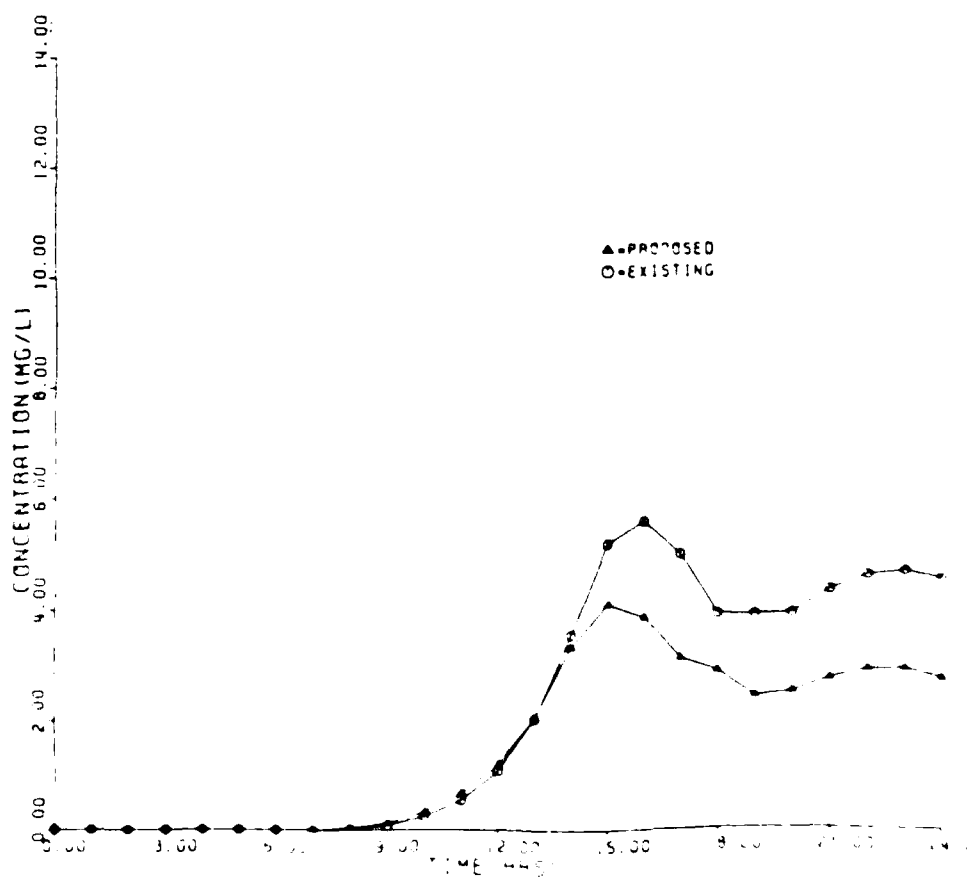
HIGH FLOW - INSTANTANEOUS INJECTION
GAGE 1 SOUTHEAST OF GRASSY ISLAND
N=15,M=20



HIGH FLOW - INSTANTANEOUS INJECTION
GAGE 2 MAIN CHANNEL
APP. 1/2 MI. NORTH OF FOX RIVER MOUTH



HIGH FLOW - INSTANTANEOUS INJECTION
GAGE 3 WEST OF MAIN CHANNEL
N=20,M=55



Chromatogram showing the separation of 1,2-dichloroethane (triangles) and 1,1-dichloroethane (circles). The x-axis is labeled 'TIME (min)' and ranges from 0 to 24. The y-axis is labeled 'COUNTS' and ranges from 0 to 10,000. The 1,2-dichloroethane peak is at approximately 15.5 minutes, and the 1,1-dichloroethane peak is at approximately 17.5 minutes.

NO-A189 076

LOWER GREEN BAY HYDRODYNAMIC AND MASS TRANSPORT:
NUMERICAL MODEL STUDY(U) COASTAL ENGINEERING RESEARCH
CENTER VICKSBURG MS A SWAIN ET AL. DEC 87

2/2

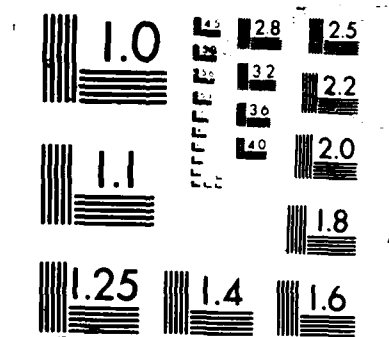
UNCLASSIFIED

CERC-MP-87-19

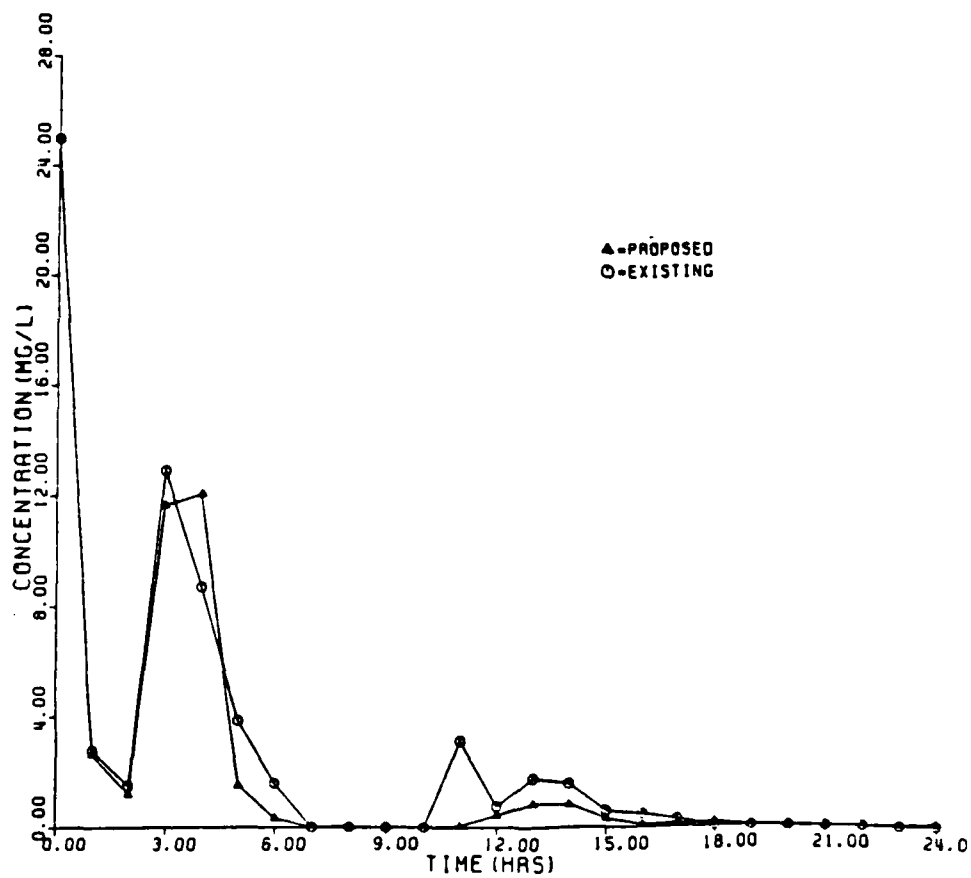
F/G 0/8

ML

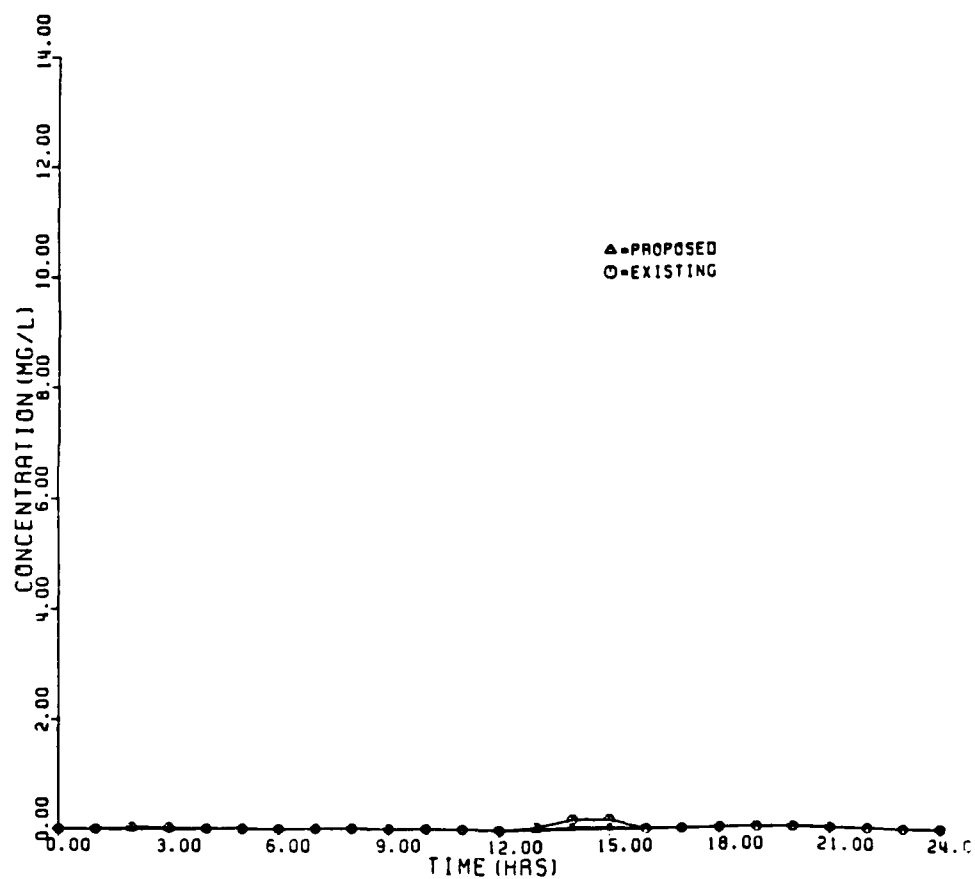




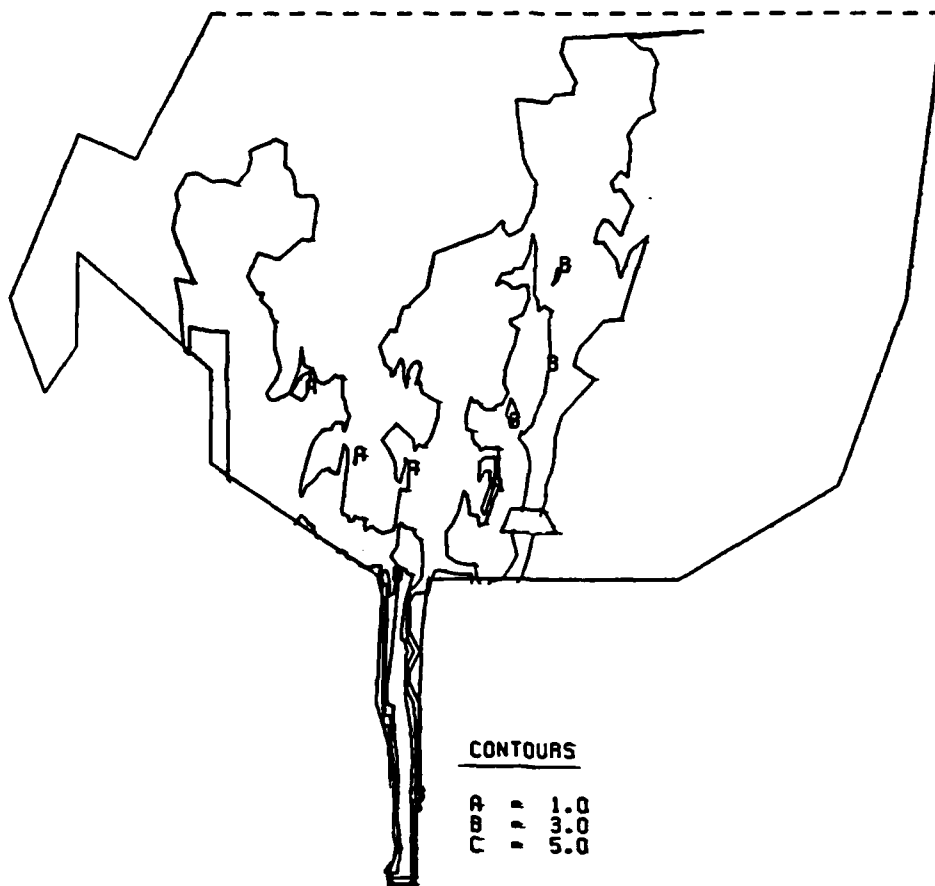
HIGH FLOW - INSTANTANEOUS INJECTION
GAGE 5 MOUTH OF FOX RIVER
N=24, M=39



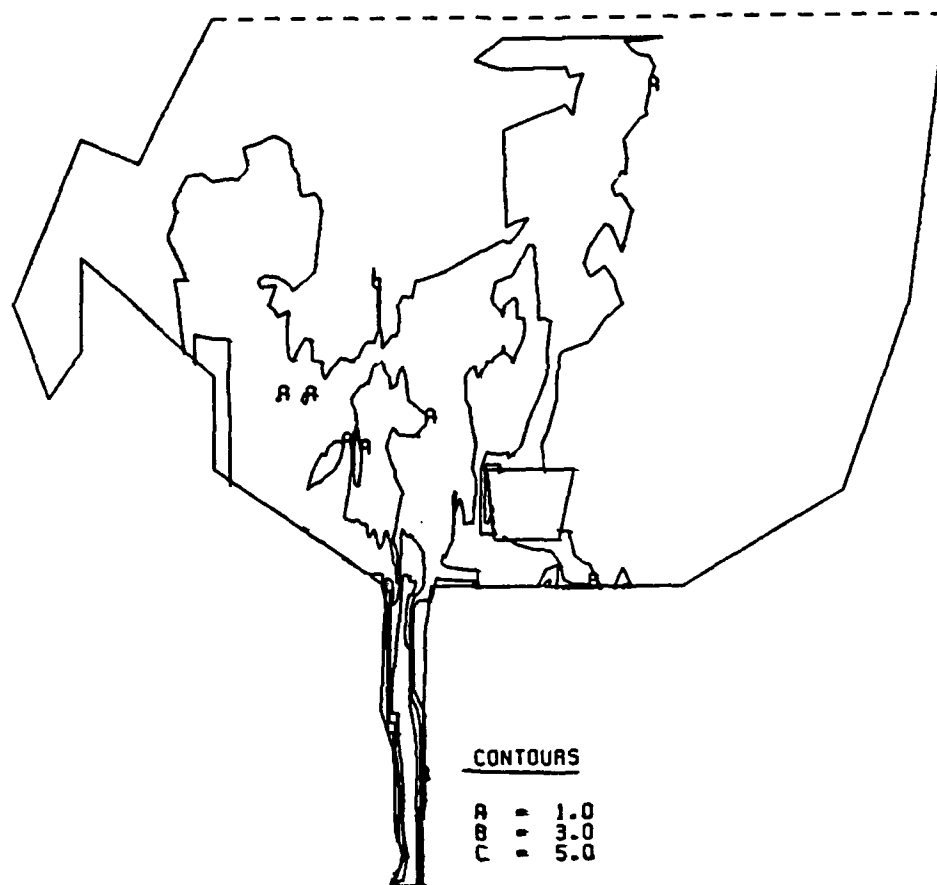
HIGH FLOW - INSTANTANEOUS INJECTION
GAGE 6 FOX RIVER
N=32,M=38



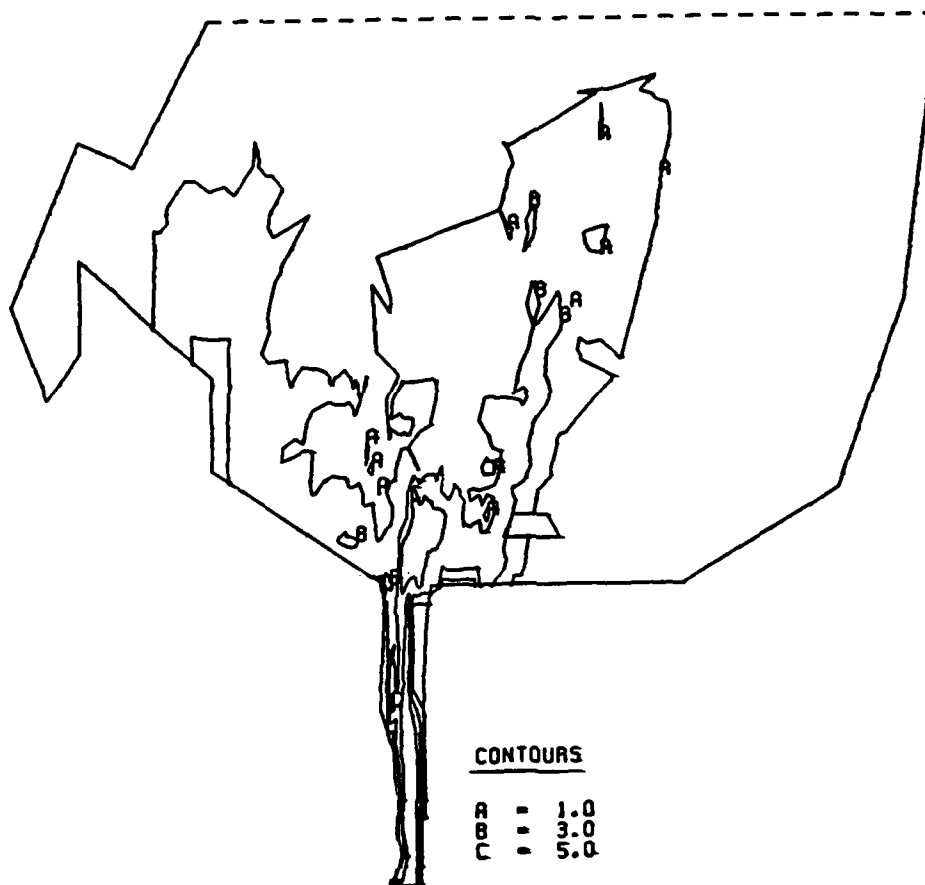
LOW FLOW, EXISTING CDF
TIME = 91 HR, ITIME=5460



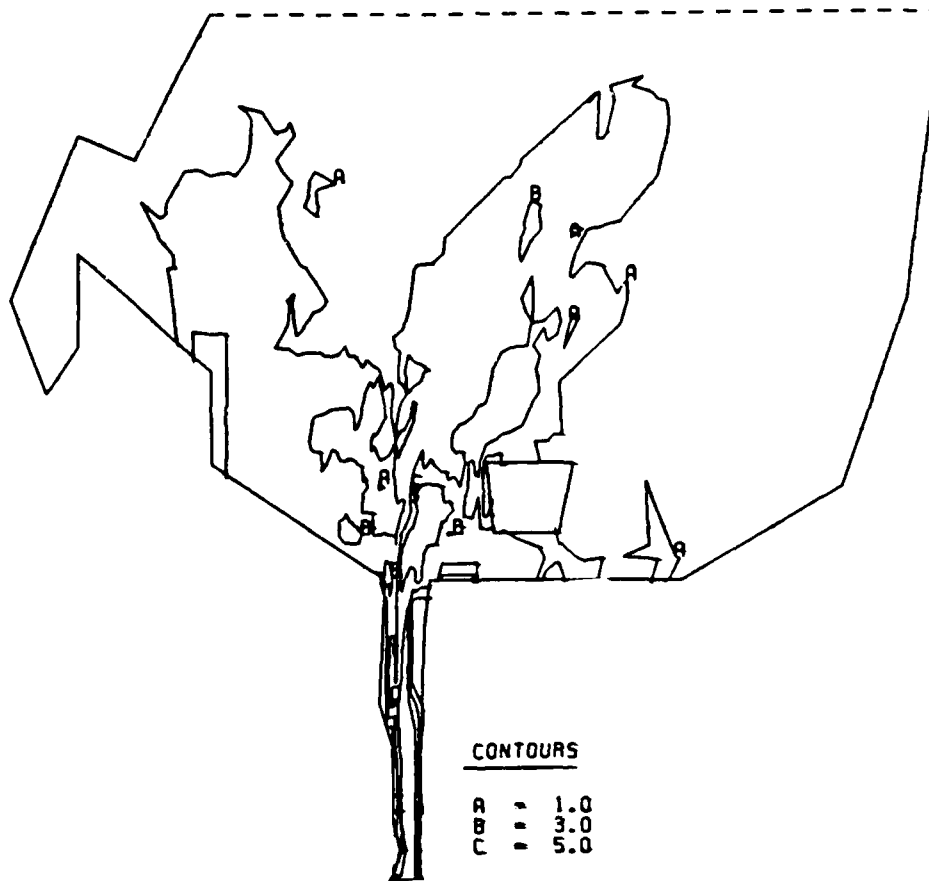
L3W FLOW, PROPOSED CDF
TIME = 91 HR, ITIME=5460



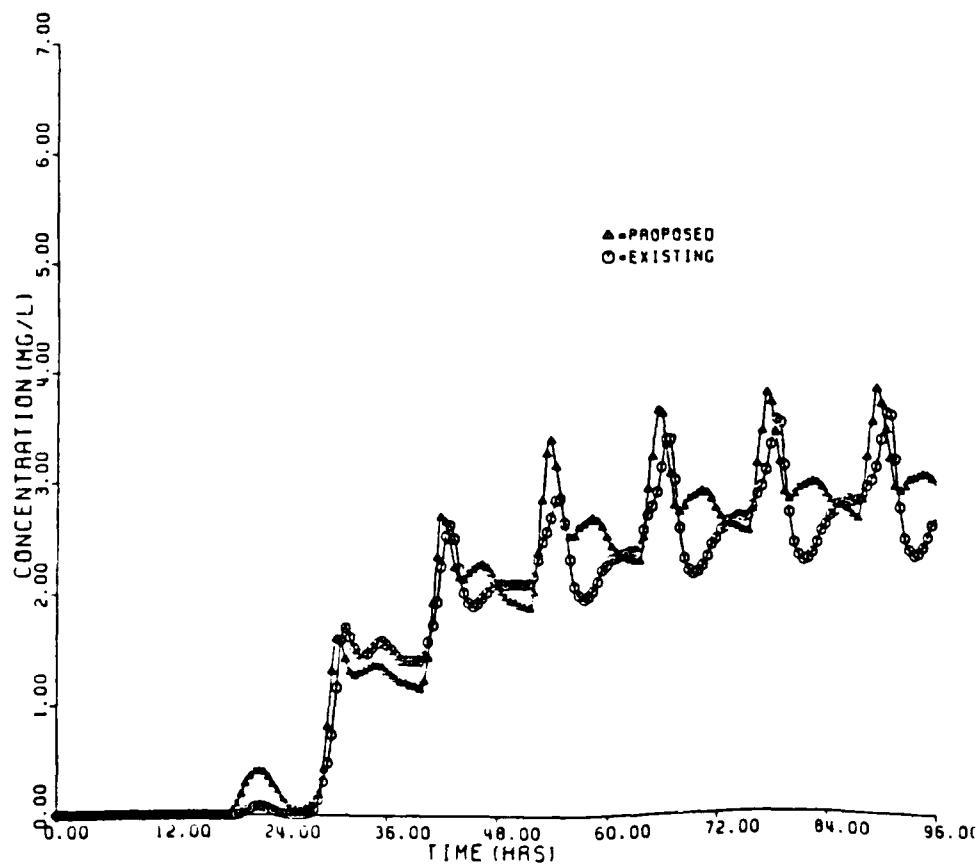
LOW FLOW, EXISTING CDF
TIME = 96 HR, ITIME=5760



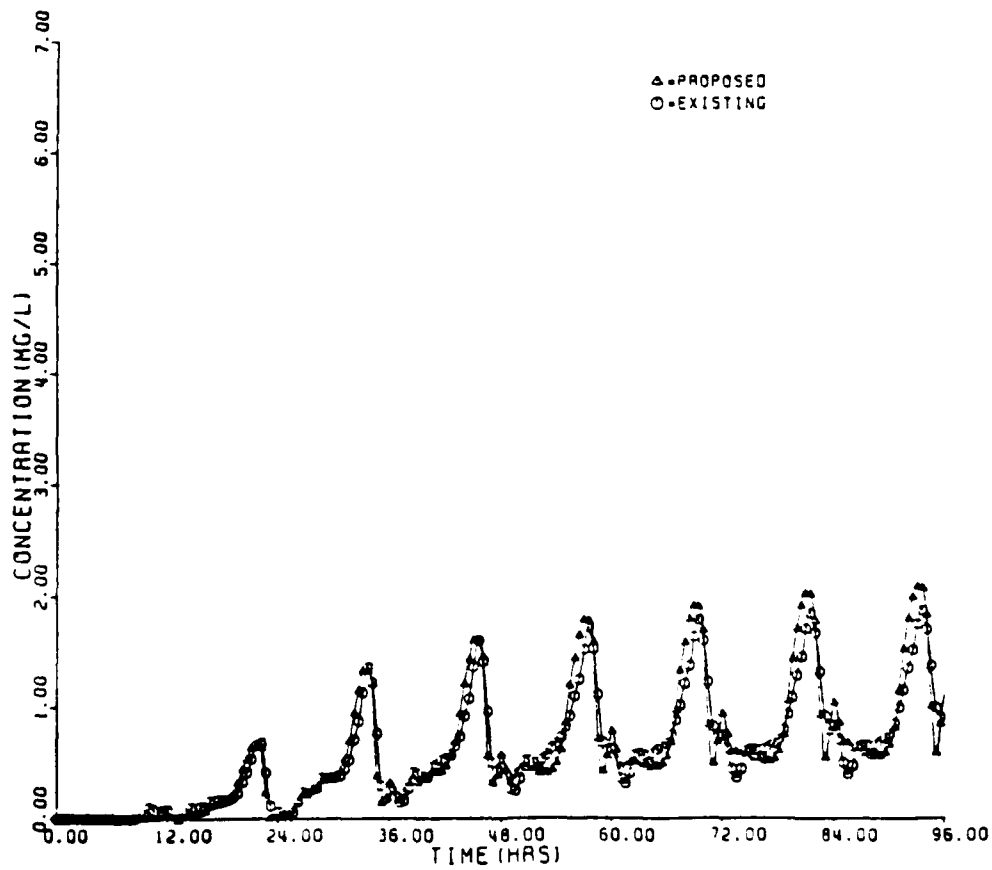
LOW FLOW, PROPOSED CDF
TIME = 96 HR, ITIME=5760



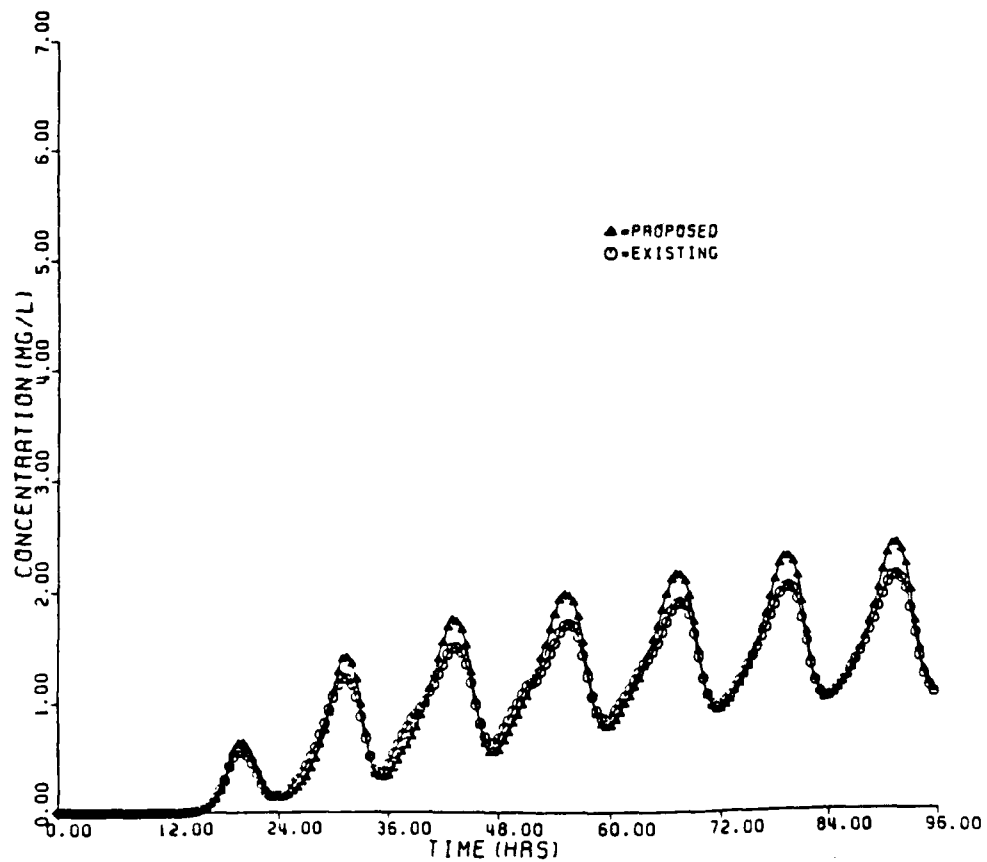
LOW FLOW - BOUNDARY INJECTION
GAGE #1 SOUTHEAST OF GRASSY ISLAND
N=15,M=20



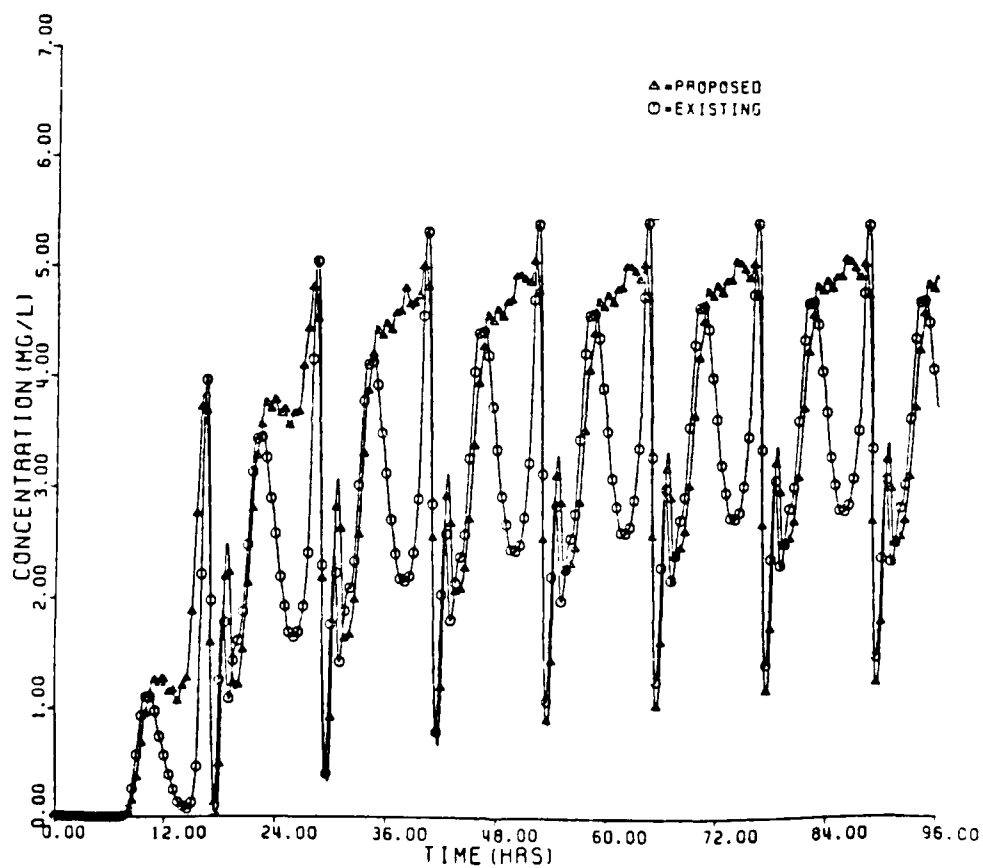
LOW FLOW - BOUNDARY INJECTION
GAGE 2 MAIN CHANNEL
APP 1/2 MI NORTH OF FOX RIVER MOUTH
N = 20, M = 39



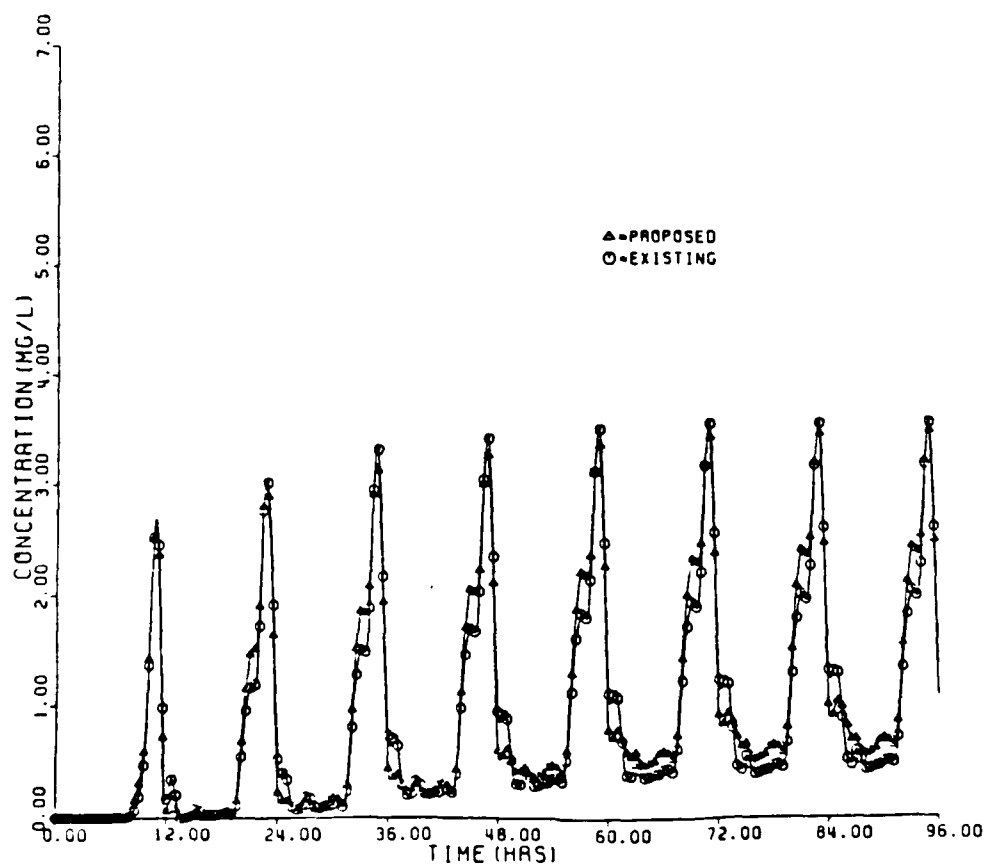
LOW FLOW - BOUNDARY INJECTION
GAGE 3 WEST OF MAIN CHANNEL
N=20,M=55



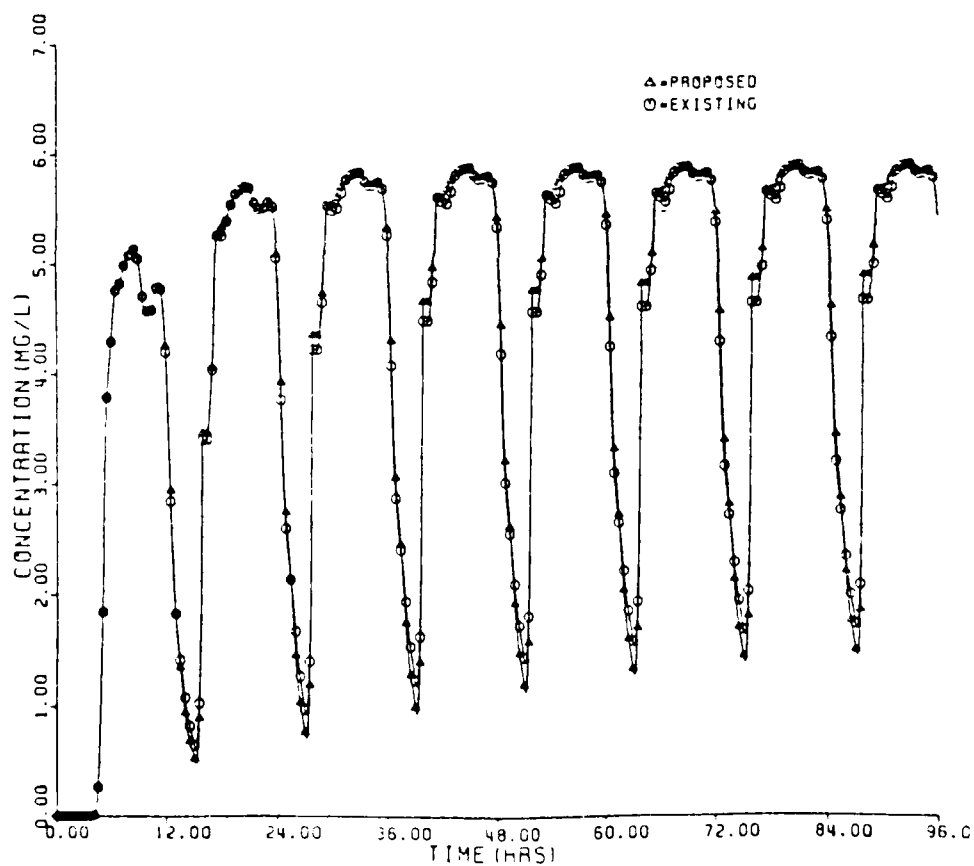
LOW FLOW - BOUNDARY INJECTION
GAGE 4 WEST OF CDF
N=22,M=29



LOW FLOW - BOUNDARY INJECTION
GAGE 5 MOUTH OF FOX RIVER
N=24,M=39



LOW FLOW - BOUNDARY INJECTION
GAGE 6 FOX RIVER
N=32,M=38



APPENDIX A: NOTATION

a,b,c	Regional constants derived from stretching transformation of coordinate system
A,B	Coefficient matrixes
C	Chezy friction coefficient
C_1	Constant of proportionality
d	Total depth of water column $d = \eta - h$
f	Coriolis parameter
F_x, F_y	External forcing functions in x- and y-direction, respectively (i.e., wind stress)
g	Acceleration due to gravity
h	Local ground (cell) elevation above datum
K^*	Dispersion coefficient
K_x^*, K_y^*	Effective dispersion coefficients
k	Integer time-step counter
n	Dimensionless parameter used to characterize stability criterion
R	Rate of water volume change in the system (for example through rainfall or evaporation)
s	Vertically integrated constituent concentration
t	Time
u	Vertically averaged water velocity in x-direction
U	Matrix consisting of η , u , and v as functions of x , y , and t
U^*	Value of U at an intermediate time-step level ($K+1$) time level, where k counts time levels
U_*^1	Shear velocity
v	Vertically averaged water velocity in x-direction
V	Largest velocity encountered at a computational cell
x,y	Cartesian coordinate system axes names
X	Physical distance
Z	Computational distance
Δt	Time-step
$\Delta x, \Delta y$	Length of computational cell in x- and y-directions
ϵ	Eddy viscosity coefficient
η	Water-surface elevation above datum
η_a	Hydrostatic water elevation due to atmospheric pressure differences
λ_x, λ_y	Two-dimensional differences operators

* Intermediate time-step level
∂ Partial differential operator
 δ_x, δ_y Centered difference operators

END

DATE

FILMED

MARCH

1988

DTIC